CARIBOU MONITORING STUDY FOR THE ALPINE SATELLITE DEVELOPMENT PROGRAM AND GREATER MOOSE'S TOOTH UNIT, 2020

Joseph H. Welch
Alexander K. Prichard
Matthew J. Macander

Prepared for

CONOCOPHILLIPS ALASKA, INC.
Anchorage, Alaska

Prepared by

ABR, INC.—ENVIRONMENTAL RESEARCH & SERVICES
Fairbanks, Alaska

COVER
Aerial view during caribou surveys of the northeastern portion of the National Petroleum Reserve–Alaska. Photography by ABR.

CARIBOU MONITORING STUDY FOR THE ALPINE SATELLITE DEVELOPMENT PROGRAM AND GREATER MOOSE'S TOOTH UNIT, 2020

Prepared for

ConocoPhillips Alaska, Inc.
P.O. Box 100360
Anchorage, Alaska 99510-0360

Prepared by

Joseph H. Welch
Alexander K. Prichard
Matthew J. Macander

ABR, Inc.—Environmental Research & Services
P.O. Box 80410
Fairbanks, Alaska 99708-0410

February 2021

EXECUTIVE SUMMARY

- Caribou use of the Alpine Satellite Development and Greater Moose's Tooth Unit areas has been studied since 2001 using a combination of aerial surveys, analysis of telemetry data, and remote sensing in order to understand caribou distribution and movements prior to, during, and after development in the area, including construction of the CD-5, GMT1/MT6, GMT2/MT7 roads. This report summarizes field research conducted in 2020 and analyses of data collected over the life of the project.
- Spring 2020 air temperatures were near the 30-year average and snow melted slightly earlier than usual at the Kuparuk airport. Temperatures were variable during early and mid-June but were generally below average. From June through early August, strong winds (>10 mph) occurred frequently and temperatures were often below average. Therefore, weather conditions were generally not conducive to high insect activity for much of the 2020 insect season. Temperatures were generally above average from mid- through late-August.
- We completed 4 of 7 planned aerial transect surveys of the Greater Moose's Tooth (GMT) survey area between April and October 2020. The estimated density ranged from a maximum of 0.56 caribou/km² on 19 June to a minimum of 0.05 caribou/km² on 27 August. We observed 5 calves in the GMT survey area during the calving survey on 9–10 June.
- We completed 2 of 3 planned aerial transect surveys of the Colville River Delta (CRD) survey area during the postcalving and late summer seasons. The estimated density in the survey area was 0.17 caribou/km² during the postcalving survey on 15 June and 0.07 caribou/km² during the late summer survey on 27 August.
- We analyzed telemetry data using kernel density analysis, dynamic Brownian Bridge movement models, and species distribution models to examine seasonal patterns of movements and distribution for caribou from both the Teshekpuk Caribou Herd (TCH) and the Central Arctic Herd (CAH).
- We examined annual and seasonal spatial patterns in vegetative biomass (based on NDVI) and snow cover and snow water equivalent calculated on a regional scale using satellite imagery. We also estimated forage metrics including forage biomass and nitrogen levels based on NDVI and phenology.
- The GMT survey area is on the eastern edge of the TCH range and gets some use by TCH females throughout the year; use by TCH males is highest during July with less use in August–October and little winter use. Use of the GMT area by the CAH is rare and largely occurs during summer.
- The CRD survey area is located between the ranges of the TCH and CAH and typically has very low densities of caribou throughout the year, however large groups of caribou from both herds are occasionally observed on the delta during the summer.
- The existing ASDP and GMT infrastructure west of the Colville River is in an area that typically has low densities of caribou and is rarely crossed by collared caribou. As development expands to the west, it will occur in areas that typically have higher caribou densities areas and are used more by migrating caribou.
- Species distribution models indicated that broad geographic patterns were important factors influencing caribou distribution during all seasons, but caribou distribution can also be explained by differences in vegetative biomass, landscape topography, snow cover, and habitat type.
- There were two observations of grizzly bear groups in the GMT or CRD survey areas in 2020: a sow with one cub was observed on the eastern Colville Delta on 19 August and a single adult bear was observed near the coast in the GMT survey area on 27 August. One adult polar bear was observed in the northwestern Colville Delta on 27 August. There was one observation of 2 muskoxen in

the southeastern GMT survey area and 4 observations of muskoxen groups outside the survey areas ranging in size from 1 adult to 33 adults and approximately 9 calves. A single wolverine was observed west of the GMT area on 19 June.

TABLE OF CONTENTS

LIST OF FIGURES

LIST OF TABLES

LIST OF APPENDICES

ACKNOWLEDGMENTS

This study was funded by ConocoPhillips Alaska, Inc., (CPAI) and was administered by Christina Pohl, CPAI Environmental Studies Coordinator, with support from Robyn McGhee of CPAI and Jasmine Woodland from Weston Solutions Inc. for whose support we are grateful. Valuable assistance with field logistics was provided by Mike Hauser, Zac Hobbs, and Krista Kenny. Alaska Department of Fish and Game (ADFG) biologists played crucial collaborative roles in this study by capturing caribou, deploying radio collars, and providing telemetry data under a cooperative agreement among ADFG, CPAI, and ABR. We thank ADFG biologists Lincoln Parrett and Elizabeth Lenart for their professional cooperation and assistance. Brian Person of the North Slope Borough Department of Wildlife Management (NSB) provided GPS and satellite telemetry data, valuable information, and advice. Bob Gill of 70 North LLC and Bob Eubank of North River Air provided safe and efficient piloting of survey airplanes under flying conditions that often were less than optimal. Assistance in the field was provided by ABR employees Nick Moser, Tim Obritschkewitsch, Kelly Lawhead, Sam Vanderwaal, and Robert McNown. Support during data collection, analysis, and report production was provided by Christopher Swingley, Dorte Dissing, Will Lentz, Pamela Odom, and Tony LaCortiglia. Review by Adrian Gall of ABR improved this report.

INTRODUCTION

BACKGROUND

The caribou monitoring study for the Alpine Satellite Development Program (ASDP) and Greater Moose's Tooth (GMT) Unit is being conducted on the Arctic Coastal Plain of northern Alaska in the northeastern portion of the National Petroleum Reserve–Alaska (NPRA) and the adjacent Colville River delta (Figure 1), an area that is used at various times of the year by two neighboring herds of barren-ground caribou (*Rangifer tarandus granti*)—the Teshekpuk Caribou Herd (TCH) and the Central Arctic Herd (CAH). The TCH generally ranges to the west and the CAH to the east of the Colville River delta (Person et al. 2007, Arthur and Del Vecchio 2009, Wilson et al. 2012, Parrett 2015a, Lenart 2015, Nicholson et al. 2016).

The TCH tends to remain on the coastal plain year-round. Most calving occurs around Teshekpuk Lake and the primary area of insect-relief habitat in midsummer is the swath of land between Teshekpuk Lake and the Beaufort Sea coast (Kelleyhouse 2001; Carroll et al. 2005; Parrett 2007, 2015a; Person et al. 2007; Yokel et al. 2009; Wilson et al. 2012). Since 2010, the calving distribution of the TCH has expanded, with some calving occurring as far west as the Ikpikpuk River and west of Atqasuk (Parrett 2015a; Prichard et al. 2019a).

Most TCH caribou winter on the Arctic Coastal Plain (hereafter, the coastal plain), generally west of the Colville River, although some caribou occasionally overwinter in the Brooks Range or with the Western Arctic Herd (WAH) in western Alaska (Carroll et al. 2005, Person et al. 2007, Parrett 2015a). In a highly unusual movement, many TCH animals wintered far to the east in the Arctic National Wildlife Refuge (ANWR) in 2003–2004 following an October rain-on-snow event (Carroll et al. 2004, Bieniek et al. 2019).

The TCH increased substantially in size from a few thousand animals in the mid-1970s, to 40,000+ in the early 1990s (Figure 2; Parrett 2015a). The TCH experienced a dip in numbers in the mid-1990s but increased steadily from 1995 to its peak estimated size of 68,932 animals in July 2008 (Parrett 2015a). The herd subsequently declined 19% by July 2011 when photocensus results estimated the herd at 55,704 animals (Parrett 2015a). Later photocensus results indicated the herd had decreased 30% from 2011 to 2013 to 39,172 animals but stabilized to 41,542 (SE = 3,486) by July 2015 and increased to a minimum of 56,255 by July 2017 (Klimstra 2018, Parrett 2015b). Although new higher-resolution digital photography introduced in 2017 may have contributed to higher population counts since 2015, the increase in estimated herd size indicates that the TCH has remained stable or increased since 2015.

Concentrated calving activity by the CAH tends to occur in two areas of the coastal plain, one located south and southwest of the Kuparuk oilfield and the other east of the Sagavanirktok River (Wolfe 2000, Arthur and Del Vecchio 2009, Lenart 2015, Nicholson et al. 2019). CAH caribou calving in the western area exhibit localized avoidance of the area within 2–5 km of active roads and pads during and for 2–3 weeks immediately after calving (Dau and Cameron 1986, Cameron et al. 1992, Lawhead et al. 2004, Johnson et al. 2020, Prichard et al. 2020a). The CAH typically moves to the Beaufort Sea coast during periods of mosquito harassment which generally begins in late June (White et al. 1975, Dau 1986, Lawhead 1988). The majority of the CAH winter in or south of the Brooks Range, predominantly east of the Dalton Highway/ Trans-Alaska Pipeline (TAPS) corridor (Arthur and Del Vecchio 2009, Lenart 2015, Nicholson et al. 2016), although many animals have remained north of the Brooks Range in the foothills or on the coastal plain in recent years (Prichard et al. 2019b, 2019c; E. Lenart, ADFG, pers. comm.).

From the early 1970s to 2002, the CAH grew at an overall rate of 7% per year (Figure 2; Lenart 2009). The herd grew rapidly from ~5,000 animals in the mid-1970s to the early 1990s, reaching a minimum count of 23,444 caribou in July 1992 before declining 23% to a minimum count of 18,100 caribou in July 1995, similar to the decline observed in the TCH during that period. The herd then increased to an estimated 68,442 animals in July 2010 (Lenart 2015). The herd subsequently declined to an estimated 50,753 animals by July 2013 (Lenart 2015) and 22,630 animals by July

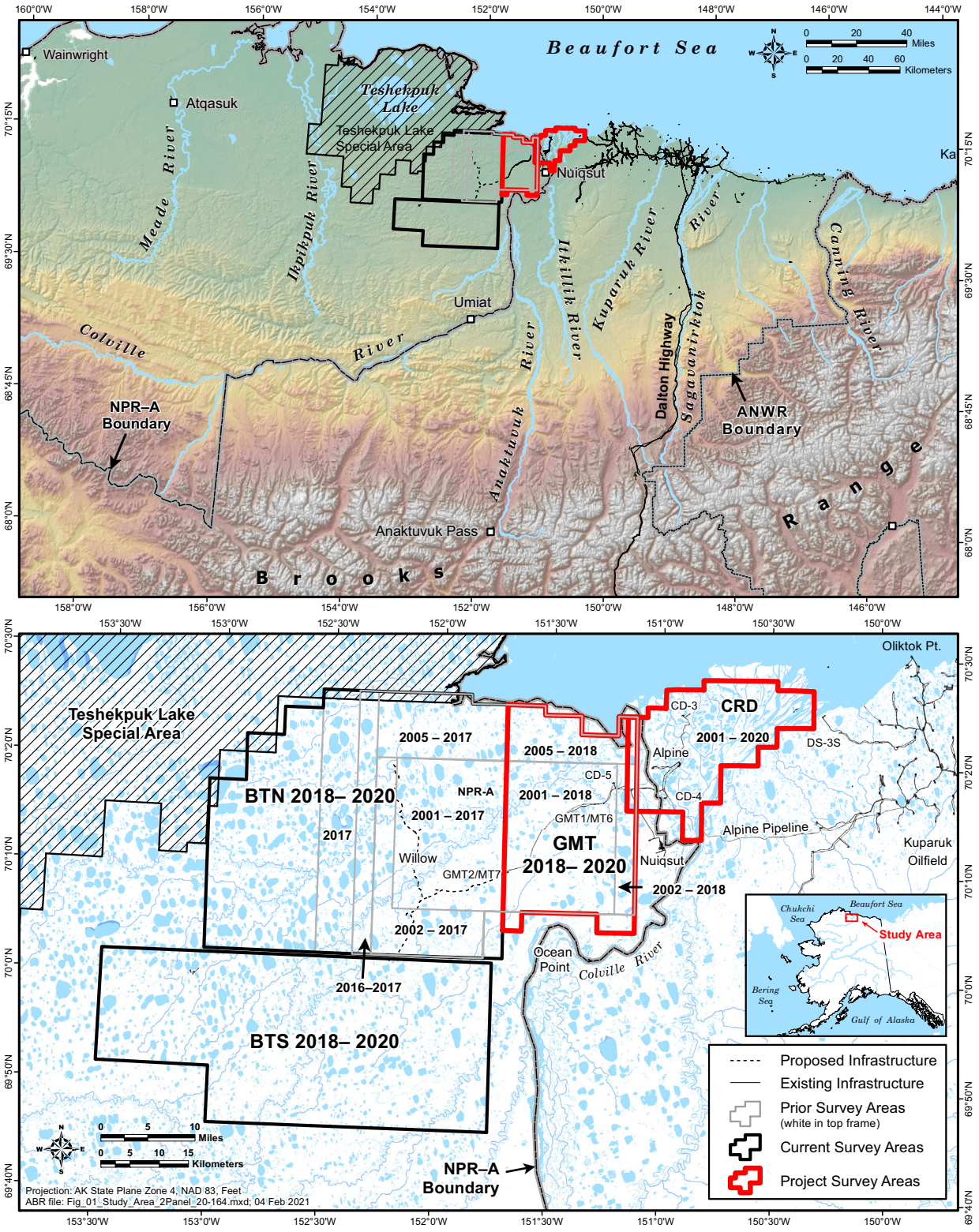

Figure 1. Location of the caribou monitoring study area on the central North Slope of Alaska and detailed view showing locations of the GMT and Colville River Delta survey areas, 2001–2020.

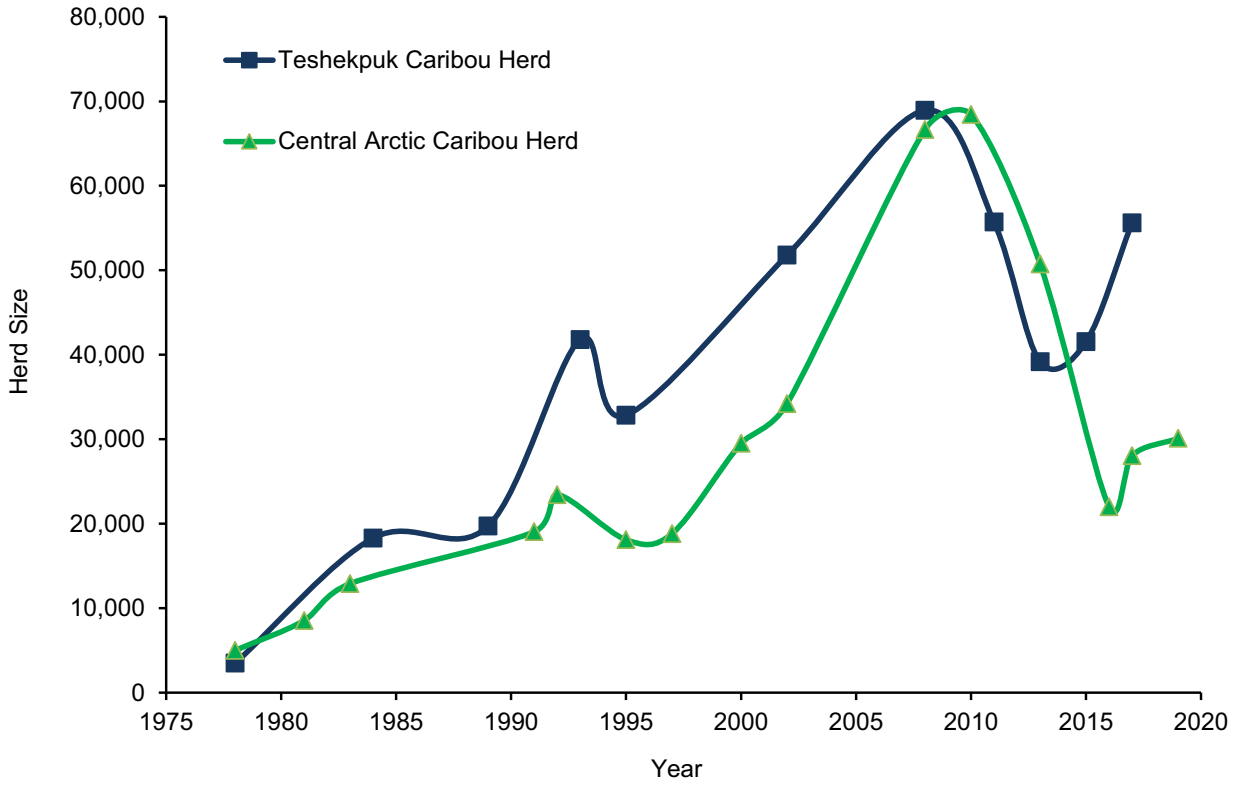

Figure 2. Population size of the Teshekpuk and Central Arctic caribou herds, 1975–2020, based on Alaska Department of Fish and Game census estimates (see text for details).

2016 (Lenart 2017) but increased to 30,069 by July 2019 (Lenart 2019). The magnitude of the decline from 2013 to 2016 may have been affected by emigration of some CAH animals to the Porcupine Caribou Herd (PCH) and the TCH, with which the CAH often intermixes on winter range (ADFG 2017, Prichard et al. 2020b).

This monitoring study builds on prior research funded by ConocoPhillips Alaska, Inc., (CPAI) and its heritage companies Phillips Alaska, Inc., and ARCO Alaska, Inc., that was conducted on the Colville River delta and adjacent coastal plain east of the delta (Alpine transportation corridor) beginning in 1992 and in the northeastern portion of the NPRA beginning in 1999 (Johnson et al. 2015; Jorgenson et al. 1997, 2003, 2004). Since 1990, contemporaneous, collaborative telemetry studies of caribou distribution and movements have been conducted in the region west of the Colville River by ADFG, the North Slope Borough (NSB), and the Bureau of Land Management (BLM) (Philo et al. 1993, Carroll et al. 2005, Person et al. 2007, Wilson et al. 2012, Parrett 2015a, Prichard et al. 2019b, 2019c). Consultants working for BP Exploration (Alaska), Inc., conducted aerial transect surveys over much of the TCH calving grounds during 1998–2001 (Noel 1999, 2000; Jensen and Noel 2002; Noel and George 2003).

STUDY OBJECTIVES

Evaluation of the natural and anthropogenic factors affecting caribou in the study area fall into two broad categories: those affecting movements of individuals and those affecting distribution of herds. Clearly, these categories are linked and are not mutually exclusive, but the applicability of study methods differs between them. Information on the potential effects of development on caribou distribution can be collected using a variety of methods, including aerial transect surveys, radio telemetry, time-lapse cameras, and observations by

local subsistence users. Information about the potential effects on caribou movements, however, cannot be addressed adequately without employing methods such as radio telemetry that allow consistent tracking of individually identifiable animals.

Several broad objectives were identified for study:

1. Evaluate the seasonal distribution, abundance, and movements of caribou in the study area, using a combination of historical and current data sets from aerial transect surveys and radio telemetry data obtained for this study and from ADFG under a cooperative agreement. Specific questions included:
    a) Which herds use the study area?
    b) How do patterns of seasonal use differ among herds?
2. Characterize important habitat conditions, such as snow cover, spatial pattern and timing of snowmelt, seasonal flooding (if possible), and estimated biomass of new vegetative growth in the study area by applying remote-sensing techniques.
3. Compare caribou distribution with habitat distribution, remote-sensing data, and other landscape features to better understand factors influencing the seasonal distribution of caribou and evaluate the potential impacts of new development.
4. Record and summarize observations of other large mammals in the study area.

STUDY AREA

CPAI began funding caribou surveys in the northeastern NPRA in 2001–2004. These studies continued during 2005–2014 under the North Slope Borough (NSB) Amended Development Permit 04-117 stipulation for the CD-4 drill site project (constructed during winter 2004–2005) which called for a 10-year study of the effects of development on caribou. The study area was specified as the area within a 48-km (30-mi) radius around the CD-4 drill site (Lawhead et al. 2015). Initially, aerial transect surveys were conducted in 3 survey areas which encompassed most of that 48-km radius (Lawhead et al. 2015): the NPRA survey area (expanded from 988 km² in 2001 to 1,310 km² in 2002; 1,720 km² in 2005); the Colville River Delta (CRD) survey area that encompasses CD-1 through CD-4 (494 km²); and the Colville East survey area (1,432–1,938 km², depending on the survey and year). Although 2014 was the tenth year of study, the NSB required continued studies for the GMT2/MT7 rezoning process. In 2016, the study area was redefined to focus on the NPRA and CRD survey areas, so results for the final year of aerial surveys in the Colville East survey area were reported elsewhere (Prichard et al. 2018a). In 2016 and 2017, the NPRA survey area was expanded westward by 1 and 2 transects, respectively (1,818 km² in 2016; 2,119 km² in 2017). In November 2018, the North Slope Borough adopted Ordinance Serial No. 75-06-72, consolidating previous ordinances and rezoning lands for the GMT2/MT7 area as resource development districts. This ordinance required CPAI to fund a caribou study to use "a landscape analysis to investigate the distribution and movements of caribou around the Colville River Delta adjacent areas including all Alpine and associated developments to assess habitat relationships and possible impacts from development."

In 2018, the NPRA survey area was therefore again redefined to focus on the three recently constructed drill sites,CD-5 constructed in the winter 2013–2014, GMT1/MT6 constructed in winter 2016–2017, and GMT2/MT7 constructed starting in winter 2018–2019 and continuing as of report publication, as well as their connecting access roads and pipelines (Figure 1, bottom panel). The newly defined Greater Mooses Tooth (GMT) survey area (776.6 km²) encompasses the portion of the previous NPRA survey area east of GMT2/MT7. It also includes the Nuiqsut Spur Road that was constructed by the Kuukpik Corporation in winter 2013–2014 to connect the village of Nuiqsut to the CD-5 access road. Although that road is not part of CPAI's infrastructure, its presence in the study area warrants its inclusion in this analysis.

The portion of the previous NPRA survey area west of GMT2/MT7, which includes the Willow prospect within the Bear Tooth Unit

(BTU), was expanded west and defined as the Bear Tooth North (BTN) survey area and the portion of the Bear Tooth Unit to the south of the Willow prospect was defined as the Bear Tooth South (BTS) survey area. Data from these two areas are reported elsewhere (Welch et al. *in prep.*). To provide a wider context to analytical results and avoid duplication, some of the analyses in this report were conducted for the combined survey areas (GMT, BTN, and BTS) and those results are included in both this report and the BTU report.

The study area is located on the central Arctic Coastal Plain of northern Alaska (Figure 1, top). The climate in the region is arctic maritime (Walker and Morgan 1964). The summer thaw period lasts about three months (June–August) and the mean summer air temperatures in Nuiqsut during 1990–2020 range from 6.2–9.9°C (43.2–49.9°F; http://climate.gi.alaska.edu/Climate/Normals, accessed 27 January 2020) with a strong regional gradient of summer temperatures increasing with distance inland from the coast (Brown et al. 1975). Mean summer precipitation is <8 cm (3.1 in), most of which falls as rain in August. The soils are underlain by permafrost and the temperature of the active layer of thawed soil above permafrost ranges from 0 to 10 °C (32–50 °F) during the growing season.

Spring is brief, lasting about 3 weeks from late May to mid-June, and is characterized by the flooding and break-up of rivers and smaller tundra streams. In late May, water from melting snow flows both over and under the ice on the Colville River, resulting in flooding on the Colville River delta that typically peaks during late May or the first week of June (Walker 1983). Break-up of the river ice usually occurs when floodwaters are at maximal levels. Water levels subsequently decrease throughout the summer, with the lowest levels occurring in late summer and fall, just before freeze-up (Walker 1983; annual hydrology reports to CPAI by Michael Baker Jr., Inc.). Summer weather is characterized by low precipitation, overcast skies, fog, and persistent northeasterly winds. The less common westerly winds often bring storms that are accompanied by high wind-driven tides and rain (Walker and Morgan 1964). Summer fog occurs more commonly at the coast and on the delta than it does farther inland.

METHODS

To evaluate the distribution and movements of TCH and CAH caribou in the study area in 2019, ABR biologists conducted aerial transect surveys, calculated remote sensing metrics from satellite imagery, and analyzed existing telemetry data sets provided by ADFG, NSB, BLM, and the U.S. Geological Survey (USGS), and from GPS collars funded by CPAI and deployed by ADFG specifically for this study in 2006–2010, 2013–2014, and 2016–2017. Most telemetry collars were scheduled to record one location every 2 hours during summer with less frequent locations during the winter; a typical collar deployment lasted 3 years.

Eight seasons per year were used for analysis of telemetry and aerial survey data, based on mean movement rates and observed timing of caribou life-history events (adapted from Russell et al. 1993 and Person et al. 2007): winter (1 December–30 April); spring migration (1–29 May); calving (30 May–15 June); postcalving (16–24 June); mosquito harassment (25 June–15 July); oestrid fly harassment (16 July–7 August, a period that also includes some mosquito harassment); late summer (8 August–15 September); and fall migration, a period that includes the breeding season, or rut (16 September–30 November).

WEATHER AND INSECT CONDITIONS

To estimate spring and summer weather conditions in the area during 2020, we used meteorological data from National Weather Service reporting stations at Kuparuk and Nuiqsut. Thawing degree-day sums (TDD; total daily degrees Celsius above zero) were calculated using average daily temperatures at the Kuparuk airstrip. Average index values of mosquito activity were estimated based on hourly temperatures from Nuiqsut using equations developed by Russell et al. (1993). The estimated probability of oestrid-fly activity was calculated from average hourly wind speeds and temperatures recorded at Nuiqsut using equations developed by Mörschel (1999).

CARIBOU DISTRIBUTION AND MOVEMENTS

AERIAL TRANSECT SURVEYS

Transect surveys provided information on the seasonal distribution and density of caribou in the study area. Surveys of the GMT and CRD survey areas (Figure 1, bottom) were conducted periodically from June to October 2020 in a fixed-wing airplane (Cessna 185 or 207), following the same procedures used since 2001 (ADFG permit number 20-094; Lawhead et al. 2015 and references therein). In 2020, seven aerial transect surveys in the GMT survey area were scheduled for mid-April (late winter), mid-May (spring migration), early June (calving), late June (postcalving), late July (oestrid fly), late August (late summer), and late September (fall migration). Surveys in the CRD survey area were scheduled for the postcalving, oestrid fly, and late summer seasons to correspond to seasons when caribou were most likely to be present based on previous aerial survey results and examination of available telemetry data. Due to the global coronavirus pandemic, April and May surveys were not conducted.

During all aerial surveys, 2 observers looked out opposite sides of the airplane. The pilot navigated the airplane along transect lines using a GPS receiver and maintained an altitude of ~150 m (500 ft) above ground level (agl). Transect lines were spaced at intervals of 3.2 km (2 mi), following section lines on USGS topographic maps (scale 1:63,360). Observers counted caribou within an 800-m-wide strip on each side of the airplane, thus sampling ~50% of the survey area on each survey. The number of caribou observed in the transect strips was therefore doubled to estimate the total number of caribou in the survey area. The strip width was delimited visually for the observers by placing tape markers on the struts and windows of the aircraft, as recommended by Pennycuick and Western (1972) or by measuring distances to recognizable landscape features displayed on maps in GPS receivers.

When caribou were observed within the transect strip, the perpendicular location on the transect centerline was recorded using a GPS receiver, the numbers of "large" caribou (adults and yearlings) and calves were recorded, and the perpendicular distance from the transect centerline was estimated in four 100-m or 200-m intervals, depending on the strip width. For plotting locations, the midpoint of the distance interval was used (e.g., 300 m for the 200–400-m interval). Thus, the maximal mapping error was estimated to be ~100 m. Confidence intervals for estimates of total caribou and calves were calculated with a standard error formula modified from Gasaway et al. (1986), using 3.2-km segments of the transects as the sample units.

DENSITY MAPPING

To map seasonal densities of caribou for the period 2002–2020, we used the inverse distance-weighted (IDW) interpolation technique of the *gstat* package (Pebesma 2004) in program *R* (R Core Team 2020). We conducted IDW calculations for all aerial survey data located within the current GMT and BTU survey areas, consistent with previous and contemporary reports (Prichard et al. 2019b, Welch et al. *in prep.*). Transect strips in the survey areas were subdivided into grid cells. Each grid cell was 1.6 km wide by 1.6 or 3.2 km long, depending on the transect length. We calculated density in each grid cell by dividing the total number of caribou observed in a grid cell on each survey by the land area in the grid cell. The best power (from 1 to 1.2) and the best number of adjacent centroids (from 10 to 24) to use in the calculations were selected based on the values that minimized the residual mean square error. This analysis produced color maps showing surface models of the estimated density of all caribou (large caribou plus calves) observed over the entire analysis area for each season.

RADIO TELEMETRY

Satellite Collars

Satellite (Platform Transmitter Terminal; PTT) telemetry used the Argos system (operated by CLS America, Inc.; CLS 2016) and locations were transferred monthly to the NSB for data archiving. Locations were transmitted either at 6 h/day for a month after deployment and then 6 h every other day throughout the year, or once every 6 days in winter and every other day during summer (Lawhead et al. 2015). The CAH satellite collars were programmed to operate 6 h/day or 6 h

every 2 days (Fancy et al. 1992, Lawhead et al. 2015).

Satellite-collar data were obtained from ADFG, NSB, and BLM for TCH animals during the period July 1990–November 2019 (Lawhead et al. 2006, 2007, 2008, 2009, 2010, 2011, 2012, 2013, 2014, 2015; Person et al. 2007; Prichard et al. 2017, 2018b, 2019c, this study) and for CAH caribou during the periods October 1986–July 1990 (from USGS), July 2001–September 2004, and April 2012–November 2019 (Cameron et al. 1989, Fancy et al. 1992, Lawhead et al. 2006, Lenart 2015; Table 1). In the TCH sample (based on herd affiliation at capture), 186 collars deployed on 166 different caribou (86 females, 80 males) transmitted signals for a mean duration of 571 days per collar. The CAH 1986–1990 sample included 17 caribou (16 females, 1 male). The CAH 2001–2004 and 2012–2020 deployment samples included 24 collars deployed on 24 caribou (16 females, 8 males), transmitting for a mean duration of 641 days per collar. Only collars that transmitted for >14 d were included in analysis. Satellite telemetry locations are considered accurate to within 0.5–1.0 km of the true locations (CLS 2016), but the data require screening to remove spurious locations (Lawhead et al. 2015).

GPS Collars

GPS collars purchased by BLM, NSB, ADFG, and CPAI (TGW-3680 GEN-III or TGW-4680 GEN-IV store-on-board configurations with Argos satellite uplink, manufactured by Telonics, Inc., Mesa, AZ) were deployed 317 times by ADFG biologists on 223 different TCH caribou (208 females, 15 males; Table 1) during 2004 and 2006–2020, with a mean deployment duration of 668 days. GPS collars (purchased by CPAI and ADFG) were deployed 182 times on 127 different female CAH caribou during 2003–2020, with a mean duration of 600 days. Only collars that transmitted for >14 d were included in analysis. Collars were programmed to record locations at 2-, 3-, 5-, or 8-h intervals, depending on the desired longevity of the collar (Arthur and Del Vecchio 2009, Lawhead et al. 2015).

GPS collars were deployed on female caribou, with the exception of 15 collars deployed on TCH males. Females are preferred for GPS collar deployment because the collar models used are subject to antenna problems when using the expandable collars that are required for male caribou due to increased neck size during the rut (Dick et al. 2013; C. Reindel, Telonics, pers. comm.). Caribou were captured by ADFG

Table 1. Number of TCH and CAH radio-collar deployments and total number of collared animals that provided movement data for the ASDP & GMT caribou study.

Herd [a] / Collar Type	Years	Female		Male		Total Deployments
		Deployments	Individuals	Deployments	Individuals	
Teshekpuk Herd						
VHF collars [b]	1980–2005	n/a		n/a		212
Satellite collars	1990–2020	97	86	89	80	186
GPS collars	2004–2020	299	208	18	15	317
Central Arctic Herd						
VHF collars [b]	1980–2005	n/a		n/a		412
Satellite collars	1986–1990	16		1		17
Satellite collars	2001–2004	10	10	2	2	12
Satellite collars	2012–2020	6	6	6	6	12
GPS collars	2003–2020	182	127	0	0	182

[a] Herd affiliation at time of capture.
[b] n/a = not available, but most collared animals were females.

personnel by firing a handheld net-gun from a Robinson R-44 piston-engine helicopter. In keeping with ADFG procedures for the region, no immobilizing drugs were used.

Data reports from Argos satellite uplinks were downloaded daily from CLS America, Inc., (Largo, MD) and the full dataset was downloaded after the collars were retrieved. Data were screened to remove spurious locations using methods described in Lawhead et al. (2015).

SEASONAL OCCURRENCE IN THE STUDY AREA

Seasonal use of the GMT and CRD survey areas was evaluated using two methods. The first method was to calculate the proportion of each monthly utilization distribution from kernel density estimation within the survey areas, by sex and herd, after first removing the portion of each seasonal utilization distribution contour that overlapped the ocean. The second method was to examine GPS- and satellite-collar data to describe movements of individual caribou in the immediate vicinity of existing ASDP infrastructure. All GPS-collared TCH segments were mapped to visualize movements in the study area. Then, to summarize crossings of the newly developed GMT1/MT6 and GMT2/MT7 roads, we also calculated the proportion of collared caribou that crossed each road during each season and year combination. Few collared CAH animals of either sex or TCH males were available for analysis, so we only summarized TCH females. Locations within 30 days of collaring were removed and animals with locations for less than half a season or fewer than 30 locations per season were excluded from analysis for that season.

To calculate kernels, we first calculated the mean location of each caribou for every 2-day period during the year. We used fixed-kernel density estimation in the *ks* package for *R* (Duong 2017) to create utilization distribution contours of caribou distribution for every 2-day period throughout the year (all years combined). We then calculated an average utilization distribution for each combination of season, herd, and sex. By calculating the average of utilization distribution based on the mean location for each animal we were able to account for movements within a season while not biasing the calculation due to autocorrelation among locations for a single caribou or due to unequal sample sizes among caribou. The plug-in method was used to calculate the bandwidth of the smoothing parameter. Because caribou are sexually segregated during some seasons, kernels were analyzed separately for females and males, although the sample size for male CAH caribou was insufficient to allow kernel density analysis. We also calculated a separate kernel for parturient TCH females during the calving season to delineate the calving range of the TCH.

To visualize caribou movements of caribou outfitted with GPS collars, we used dynamic Brownian Bridge Movement Models (dBBMM) to create utilization distribution maps of movements based on the locations of collared individuals (Kranstauber et al. 2014). These dBBMM models, a modification of earlier Brownian bridge models (Horne et al. 2007), use an animal's speed of movement and trajectory calculated from intermittent GPS locations to create a probability map describing relative use of the area traversed. We computed the 95% isopleth of movements for each individual TCH caribou outfitted with a GPS collar in the area and then overlaid the isopleth layers for each season to calculate the relative proportion of collared caribou using each 100-m pixel. This visualization displays the seasonal use of the area by TCH caribou as a function of both caribou distribution and movements. The dBBMM models were computed using the *move* package in *R* (Kranstauber et al. 2017).

REMOTE SENSING

The remote sensing methods are summarized here, a full description of remote sensing methods can be found in Appendix A. We analyzed 2020 snow cover and 2000–2020 vegetation greenness using gridded, daily reflectance and snow-cover products from MODIS Terra and Aqua sensors. The snow-cover data were added to the data compiled for 2000–2019 (see Lawhead et al. 2015 and Prichard et al. 2017 and 2018b for detailed description of methods). The entire vegetation index record, based on atmospherically corrected surface reflectance data, was processed to ensure comparability of greenness metrics.

SNOW COVER

Snow cover was estimated using the fractional snow algorithm developed by Salomonson and Appel (2004). A time series of images covering the April–June period was analyzed for each year during 2000–2020. Pixels with >50% water (or ice) cover were excluded from the analysis. For each pixel in each year, we identified:

- The first date with 50% or lower snow cover (i.e., "melted")
- The closest prior date with >50% snow cover (i.e., "snow")
- The midpoint between the last observed date with >50% snow cover and the first observed date with <50% snow cover, which is an unbiased estimate of the actual snowmelt date (the first date with <50% snow cover)
- The duration between the dates of the two satellite images with the last observed "snow" date and the first observed "melted" date, providing information on the uncertainty in the estimate of snowmelt date. When the time elapsed between those two dates exceeded one week because of extensive cloud cover or satellite sensor malfunction, the pixel was assigned to the "unknown" category.

VEGETATIVE BIOMASS

The Normalized Difference Vegetation Index (NDVI; Rouse et al. 1973) is used to estimate the biomass of green vegetation within a pixel of satellite imagery at the time of image acquisition (Rouse et al. 1973). The rate of increase in NDVI between two images acquired on different days during green-up has been hypothesized to represent the amount of new growth occurring during that time interval (Wolfe 2000, Kelleyhouse 2001, Griffith et al. 2002). NDVI is calculated as follows (Rouse et al. 1973; http://modis-atmos.gsfc.nasa.gov/NDVI/index.html):

$$NDVI = (NIR - VIS) \div (NIR + VIS)$$

where:

NIR = near-infrared reflectance (wavelength 0.841–0.876 μm for MODIS), and

VIS = visible light reflectance (wavelength 0.62–0.67 μm for MODIS).

NDVI during the calving period (NDVI_Calving) was calculated from a 10-day composite period (1–10 June) for each year during 2000–2020 (adequate cloud-free data were not available to calculate NDVI_Calving over the entire study area in some years). NDVI values near peak lactation (NDVI_621) were interpolated based on the linear change from two composite periods (15–21 June and 22–28 June) in each year. NDVI_Rate was calculated as the linear change in NDVI from NDVI_Calving to NDVI_621 for each year. Finally, NDVI_Peak was calculated from all imagery obtained between 21 June and 31 August each year during 2000–2020. Due to the availability of new forage models, NDVI_Calving, NDVI_621, NDVI_Rate, and NDVI_Peak were not included in analyses of caribou distribution in 2020, but we included summaries of these metrics in this report for comparison with previous reports.

FORAGE MODELING

We applied forage models from Johnson et al. (2018) that incorporate daily NDVI values as well as habitat type, distance to coast, and days from peak NDVI to predict biomass, nitrogen, and digestible energy for a given location on a given day. These models may provide metrics that are more directly related to caribou forage needs than NDVI alone.

Johnson et al. (2018) calibrated the forage models for 4 broad vegetation classes (tussock tundra, dwarf shrub, herbaceous mesic, and herbaceous wet). Following their approach, we used the Alaska Center for Conservation Science (ACCS) land cover map for Northern, Western, and Interior Alaska (Boggs et al. 2016), aggregated on the "Coarse_LC" attribute. This map is based on the North Slope Science Initiative (NSSI 2013) with the addition of the aggregation field. We calculated the modal land cover class for each 500-m pixel.

Snow water equivalent (SWE) estimates were obtained from the Daymet Version 3 model output data (Thornton et al. 2016). This model provided gridded estimates of daily weather parameters for North America and Hawaii at 1 km resolution. SWE was extracted based on the location and date.

For each date from the start of the calving season through the end of the late summer season (30 May–15 September) and for each year with telemetry locations (2002–2020) we mapped NDVI, annual NDVIMax, and days to NDVIMax. Then, we applied the equations from Johnson et al. (2018) to calculate forage nitrogen content and forage biomass for the 4 broad vegetation classes.

HABITAT CLASSIFICATION

We used the NPRA earth-cover classification created by BLM and Ducks Unlimited (2002; Figure 3) to classify habitats for analyses. The NPRA survey area contained 15 cover classes from the NPRA earth-cover classification (Appendix B), which we lumped into nine types to analyze caribou habitat use. The barren ground/other, dunes/dry sand, low shrub, and sparsely vegetated classes, which mostly occurred along Fish and Judy creeks, were combined into a single riverine habitat type. The two flooded-tundra classes were combined as flooded tundra and the clear-water, turbid-water, and *Arctophila fulv*a classes were combined into a single water type; these largely aquatic types are used very little by caribou, so the water type was excluded from the analysis of habitat preference.

Some previous reports (e.g., Lawhead et al. 2015) used a land-cover map created by Ducks Unlimited for the North Slope Science Initiative (NSSI 2013); however, discontinuities in classification methodology and imagery bisected our survey area and potentially resulted in land-cover classification differences in different portions of the survey area, and so we reverted to the BLM and Ducks Unlimited (2002) classification instead.

SPECIES DISTRIBUTION MODELING

GENERAL SUITABILITY

We fit a relationship between caribou group locations and a suite of environmental predictors that characterized weather, habitat, and topography. In previous years, we used resource selection function (RSF) models to evaluate relationships between caribou locations and explanatory variables. While still a highly valid method, RSFs are limited by the number of predictor variables and model complexity that can be incorporated into the model. Therefore, we decided to model relationships between environmental covariates and caribou distribution using the Maxent Java application (Phillips et al. 2020). Maxent is one of the most commonly used methods for computing species distribution models due to its ease of use and its predictive performance relative to other methods, especially with small sample sizes (Elith et al. 2006, Phillips et al. 2006, Warren and Seifert 2011, Merow et al. 2013). Maxent uses presence-only data and environmental variables to model a relative environmental probability distribution (suitability) across a landscape using a maximum entropy model framework (Phillips et al. 2006). Maxent is a commonly used data mining technique that compares complex combinations of variables, variable transformations, and multiple variable interactions to find the best model for predicting the distribution of training and test data (Phillips et al. 2006, Elith et al. 2011, Merow et al. 2013, Phillips et al. 2017). Because this is a data mining method, the emphasis is modeling predictions (mainly maps). As a result, the reported relationships between caribou distribution and environmental variables are more likely to be due to spatial correlation rather than causal relationships when compared to methods like RSF. However, Maxent provides tools for evaluating model performance and validity, variable contributions and relationships, and species distribution model (SDM) maps for investigation.

We used the same method for selecting caribou location data for Maxent as we did for the previously used RSF models (Prichard and Welch 2020, Prichard et al. 2020c). We included group locations from aerial surveys and locations from GPS-collared individuals. Locations from animals outfitted with satellite-collars (PTT) were not used in these analyses due to the lower accuracy of locations from those collars. We used caribou locations from aerial transect surveys conducted during 2002–2020 in the BTN, BTS, and GMT combined survey areas, but the seasonal sample sizes for the CRD survey area were too small to

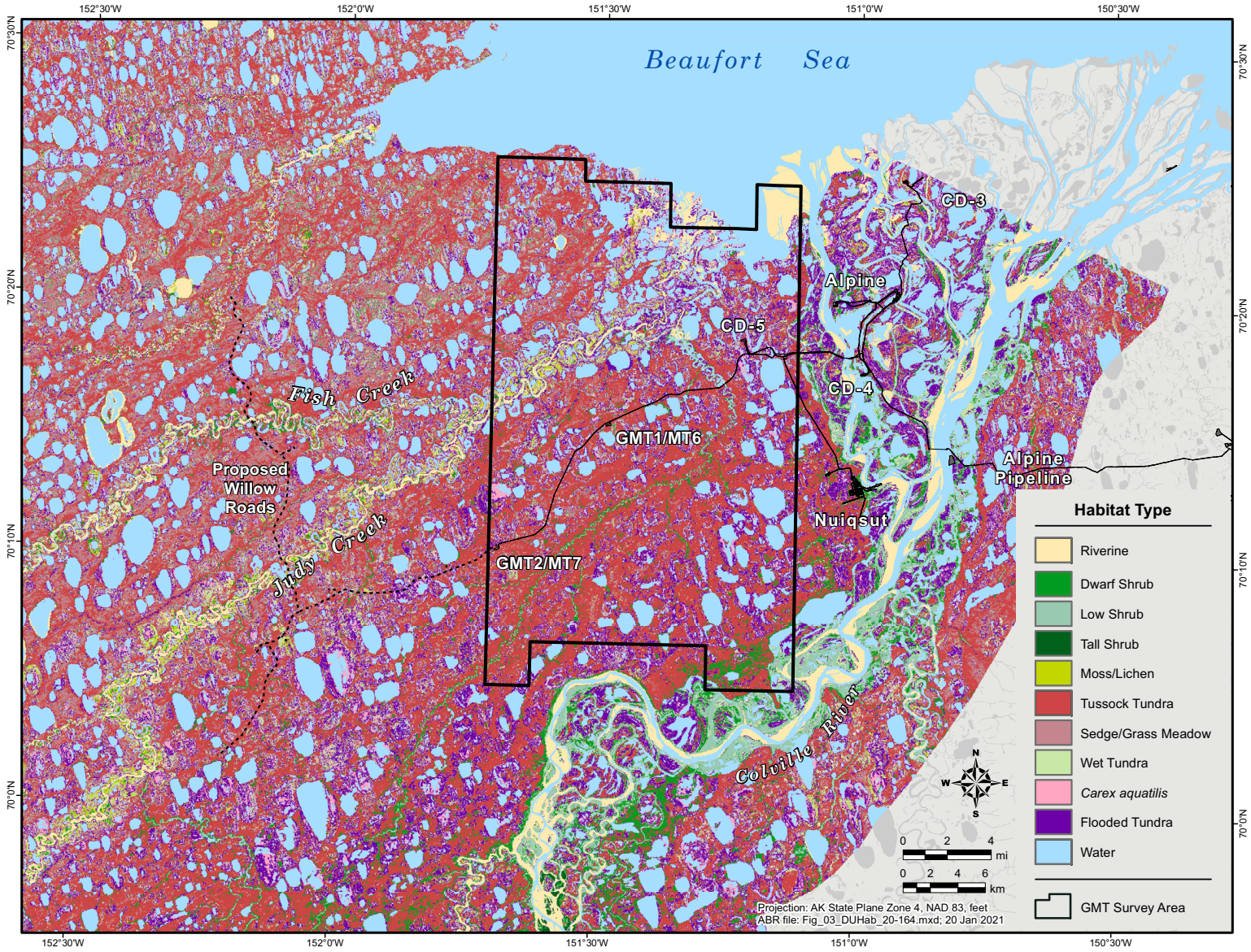

Figure 3. Habitat types used for caribou habitat-selection analysis in the NPRA survey area (adapted from BLM and Ducks Unlimited 2002).

support analysis. The available GPS-collar data spanned the period 11 May 2003–30 December 2020 and were filtered to include only locations falling within the aerial survey area. We subsampled GPS locations at 48-h intervals in all seasons to standardize the time between GPS-collar locations, maintain an adequate sample size, and reduce the effect of autocorrelation on results (Lair 1987, McNay et al. 1994). We assumed that 48 h was enough time for a caribou to move across the entire study area, thereby minimizing autocorrelation. We excluded caribou locations in waterbodies on the habitat map and in areas that were excluded from the NDVI calculations because they were predominantly water-covered.

For each actual caribou or caribou group location, we generated 25 random locations in non-water habitats within the same survey area as the actual location. We were therefore testing for selection at the level of specific areas or attributes for animals that were within the survey area. For this analysis we use the terms "selection" and "avoidance" to refer to attributes that are used more than expected or less than expected by caribou, when compared with random points.

We ran seasonal models to compare actual caribou locations to random locations using the following explanatory variables: habitat type (merged into the eight non-water categories; Figure 3), mean annual precipitation (MAP; Crookston and Rehfeldt 2010), degree-days greater than 5 °C (DD5; Crookston and Rehfeldt 2010), annual moisture index (AMI; Dunk et al. 2019), elevation, aspect (categorical variable with 8 directions and flat), slope, local elevational difference (LED; Dunk et al. 2019), topographic position index (TPI; Jenness et al. 2013), terrain ruggedness index (TRI; Wilson et al. 2007), topographic ruggedness index (TRI2; Riley et al. 1999), topographic wetness index (TWI; Theobald 2011) and flat and gentle sloping landforms (Theobald 2011).

AMI was calculated as the ratio of the square root of (DD5)/MAP, LED was calculated as the difference between the elevation of a pixel and the minimum elevation within a 27 pixel radius, TPI compares the elevation of each pixel to the mean elevation of cells within a defined radius. High TPI values indicate that a pixel has a high elevation relative to adjacent pixels (e.g., ridgetops), TRI was calculated as the mean of the absolute difference between the elevation of a pixel and the elevation of the 8 pixels surrounding it, TRI2 was calculated as the standard deviation of the elevation within a 3x3 rectangular window centered on a pixel, and TWI represents the relative water accumulation potential based on factors related to slope and hillshade. Because the spatial scale that caribou may select these features is unknown, we calculated these variables at 5 different spatial scales. Mean proportions of each variable were calculated at the 120 m scale using the Aggregate Tool and at the 0.5 km, 1.0 km, 2.0 km, and 3.2 km scales using the Focal Statistics Tool in ArcGIS Pro.

Additionally, we used daily NDVI, daily nitrogen, daily biomass, maximum NDVI, and daily snow water equivalent (SWE) at each location and time used in the analysis. These we calculated based on 500-m pixels. We calculated landscape ruggedness (Sappington et al. 2007) over a 150-m by 150-m box centered at each 30-m pixel. The median snow-free date (date at which the pixel is typically snow-free [Macander et al. 2015]), distance to coast, and west-to-east distribution were calculated for each location used in the analysis. Because of the different seasonal importance of these variables, the median snow-free date was used only for the winter, spring migration, and calving seasons, SWE was only used for the winter and spring migration seasons, and daily NDVI, nitrogen, and biomass variables were used only for the snow-free seasons (calving, postcalving, mosquito, oestrid fly, and late summer seasons).

While Maxent is computationally capable of handling many model coefficients that may be highly correlated (Elith et al. 2011, Phillips et al. 2017), high levels of correlation among variables can limit the ability to interpret the influence of specific variables and it is recommended to remove highly correlated variables (Merow et al. 2013). We therefore used a two-step process to reduce the number of variables, simplify the model, and aid in interpretation. In the first step, we selected a single spatial scale for each variable. For each season, we first calculated the test-ratio, the ratio of the mean values of environmental variables at caribou group locations to the mean of the randomly generated background locations, at each of the 5 spatial

scales. A large test ratio indicates that the values of that variable are more different at locations used by caribou compared to random locations and therefore, suggests some selection of that variable by caribou. For each variable, we only retained the spatial scale with the largest test ratio (Dunk et al. 2019). This produced the scale-defined variable dataset (one spatial scale for each variable). For the second stage of variable selection, we removed highly correlated variables. We categorized variables into three groups: weather, habitat, and topography. We then calculated the Variance Inflation Factor (VIF) for all variables within each of these categories and removed variables with VIF values >5. Once inter-category VIFs were <5, we calculated the VIFs for all remaining variables combined and used a relaxed threshold. We removed variables if the VIF > 10. The relaxed VIF threshold was a compromise to retain variables while still minimizing the amount of correlation among variables. All calculations were performed in R (R version 4.0.2, R Core Team 2020) using the 'usdm' and 'raster' packages (Hijmans 2020, Naimi et al. 2014).

After determining the set of explanatory variables to be used, we ran the Maxent models for each season individually. By default, Maxent automatically generates background points from within a single study area, which does not work for this analysis because our random locations are drawn from within the bounds of multiple survey areas. Therefore, we used the samples-with-data (SWD) method in Maxent where the user supplies datasets with environmental data already extracted for both used and random points (Phillips 2017). We allowed Maxent to automatically choose among linear, quadratic, product (interactions), hinge (similar to splines), and categorical forms of variables and allowed Maxent to use locations with some missing values of explanatory variables. Hinges can be applied multiple times to the same function, providing for a very flexible framework to model relationships in the data (Elith et al. 2011). We used 1,000 maximum iterations and allowed samples with some NULL values to be included. All other settings were left at default.

Ideally, the Maxent model will fit the training data well but also generalize outside of sampled locations (Phillips et al 2006). To avoid overfitting the training data, Maxent employs L1 regularization to constrain modeled distributions to lie within a certain interval around the empirical mean rather than matching it exactly (Phillips et al. 2006, Warren and Seifert 2011, Merow et al. 2013). Maxent allows users to vary the constant regularization multiplier (RM) that penalizes all parameters to reduce over-fitting and shrinks coefficients towards or to zero, thus reducing the number of parameters in the model. Lower values of the RM can lead to overly complicated models, overparameterization, and overfitting, while values that are too high can lead to overly simplified models that overpredict suitability (Cao et al. 2013). The Maxent default value of 1 has been optimized to best balance between overfitting and overgeneralizing the data and was based on a dataset from 226 species from 6 regions around the world (Phillips and Dudik 2008, Elith et al. 2006). However, models using this default value sometimes overfit the training data or can be overly simplistic (Anderson and Gonzalez 2011, Warren and Seifert 2011, Cao et al. 2013, Merrow et al. 2013, Radosavljevic and Anderson 2014). Many different researchers have investigated the best method for optimizing the RM (Warren and Seifert 2011, Cao et al. 2013, Radosavljevic and Anderson 2014, Galante et al. 2018).

For all models, Maxent provides receiver operating characteristic (ROC) curves with an associated area under the curve (AUC) that can be used to assess model performance (Phillips 2017). We chose to use the AUC value of withheld test data (AUCtest) as a metric to optimize the RM value as described in Warren and Seifert (2011) because this metric performed very well when sample sizes are large (>1,000 locations), which was often the case with our analyses. We therefore ran our models with RMs of 0.75, 1, 2, 3, 4, 5, and 6 and chose the model with the highest AUCtest. We ran the initial models on a random selection of 80% of the data (training data) and used the remaining 20% of locations to independently assess the model performance (test data). Once the top model based on AUCtest was identified, the Maxent model was re-run with the best RM and 100% of the data for training.

To assess variable importance, Maxent calculates a permutation importance value for each variable in the model. The permutation importance value is equal to the drop in AUC the training data

(AUCtrain) when Maxent randomly changes the values of each variable in turn and re-runs the model. A large drop in AUCtrain indicates that the variable was important to overall performance. Maxent also provides response curves to show the relationship between each explanatory variable and the predicted suitability. These curves represent the effect of changing the values of one variable while holding all other variables in the model constant. AUC values from 0.7–0.8 are generally considered to acceptable model performance, 0.8–0.9 indicate excellent model performance, and >0.9 indicate outstanding model performance (Hosmer and Lemeshow 2000). Results of the model were mapped using the cloglog function (complimentary log-log), which is currently the best transformation for estimating the probability of presence (Fithian et al. 2015, Phillips et al. 2017).

In order to map the suitability results, we needed to use a consistent set of rasters for each season. Because some variables varied over time, we used the median values of daily NDVI, nitrogen, biomass, and SWE calculated at the midpoint of each season, median yearly maxNDVI, and the median date of snowmelt since 2002 as input variables for the suitability maps.

DISTRIBUTION AND INFRASTURCTURE

We used the SDM output from the seasonal analyses to model the potential impacts of infrastructure on caribou distribution. A second model for each season was built using just 2 variables: the suitability map from the initial SDM model; and the distance to roads/pads. The SDM variable represented the predicted suitability of each pixel across the landscape as estimated from the first Maxent model without a distance to roads variable. We then used distance to road/pad as a second variable to estimate the influence of distance to road after accounting for all of the other variables influencing caribou distribution. Including the distance to road/pad variable results in an estimate of how much this information improves the model. We limited our data to locations from 2019 and 2020 after all current roads in the GMT survey area were constructed. Because we were most interested in evaluating the potential impact to caribou near roads and pads, distances beyond 10 km were set to 10 km. Decline in caribou distribution near roads has been reported to occur within approximately 2–5 km during calving for the CAH (Dau et al. 1985, Dau and Cameron 1992, Lawhead et al. 2004, Johnson et al. 2020), therefore our maximum distance corresponds to twice the maximum expected area of decline.

OTHER MAMMALS

Observations of other large mammals were recorded during field surveys (both aerial and ground-based) for this and other wildlife studies conducted for CPAI. Observations in other survey areas were summarized in separate reports (Prichard and Welch. 2021, Welch et al. *in prep*.).

RESULTS

WEATHER CONDITIONS

Air temperatures in spring 2020 were near the 30-year average (1983–2020) and snow melted slightly earlier than usual at the Kuparuk airport (Figure 4, Appendix C). Approximately half of the snowpack melted during 9–10 May when temperatures reached 1.7 °C (35.0 °F). Snow depths of approximately 10 cm (3.9 in) persisted at the Kuparuk airstrip from 10–20 May but then declined to zero or trace level by 29 May when temperatures were again above freezing. Temperatures were variable during early and mid-June but were generally below average.

Summer weather conditions can be used to predict the occurrence of harassment by mosquitoes (*Aedes* spp.) and oestrid flies (warble fly *Hypoderma tarandi* and nose bot fly *Cephenemyia trompe*) (White et al. 1975, Fancy 1983, Dau 1986, Russell et al. 1993, Mörschel 1999, Yokel et al. 2009). Mosquitoes in the study area usually emerge from the middle of June through early July depending on the timing of snowmelt and temperatures, whereas oestrid flies usually do not emerge until mid-July. Daily air temperatures in mid-June were near average but predicted mosquito harassment did not exceed 50% in late June or early July (Figure 5) and only approached 50% on two days during this period. ABR biologists conducting ground-based surveys for other projects near the Colville River delta reported moderate mosquito activity starting around 25 June.

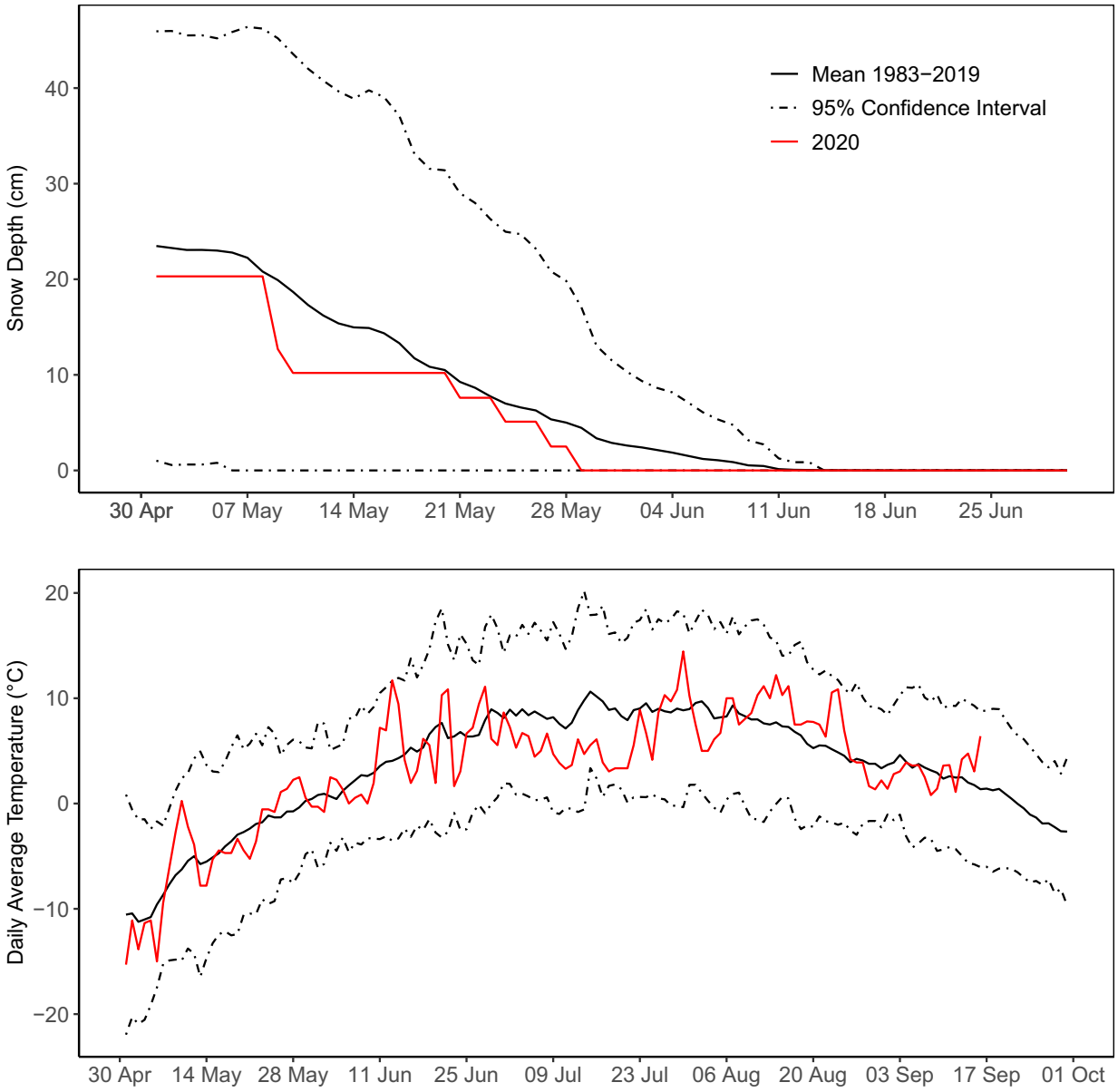

Figure 4. Snow depth at the Kuparuk airstrip during May–June 2020, compared with the long-term mean and 95% confidence interval (top panel) and daily average air temperature at Kuparuk during May–September 2020 compared with the long-term mean and 95% confidence interval (bottom panel).

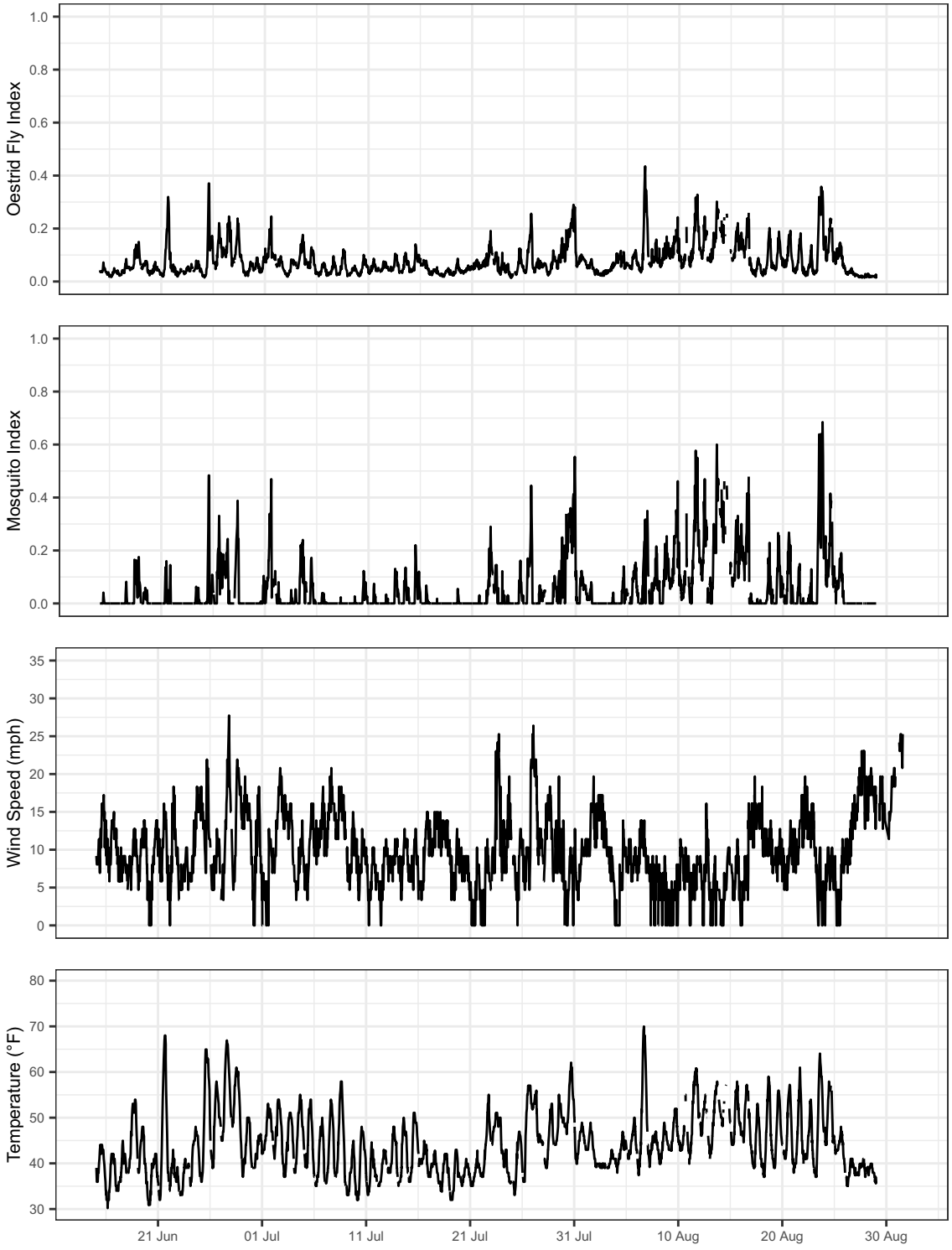

Figure 5. Hourly air temperature, wind speed, mosquito probability, and oestrid fly probability at Nuiqsut during 15 June–7 September 2020.

Weather conditions were generally not conducive to high insect activity during the remainder of the 2020 insect season. From June through early August strong winds (>10 mph) occurred frequently, and temperatures were often below average. Temperatures were generally above average for the remainder of August (Figure 4, Appendix C). This resulted in zero days with a high probability of oestrid fly harassment (>50% probability) and only 4 days with a high probability of mosquito harassment, although 3 of those days occurred in August when the severity of mosquito harassment is generally lower (Figure 5).

CARIBOU DISTRIBUTION AND MOVEMENTS

AERIAL TRANSECT SURVEYS

GMT Survey Area

Seven aerial surveys of the GMT survey area were planned between April and October 2020 (Figure 6), but 3 were cancelled and one was only partially completed. The winter and spring migration surveys were cancelled due to health concerns stemming from the emerging Covid-19 pandemic. We conducted surveys in June, with Covid-19 safety protocols in place, however the postcalving survey was conducted with only one aerial surveyor due to a non-Covid 19 illness and was limited by persistent fog in the area. The late July oestrid fly survey was cancelled due to concerns regarding high levels of subsistence hunting in the region by Nuiqsut residents.

The estimated density on the 5 partial or completed surveys ranged from a high of 0.56 caribou/km² on 19 June to a low of 0.05 caribou/km² on 27 August (Table 2, Figure 7). A total of 182 caribou (0.47 caribou/km²) were observed during the calving survey on 9–10 June, including 5 calves. Caribou density peaked on the postcalving survey on 19 June (0.56 caribou/km²), although no calves were seen. Caribou densities were reported to be high in the area during the late July period, but this resulted in high levels of subsistence hunting and cancellation of the survey. Densities declined to the lowest level of the year on the 27 August survey (0.05 caribou/km²) during the late summer season. The density of caribou then increased to a moderate density of 0.34 caribou/km² on the fall migration survey (6–7 October).

These results are within the normal seasonal ranges of caribou density observed in the GMT survey area since 2001 (Figure 7). Caribou densities tend to be highest during the fall, winter and postcalving seasons, moderate during the spring migration, calving, and late summer seasons, and lowest during the mosquito and oestrid fly seasons, although the densities during the mosquito and oestrid fly seasons can be highly variable with large groups of caribou occasionally present as occurred in 2005 when an estimated density of 19.68 caribou/km² was observed in the study area (not shown on Figure 7). In 2020, caribou densities followed these same trends, but with higher than average densities observed during June surveys.

Results from the seasonal IDW density mapping of caribou recorded on aerial surveys of the NPRA/GMT survey area during all years combined (2002–2020) also showed large differences among seasons (Figure 8). The highest mean density was observed during the oestrid fly season, but that density was strongly affected by several large groups that were observed in only one year (2005; 19.68 caribou/km²).

Colville River Delta Survey Area

Three surveys of the CRD survey area were scheduled for the postcalving, oestrid fly, and late summer seasons, but were not surveyed in other seasons due to low historical use of the Colville River delta during those periods (Figure 6, Table 2). The oestrid fly season survey was also cancelled due to high hunter activity in the area at the scheduled time of the survey. Similar to most surveys conducted in previous years, the estimated density of caribou was low on all surveys (0.07–0.17 caribou/km²) and only 4 calves were observed during the postcalving survey (Figure 6, Table 2).

RADIO TELEMETRY

Radio collars provide detailed location and movement data throughout the year for a small number of individual caribou. The telemetry data also provide valuable insight into herd affiliation and distribution, which is not available from transect surveys. Mapping of the telemetry data from satellite (PTT) and GPS collars clearly shows that the study area is located at the interface of the

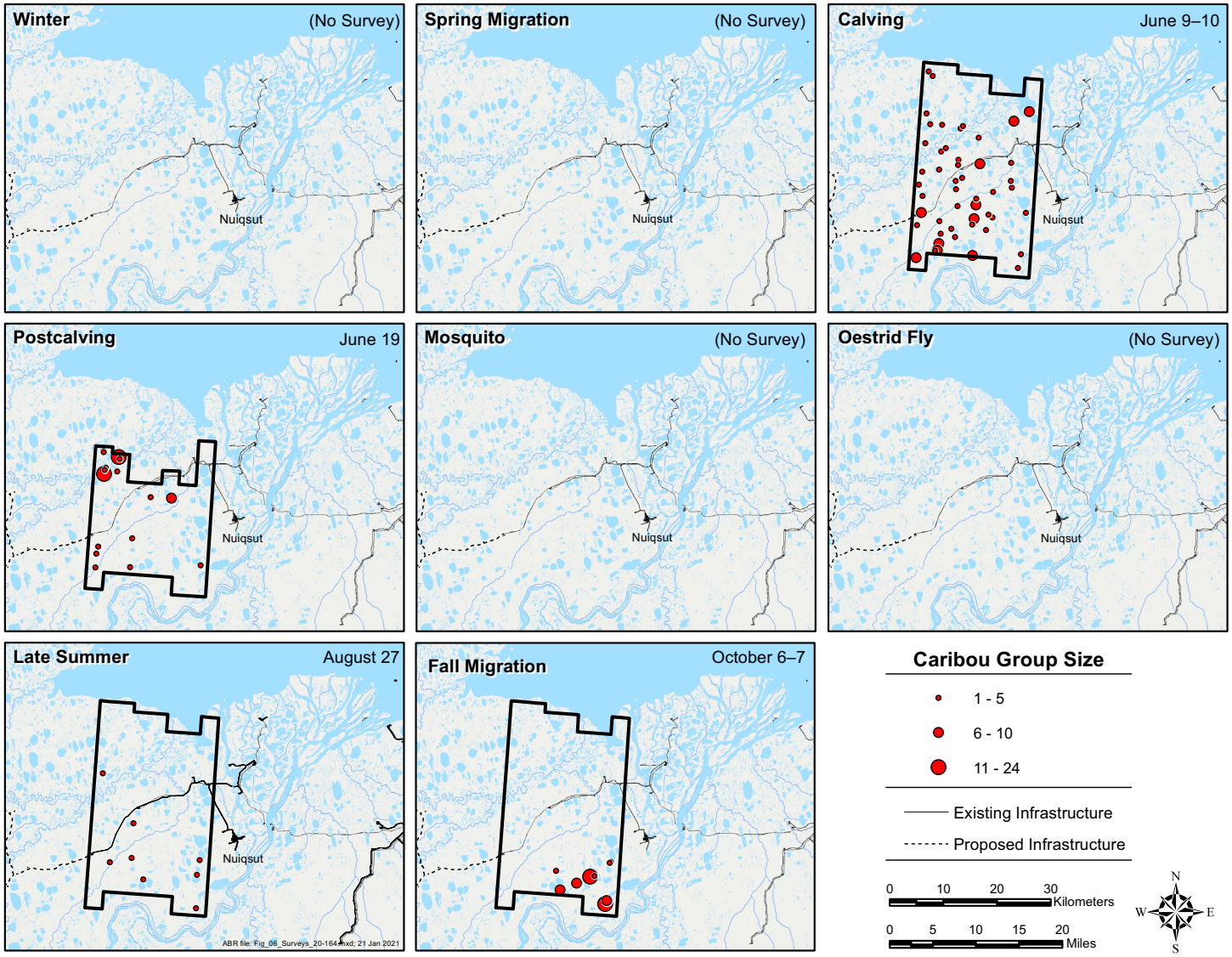

Figure 6. Distribution and size of caribou groups during different seasons in the GMT and Colville River Delta survey areas, June–October 2020.

Table 2. Number and density of caribou in the GMT and Colville River Delta survey areas, June–October 2020.

Survey Area and Date	Total Area [a]	Observed Large Caribou [b]	Observed Calves [c]	Observed Total Caribou	Mean Group Size [d]	Estimated Total Caribou [e]	SE [f]	Density (caribou/km²) [g]
GMT								
June 9–10	778	177	5	182	3.6	364	48.6	0.47
June 19	489 [h]	69	0	69	4.3	276	88.1	0.56
August 27	778	19	nr	19	2.4	38	12.9	0.05
October 6–7	778	71	nr	71	7.9	267 [i]	63.3 [i]	0.34 [i]
Colville River Delta								
June 15	494	37	4	41	4.1	82	28.8	0.17
August 27	494	17	nr	17	4.3	34	14.6	0.07

[a] Survey coverage was 50% of this area unless otherwise noted.
[b] Adults + yearlings.
[c] nr = not recorded; calves not differentiated reliably due to larger size.
[d] Mean Group Size = Observed Total Caribou ÷ number of caribou groups observed.
[e] Estimated Total Caribou = Observed Total Caribou × 2 (to adjust for 50% survey coverage).
[f] SE = Standard Error of Estimated Total Caribou, calculated following Gasaway et al. (1986), using transects as sample units.
[g] Density = Estimated Total Caribou ÷ Area.
[h] Survey coverage was 25% of this area.
[i] Applied a Sightability Correction Factor of 1.88 (Lawhead et al. 1994) to correct for low sightability due to patchy snow.

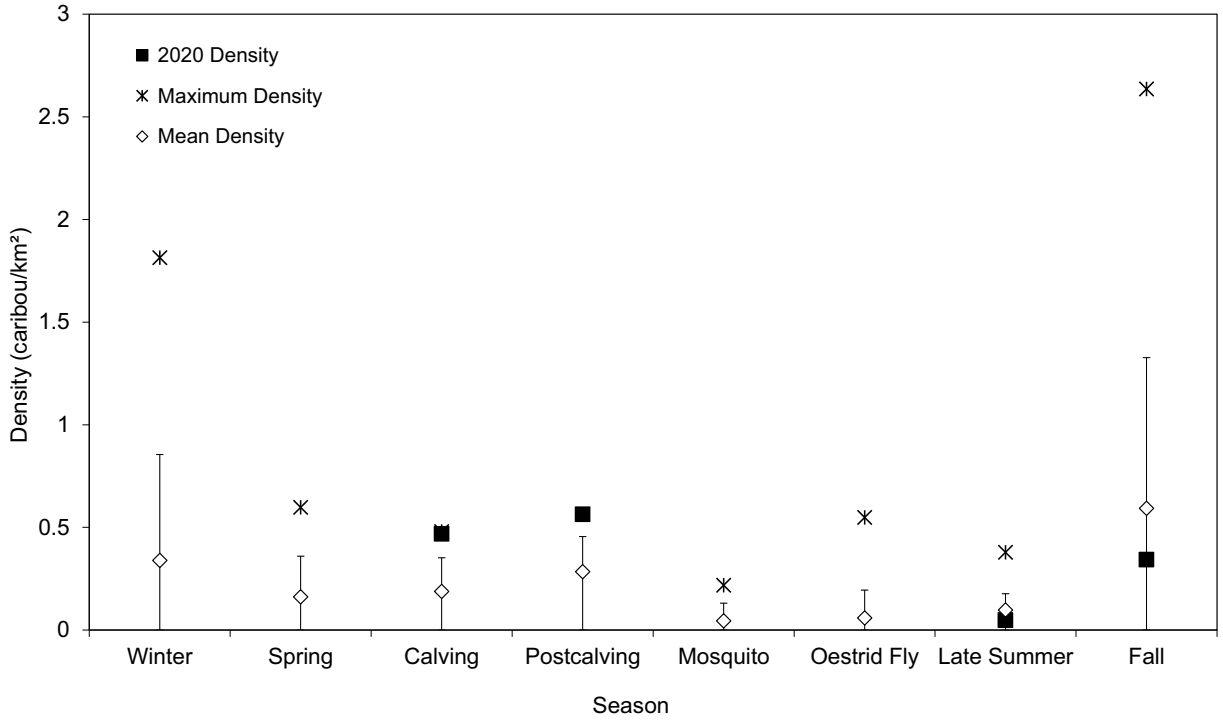

Figure 7. Seasonal density of caribou observed on 136 surveys of the GMT survey area, April–October 2001–2020. Error bars represent 95% confidence intervals. One oestrid fly survey with density 19.68 caribou/km² is not included.

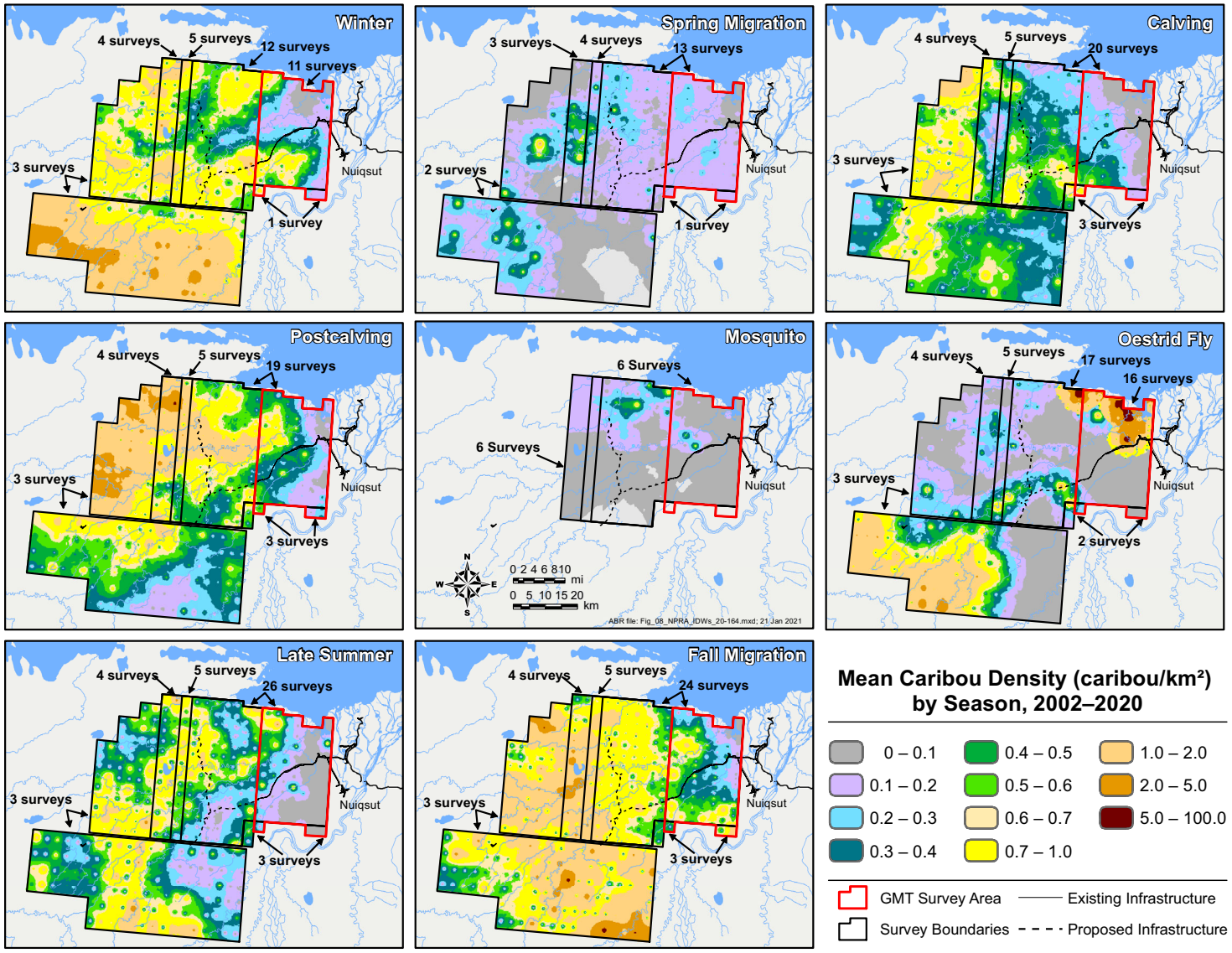

Figure 8. Seasonal density of caribou within the caribou survey areas based on IDW interpolation of aerial survey results, 2002–2020.

annual ranges of the TCH and CAH (Figures 9–10). The majority of collar locations for the TCH occurred west of the Colville River and most of the CAH occurred east of it. The composite satellite and GPS telemetry data demonstrate that, although collared TCH caribou use the study area to some extent in all seasons, use of the area peaks during the summer insect season (primarily oestrid fly season) and fall migration, followed closely by winter (Figures 9–10). The lowest level of use of the area by collared TCH caribou occurred during the spring migration, calving, and postcalving seasons.

TCH GPS Collars and dBBMMs

Mapping of TCH movements derived from the dBBMMs in the study area shows that TCH females use the GMT survey area during all seasons, although their use of the area and movement rates vary widely among seasons (Figure 11). During winter, caribou are distributed widely but show low rates of movement. During the spring migration and calving seasons, TCH females move across the study area from southeast to northwest as they migrate toward the core calving area near Teshekpuk Lake. During the postcalving and mosquito seasons, caribou largely remain west and north of the study area, often traversing the narrow corridors between Teshekpuk Lake and the ocean (Yokel et al. 2009). During the oestrid fly season, TCH females move rapidly and often tend to disperse inland away from Teshekpuk Lake with occasional large movements through the GMT survey area and some movements onto the Colville River delta. During late summer, caribou are usually found dispersed inland to the west of the GMT survey area. TCH caribou disperse widely during fall migration, including movements throughout much of the GMT survey area. The Colville River delta is used little by the TCH during all seasons (Figure 11).

KERNEL DENSITY ANALYSIS

Seasonal herd distributions were estimated using fixed-kernel density estimation, based on caribou locations from satellite and GPS collars deployed on 273 TCH females and 90 TCH males during 1990–2020 and on 138 CAH females and 8 CAH males during 2001–2020. These numbers differ from the number of collar deployments listed earlier (Table 1) because some individuals switched herds after collaring. Kernels were used to produce 50%, 75%, and 95% utilization distribution contours (isopleths), which were assumed to correspond to density classes (high, medium, and low density) for female CAH caribou and for male and female TCH caribou (Figures 12–14); the sample size of CAH males was too small to conduct this analysis for males separately. Although these analyses use data covering 20–30 years, the results are more heavily weighted for more recent years when more collars were deployed.

Female CAH caribou generally wintered between the Dalton Highway/TAPS corridor and Arctic Village, although in recent years more wintering has occurred on the north side of the Brooks Range. They then migrated north in the spring to calve in two areas on either side of the Sagavanirktok River/TAPS corridor. They spent the mosquito season near the coast and were widely dispersed across the central coastal plain on both sides of the Sagavanirktok River and Dalton Highway/TAPS corridor during the oestrid fly and late summer seasons (Figure 12). During fall migration, many collared CAH caribou crossed the Dalton Highway to return to the wintering areas.

TCH caribou generally wintered on the coastal plain between Nuiqsut and Wainwright or in the central Brooks Range near Anaktuvuk Pass, migrated to their calving grounds near Teshekpuk Lake, and spent the rest of the summer on the coastal plain, primarily between Nuiqsut and Atqasuk (Figures 13–14). Compared with females, males were more likely to overwinter in the central Brooks Range instead of on the coastal plain. They also migrated to the summer range later and were generally not distributed as far west during summer (Figures 13–14). The distribution of parturient TCH females during calving was similar to the distribution of all TCH females during calving but was more concentrated near Teshekpuk Lake (Figure 15).

Examination of the proportion of kernel densities by month showed that use of the CRD survey area by collared animals was low for both CAH and TCH caribou during the entire year (<2% of the utilization distribution) with the highest use by CAH females during the insect season (1.5% of the utilization distribution; Figure 16). Use of the

Page intentionally left blank.

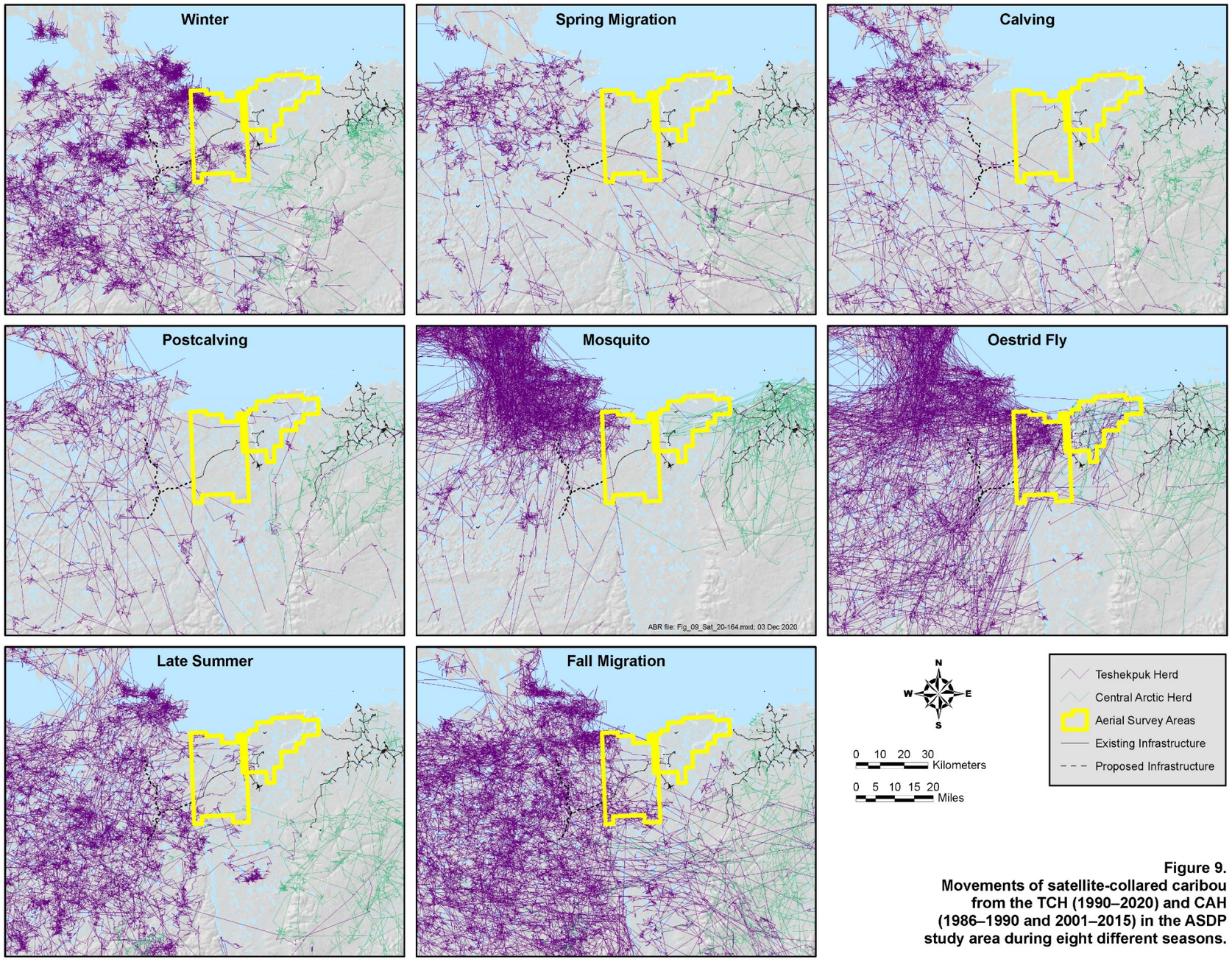

Figure 9.
Movements of satellite-collared caribou from the TCH (1990–2020) and CAH (1986–1990 and 2001–2015) in the ASDP study area during eight different seasons.

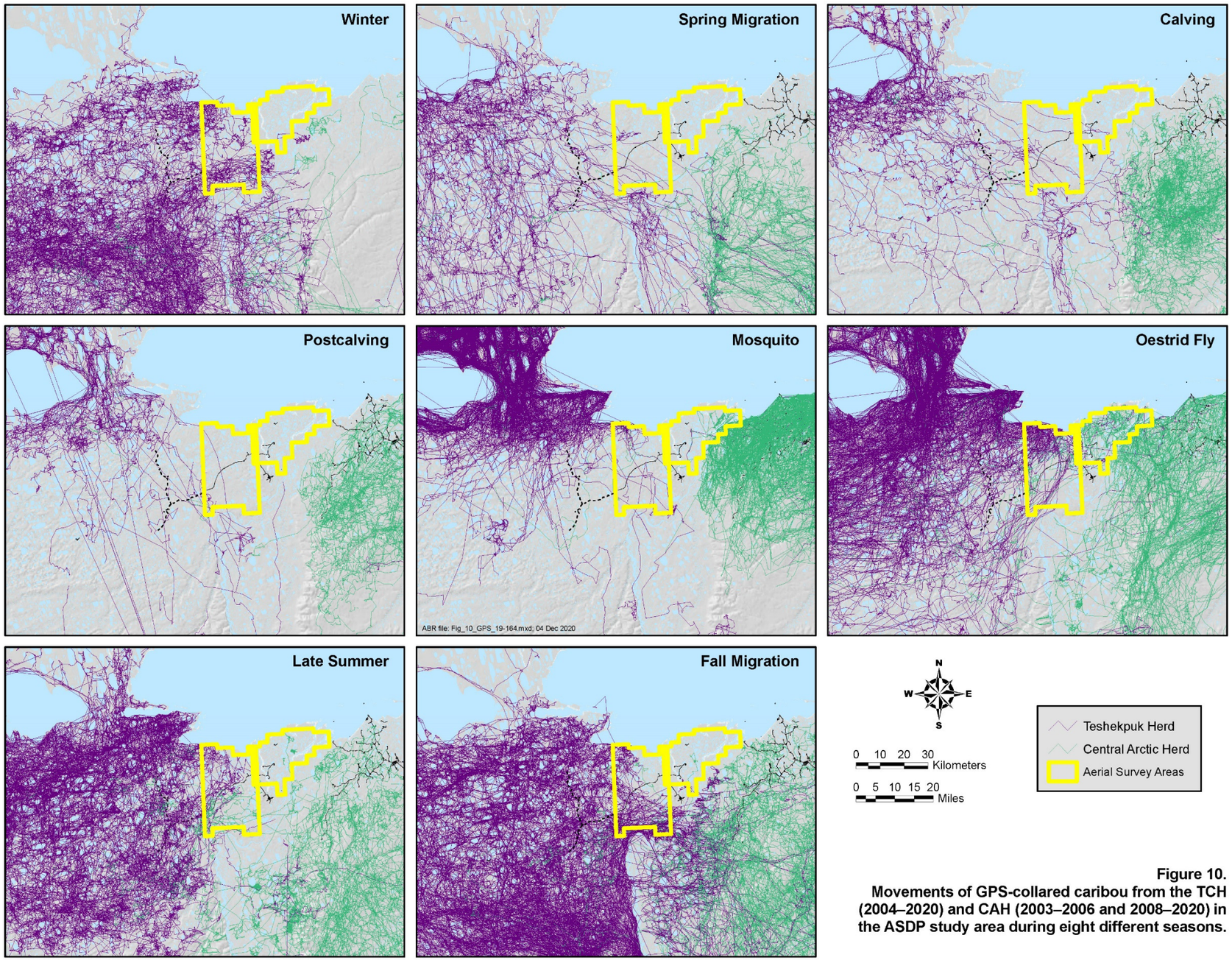

Figure 10.
Movements of GPS-collared caribou from the TCH (2004–2020) and CAH (2003–2006 and 2008–2020) in the ASDP study area during eight different seasons.

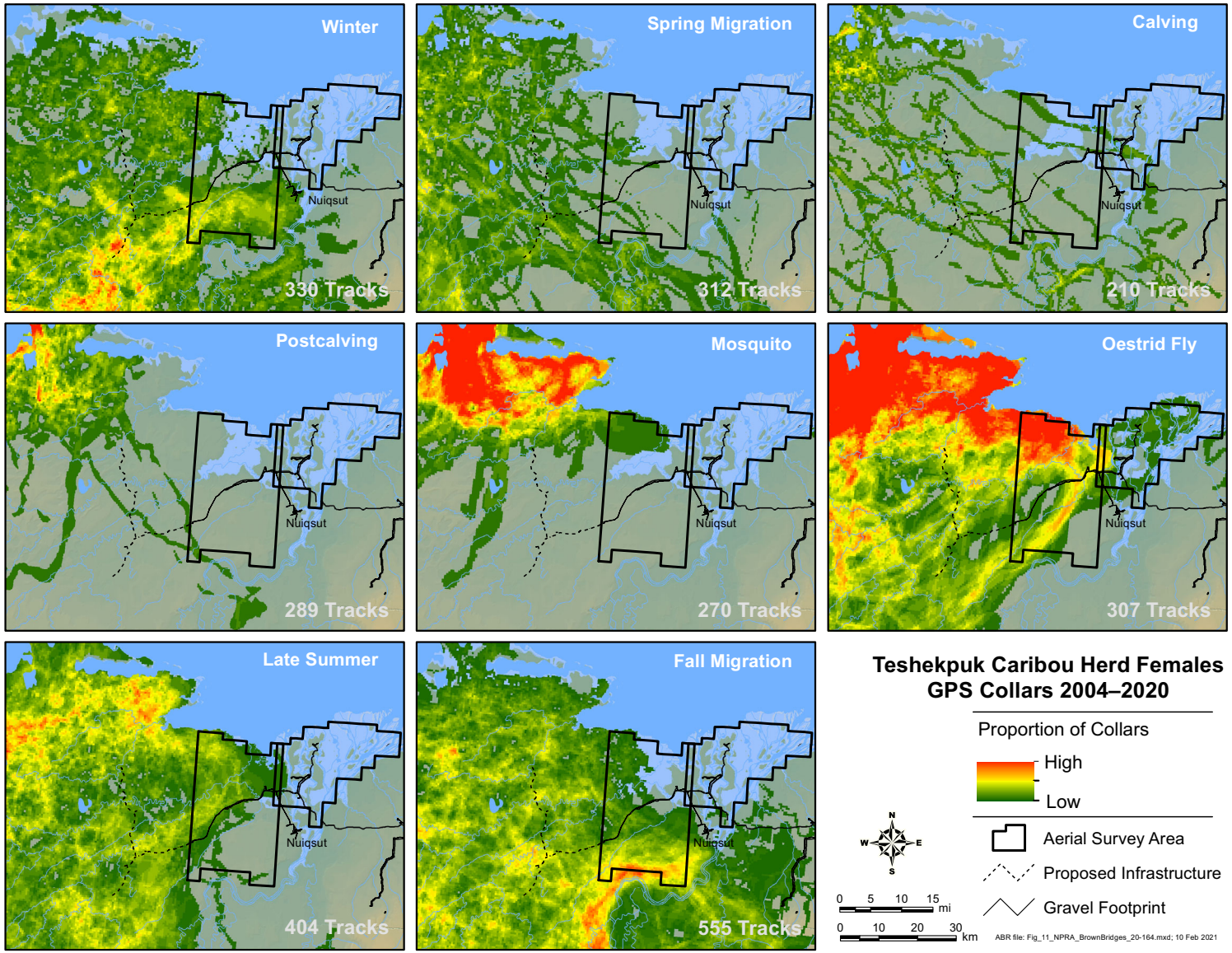

Figure 11. Proportion of GPS-collared caribou using an area based on 95% isopleth of dynamic Brownian Bridge movement models of individual caribou movements.

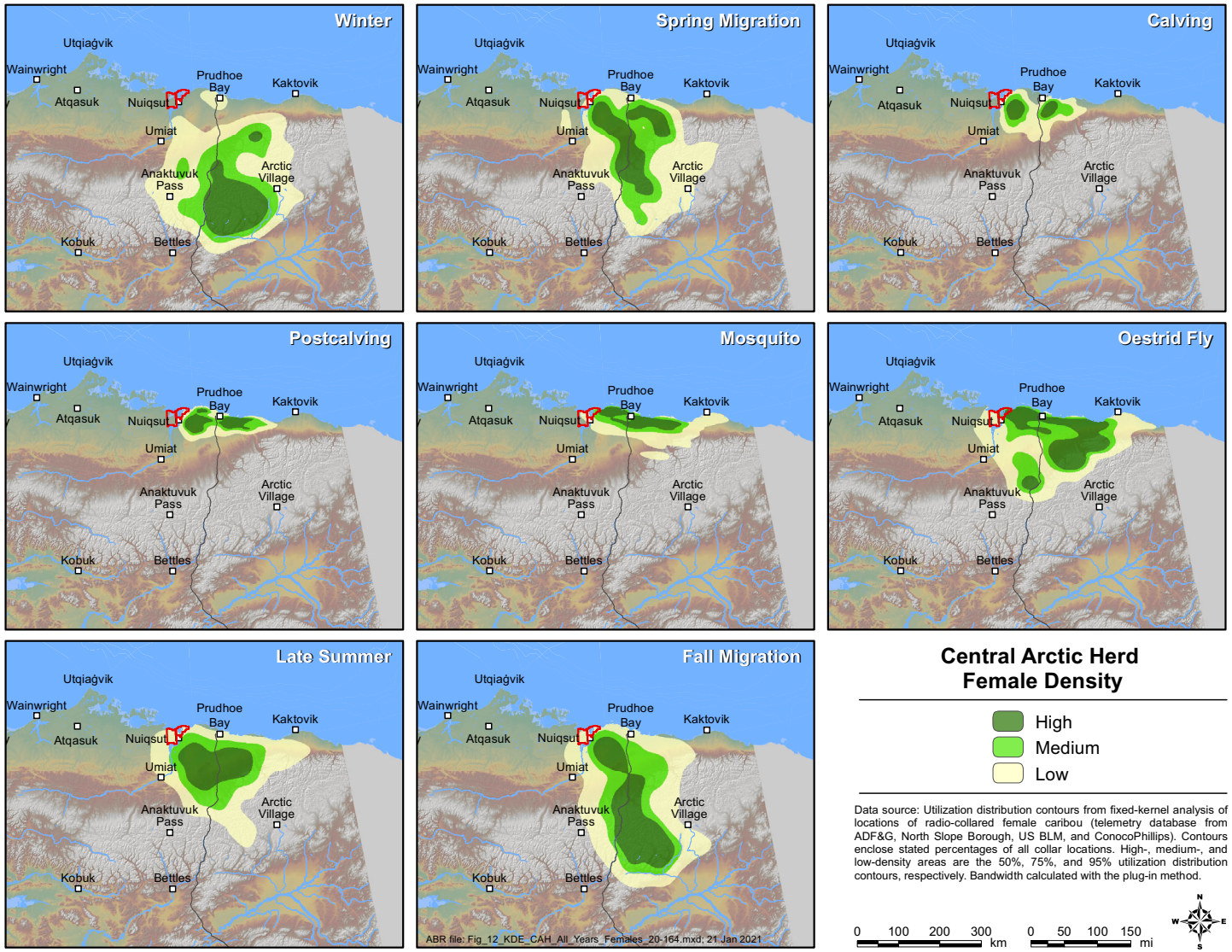

Figure 12. Seasonal distribution of CAH females based on fixed-kernel density estimation of telemetry locations, 2001–2020. Survey areas are outlined in red.

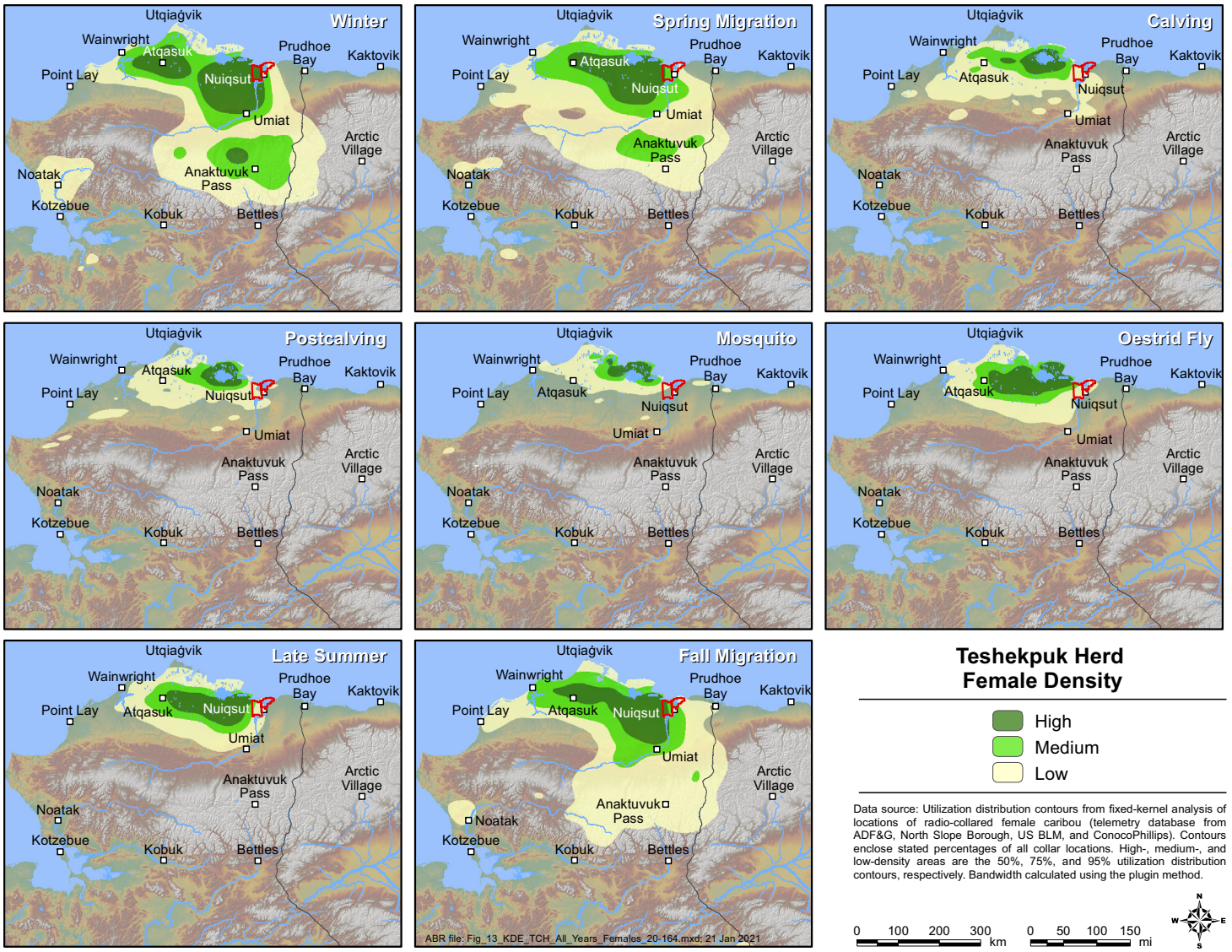

Figure 13. Seasonal distribution of TCH females based on fixed-kernel density estimation of telemetry locations, 1990–2020. Survey areas are outline in red.

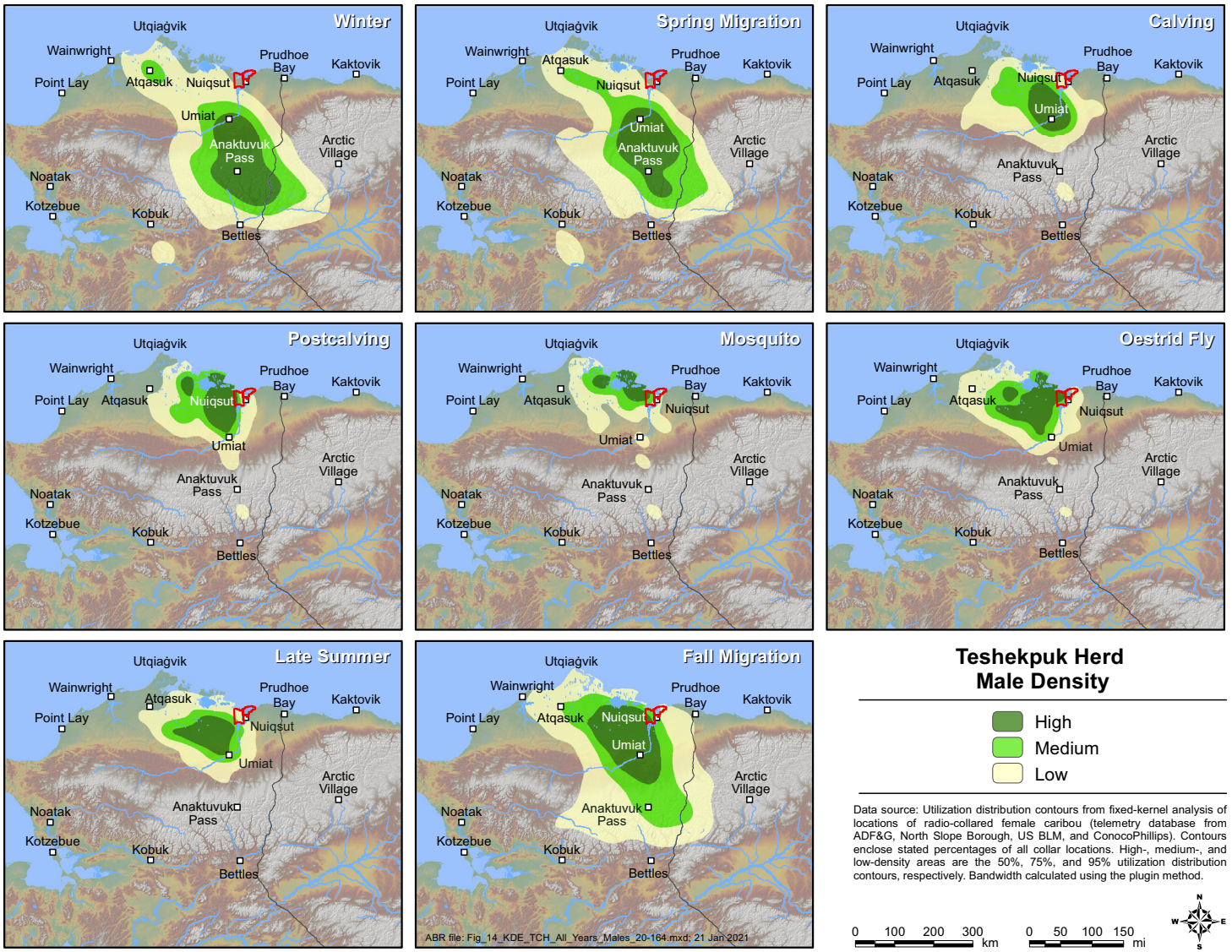

Figure 14. Seasonal distribution of TCH males based on fixed-kernel density estimation of telemetry locations, 1997–2020. Survey areas are outlined in red.

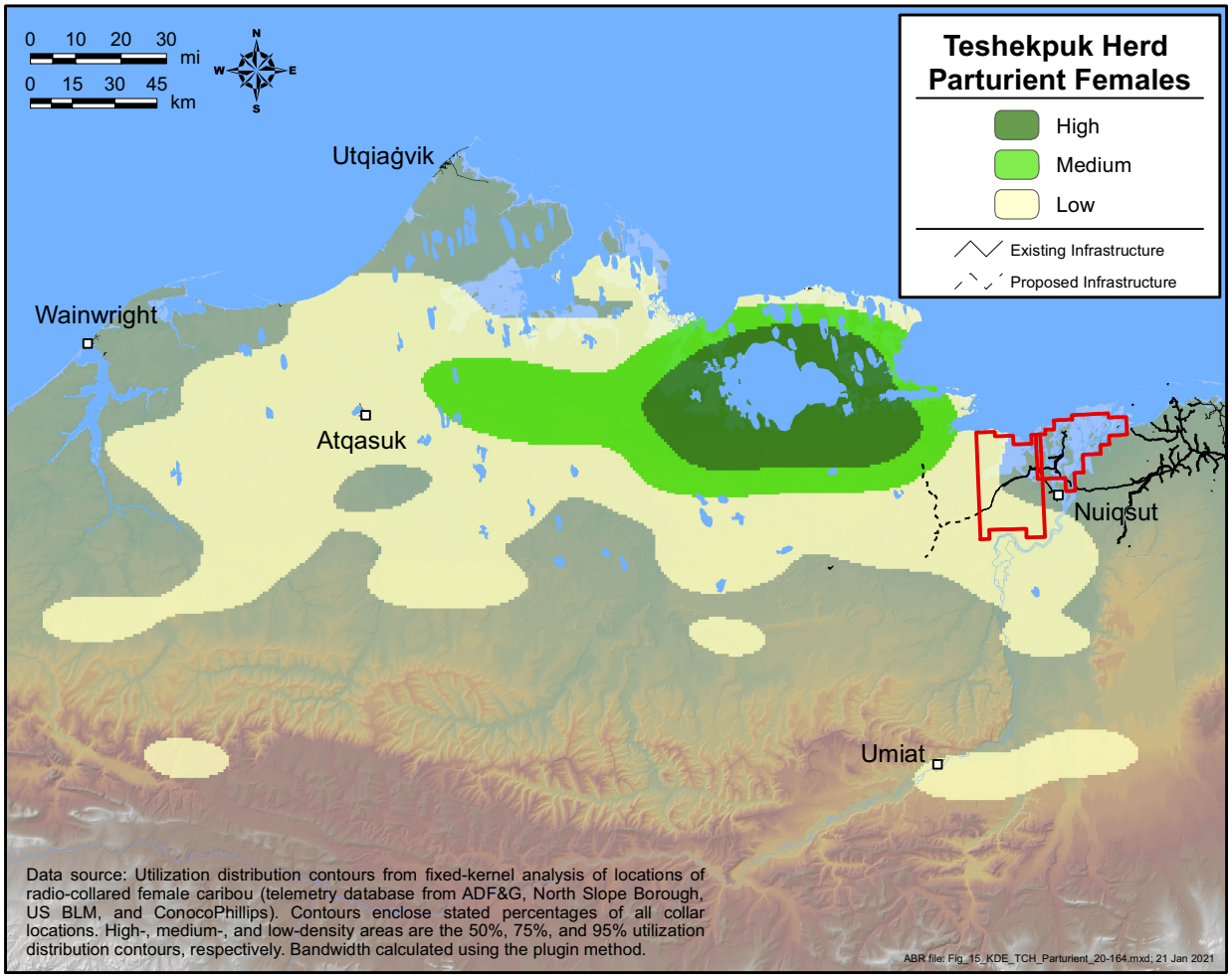

Figure 15. Distribution of parturient females of the Teshekpuk Herd during calving based on fixed-kernel density estimation of telemetry locations, 1990–2020. Survey areas are outlined in red.

CRD is episodic with large groups occasionally using the delta, usually during mid-summer when weather conditions result in movements of insect harassed caribou into the area.

Use of the GMT survey area by CAH females was consistently low all year (<1%) but peaked from July–September when the herd is typically widely dispersed across the central coastal plain. Collared TCH females used the GMT survey area at consistently low levels (<2% of total utilization) throughout the year, with the highest predicted level of use occurring in October (Figure 16). Male TCH caribou had the highest use of the GMT survey area, with use increasing sharply from near zero in May to a peak in July (3.3% of the utilization distribution) before dropping to ~1% from August through October, and then to near 0% during winter as males migrated into the foothills and mountains of the Brooks Range or toward Atqasuk (Figure 16).

MOVEMENTS NEAR ASDP INFRASTRUCTURE

Since monitoring began in the late 1980s–early 1990s with satellite collars and then with GPS collars first being deployed in 2003, movements by collared TCH and CAH caribou near ASDP infrastructure have occurred infrequently and sporadically. Movements of TCH caribou near ASDP infrastructure occur primarily during calving (early June) and the oestrid fly season (mid-July to early August; Figure 17). From

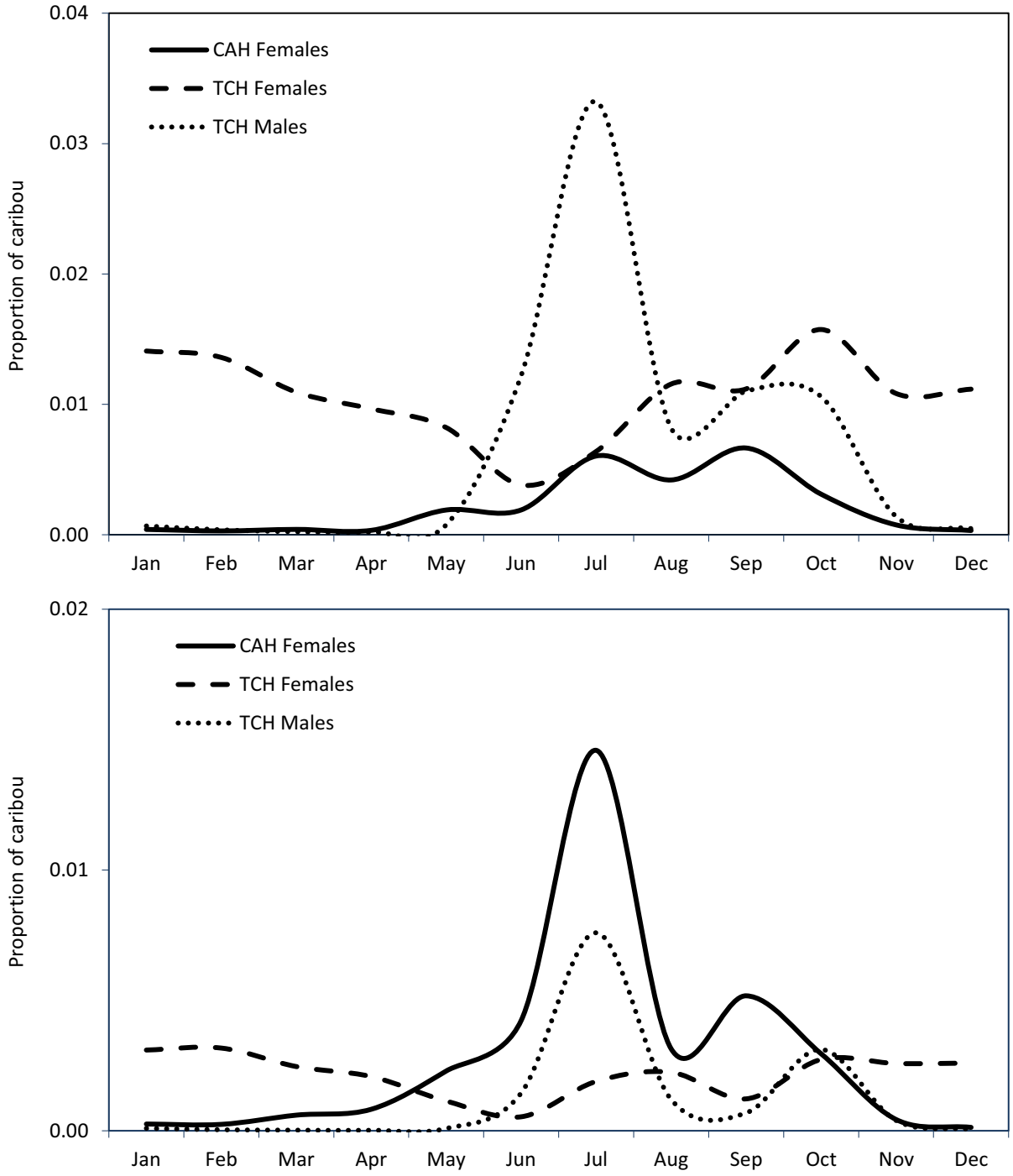

Figure 16. Proportion of CAH and TCH caribou within the GMT survey area (top panel) and Colville River Delta survey area (bottom panel), based on fixed-kernel density estimation, 1990–2020.

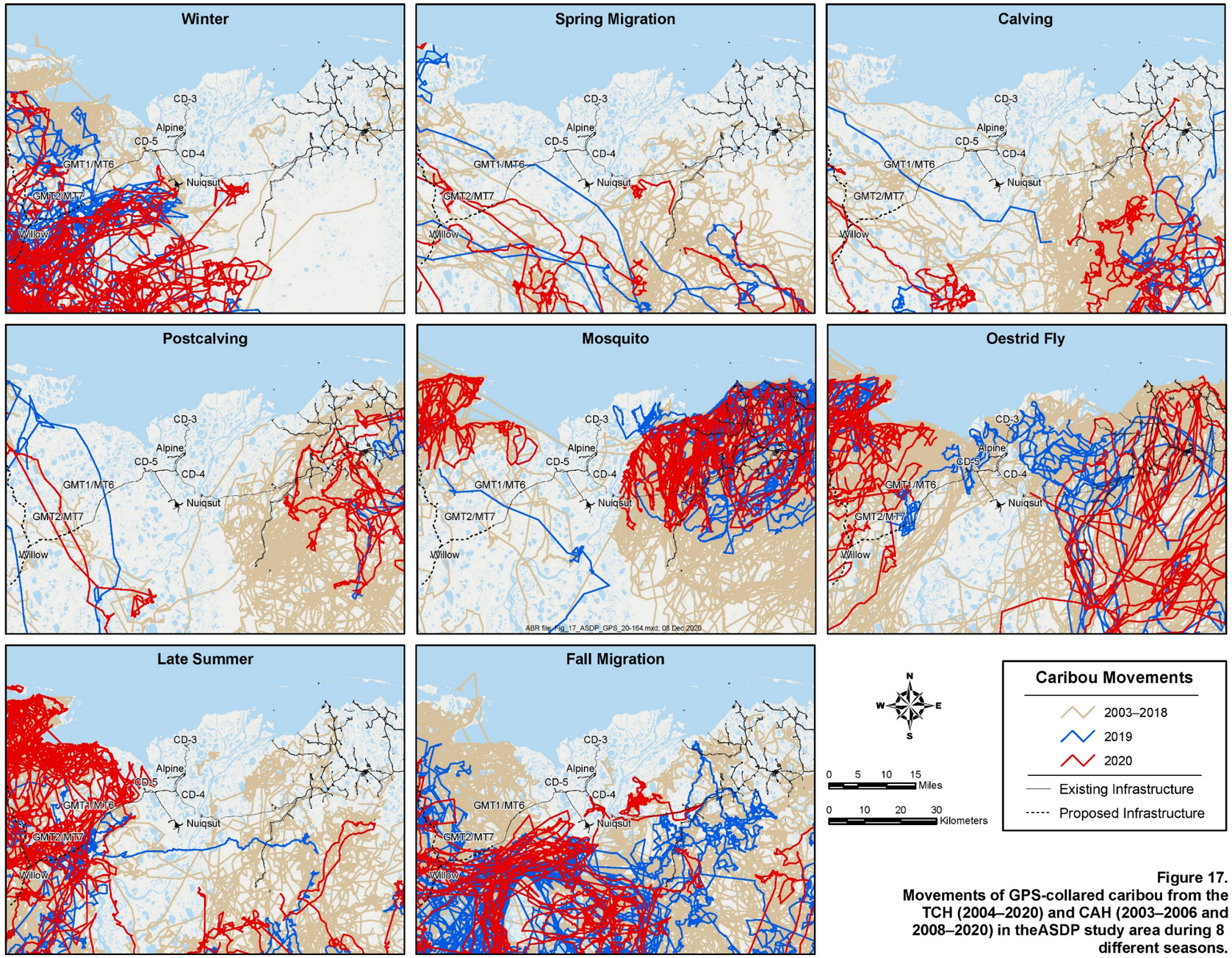

Figure 17.
Movements of GPS-collared caribou from the TCH (2004–2020) and CAH (2003–2006 and 2008–2020) in theASDP study area during 8 different seasons.

Page intentionally left blank.

December 2019 through November 2020, only one GPS-collared TCH or CAH caribou was recorded within 4 km of the CD-1 through CD-4 facilities or associated roads. During the fall migration season, this female caribou approached within 0.75 km of CD4 from south of Nuiqsut before moving off to the east following the Alpine Pipeline.

Prior to construction in winter 2013-2014, movements across the CD-5 pad and access road alignments also occurred rarely (Figure 17). Only eight TCH caribou outfitted with GPS collars and 11 TCH caribou outfitted with satellite collars crossed the CD-5 road alignment in all years prior to construction. CAH caribou have crossed the CD-5 road even less frequently than TCH caribou; only one GPS-collared CAH caribou crossed the CD-5 alignment in July 2010 and no satellite-collared CAH caribou crossed the CD-5 alignment before construction. In 2020, no GPS collared caribou crossed the CD-5 road during the oestrid fly season, but 3 caribou did approach within 4 km of the CD5 pad and road from the north before turning around (Figure 17).

Greater proportions of collared TCH have crossed the GMT1/MT6 and GMT2/MT7 road alignments than have occurred near the CD–5 road alignment, although such movements have not occurred frequently (Figure 17; Table 3) (Lawhead et al. 2015; Prichard et al. 2017, 2018c, 2019c, 2020d). Some crossings occur during the spring migration and calving seasons as caribou move north towards Teshekpuk Lake for calving and later, mosquito-relief. Very few crossings occur during the postcalving and mosquito seasons because most TCH caribou are already located to the northwest near the Beaufort Sea coast. Crossings are more common during the winter, oestrid fly, and late summer seasons as caribou disperse inland from the coast. Crossings are most common during the fall migration season and then decrease to lower rates during the winter season. During mid- and late-August 2020, 20 collared TCH caribou approached the GMT1/MT6 and GMT2/MT7 roads from the north and west. Two of these caribou crossed the road with the remainder either turning back to the west or following the road to the southwest. This was the same movement of animals that brought 3 caribou near CD–5. As late summer progressed into the fall migration season, many of these caribou joined other collared caribou and moved from west of GMT2/MT7 towards Nuiqsut before migrating south. No animals crossed the GMT1/MT6 or GMT2/MT7 roads during this movement and all animals moved between the roads and the Colville River before migrating south. A similar pattern of movements occurred during the winter of 2019/2020 when 8 caribou spent time within ~10 km of the roads, primarily between the roads and the Colville River, but never crossed any roads.

REMOTE SENSING

Because MODIS imagery covers large areas at a relatively coarse resolution (250- to 500-m pixels), it was possible to evaluate snow cover and vegetation indices over a much larger region extending beyond the study area with no additional effort or cost. The region evaluated extends from the western edge of Teshekpuk Lake east to the Canada border and from the Beaufort Sea inland to the northern foothills of the Brooks Range. The ability to examine this large region allowed us to place the study area into a larger geographic context in terms of the chronology of snow melt and vegetation green-up, both of which are environmental variables that have been reported to be important factors affecting caribou distribution in northern Alaska (Kuropat 1984, Johnson et al. 2018).

SNOW COVER

Based on observations from survey crews and records from weather stations in the area (Figure 4; Appendix C), the timing of snow melt was approximately average for most of the region in 2020. Estimated snow cover from MODIS data indicated active snowmelt was widespread in the GMT survey areas on 29 May. Southern portions of the GMT survey area were snow free on 30 May, and the entire region was generally snow-free by 4 June with the exception of a partially snow-covered area near the coast (Figure 18). For the GMT survey areas, this timing was similar to or slightly earlier than the median date of snowmelt computed for the past 20 years (Figures 19–20, Appendix D).

The median dates of snow melt for each pixel computed using 2000–2020 data (where the date of melt was known within one week) indicate that nearly all of the snow on the coastal plain typically

Table 3. Proportion of female Teshekpuk Herd caribou crossing or within 1 km of the GMT1/MT6 and GMT2/MT7 access roads, by season and year.

Season	Year(s)	Collars[a]	Crossed GMT1/MT6	1 km of GMT1/MT6	Crossed GMT2/MT7	1 km of GMT2/MT7	Crossed Either	1 km of Either
Spring Migration	2004–08	29	0	0	0	0	0	0
	2009–12	76	0	0	0.01	0.01	0.01	0.01
	2013–15	54	0	0	0.02	0.02	0.02	0.02
	2016–20	291	0	0	0	0	0	0
	All Years	450	0	0	0	0	0	0.01
Calving	2004–08	28	0	0.04	0.04	0.04	0.04	0.07
	2009–12	73	0	0	0.04	0.04	0.04	0.04
	2013–15	49	0	0	0	0	0	0
	2016–20	286	0	0	0.01	0.01	0.01	0.01
	All Years	436	0	0	0.01	0.01	0.01	0.02
Postcalving	2004–08	28	0	0	0	0	0	0
	2009–12	71	0	0	0	0	0	0
	2013–15	45	0	0	0	0	0	0
	2016–20	151	0	0	0	0	0	0
	All Years	295	0	0	0	0	0	0
Mosquito	2004–08	34	0	0	0	0	0	0
	2009–12	84	0	0	0	0	0	0
	2013–15	66	0	0	0	0	0	0
	2016–20	309	0	0	0	0	0	0
	All Years	493	0	0	0	0	0	0
Oestrid Fly	2004–08	38	0	0	0	0	0	0
	2009–12	95	0.05	0.16	0.05	0.05	0.11	0.18
	2013–15	80	0	0	0	0	0	0
	2016–20	316	0	0	0	0	0	0
	All Years	529	0.01	0.03	0.01	0.01	0.02	0.03
Late Summer	2004–08	60	0	0.02	0.02	0.02	0.02	0.02
	2009–12	94	0	0	0	0	0	0
	2013–15	78	0	0	0	0	0	0
	2016–20	390	0	0.02	0	0.02	0	0.03
	All Years	622	0	0.01	0	0.01	0	0.02
Fall Migration	2004–08	60	0	0	0.10	0.10	0.10	0.10
	2009–12	96	0	0	0	0	0	0
	2013–15	78	0	0.03	0.1	0.13	0.10	0.13
	2016–20	385	0	0	0.01	0.02	0.01	0.02
	All Years	619	0	0	0.03	0.04	0.03	0.04
Winter	2004–08	58	0	0.03	0.02	0.02	0.02	0.03
	2009–12	92	0	0	0	0	0	0
	2013–15	70	0	0.03	0.03	0.03	0.03	0.03
	2016–20	374	0	0	0.01	0.02	0.01	0.02
	All Years	594	0	0.01	0.01	0.02	0.01	0.02

[a] Locations within 30 days of collaring were removed and then animals with fewer than 50 locations or active less than half the season were removed from the analysis.

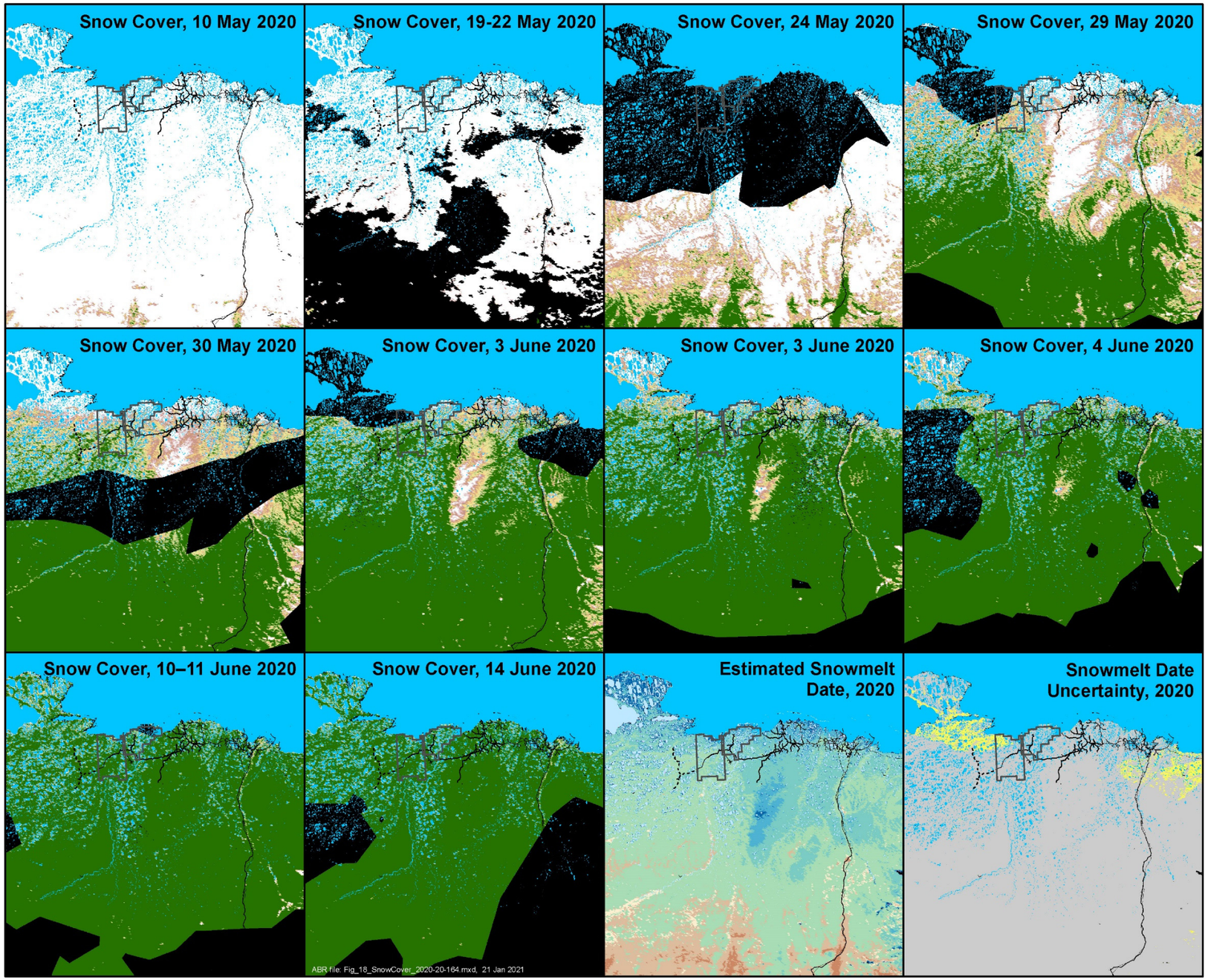

Snow Cover

Snow Fraction (240-m pixels)

- Snow Free
- < 10% Snow Cover
- 10–20% Snow Cover
- 20–30% Snow Cover
- 30–40% Snow Cover
- 40–50% Snow Cover
- 50–60% Snow Cover
- 60–70% Snow Cover
- 70–80% Snow Cover
- 80–90% Snow Cover
- > 90% Snow Cover
- Clouds or bad sensor data
- >= 50% Water Cover

Estimated Snowmelt Date, 2020

- April 30 or earlier
- May 1–17
- May 18–24
- May 25–27
- May 28–30
- May 31–June 2
- June 3–5
- June 6–8
- June 9–11
- June 12–18
- June 19-30
- July 1 or later
- Clouds or bad sensor data
- Water fraction > 50%

Uncertainty in Snowmelt Date, 2020

- Three days or less
- 4–6 days
- 7–9 days
- 10–12 days
- 13–15 days
- 16–18 days
- 19–21 days
- More than 21 days

- Aerial Survey Area
- Existing Infrastructure
- Proposed Infrastructure

0 20 40 60 mi
0 20 40 60 80 100 km

N W E S

Figure 18. Extent of snow cover between early May and mid-June on the central North Slope of Alaska in 2020, as estimated from MODIS satellite imagery.

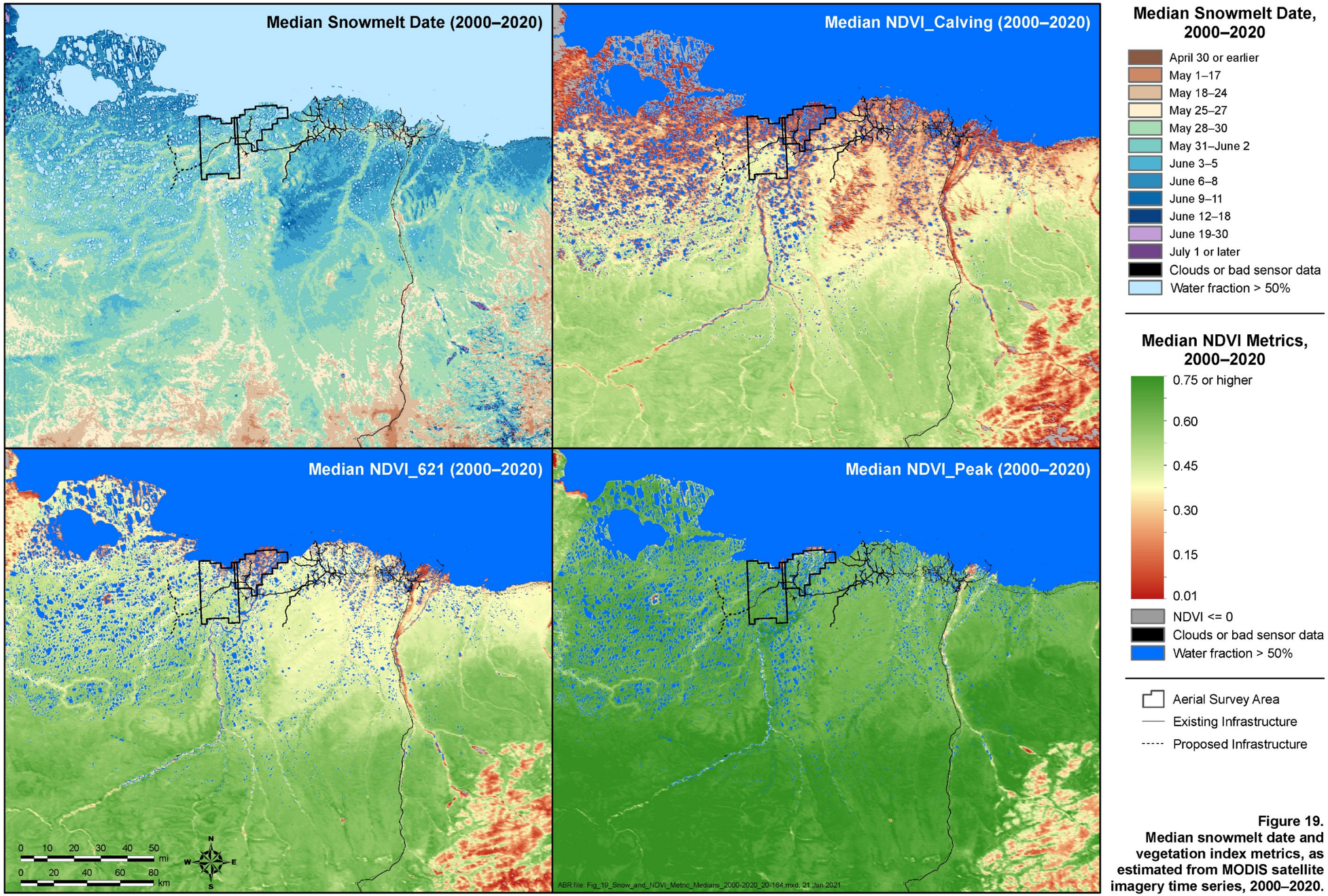

Figure 19.
Median snowmelt date and vegetation index metrics, as estimated from MODIS satellite imagery time series, 2000–2020.

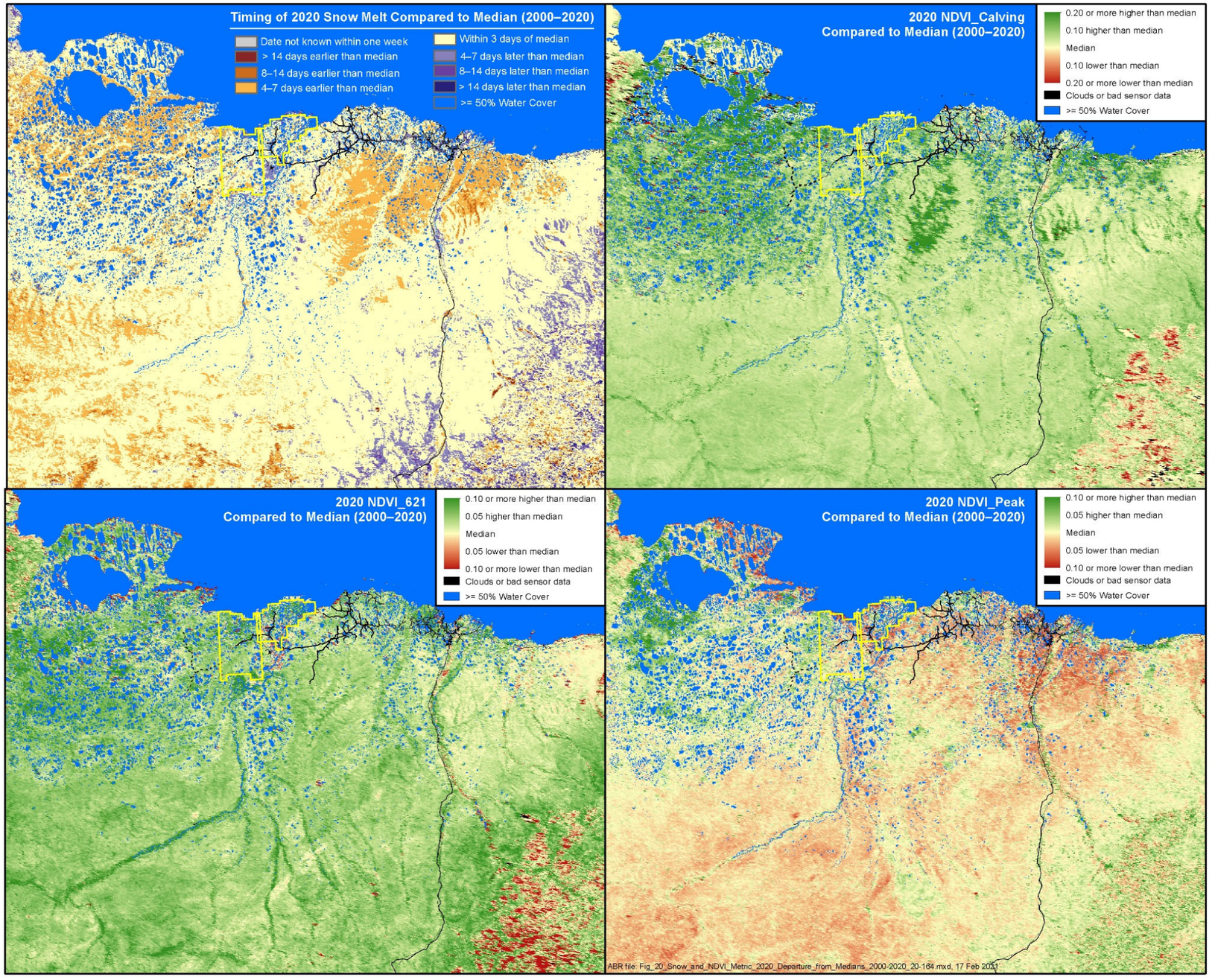

Figure 20.
Departure of 2020 values from median snowmelt date and vegetation index metrics (2000–2020), as estimated from MODIS satellite imagery time series.

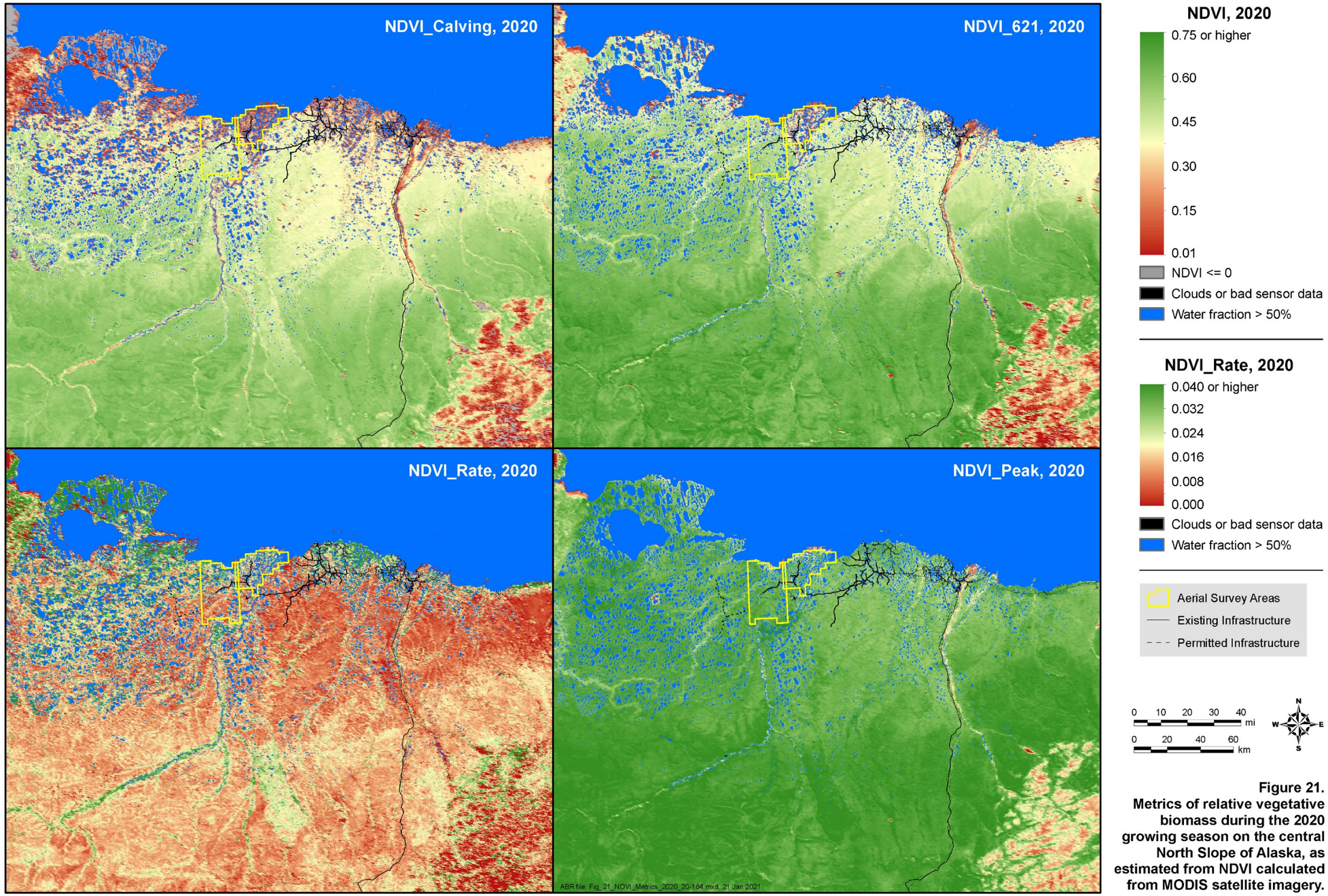

Figure 21.
Metrics of relative vegetative biomass during the 2020 growing season on the central North Slope of Alaska, as estimated from NDVI calculated from MODIS satellite imagery.

melts over a period of three weeks between 25 May and 11 June (Figure 19; Appendix D). Snow melt progressed northward from the foothills of the Brooks Range to the outer coastal plain, occurring earlier in the "dust shadows" of river bars and human infrastructure, and later in the uplands and numerous small drainage gullies southwest of the Kuparuk oilfield. The southern coastal plain, wind-scoured areas, and dust shadows typically melted during the last week of May (Figure 19). The central coastal plain and most of the Colville River delta usually melted in the first week of June, leaving snow on the northernmost coastal plain, in uplands, and in terrain features that trap snow, such as stream gullies. During the second week in June, most of the remaining snow melted, although some deep snow-drift remnants, lake ice, and *aufeis* persisted into early July (Figure 19). In the GMT survey area, snow melt occurred earliest near stream channels and a south-to-north gradient was apparent, with snow typically melting several days later near the coast. Previous comparisons of the performance of the MODIS subpixel-scale snow-cover algorithm with aggregated Landsat imagery suggest that the overall performance of the subpixel algorithm is acceptable, but that accuracy degrades near the end of the period of snow melt (Lawhead et al. 2006).

VEGETATIVE BIOMASS

Compared with the median NDVI since 2000 (Figure 19), the estimated vegetative biomass during calving (NDVI_Calving) and during peak lactation (NDVI_621) in 2020 was above normal across much of the study area (Figures 19–21; Appendices E–F). Those values are consistent with the average or slightly early snow melt in 2020. Peak NDVI was near normal in 2020 (Figure 20; Appendix G), indicating that, despite cool summer temperatures, 2020 was an average growing season overall. Therefore, the early gains in growth largely compensated for the below average temperatures in July (Figure 4). In 2020, NDVI_Rate was low in inland areas with earlier snowmelt, but high in more coastal areas where snowmelt occurred later (Figure 21). This is consistent with a rapid increase in NDVI values soon after snowmelt, as standing dead biomass is exposed and rapid new growth of vegetation occurs.

SPECIES DISTRIBUTION MODELING

GENERAL SUITABILITY

We used test-ratio calculations and VIF analysis to reduce our seasonal explanatory variable sets from an original 138 possible explanatory variables to 59 variables that were included in at least one model. In most cases, the 120m radius variable-scale had the greatest test-ratio, indicating localized habitat selection at the scale of our study area. However, for many of the habitat variables, as well as TPI, a higher test-ratio occurred at larger spatial scales during some seasons. After selecting the variable-scale with the highest test-ratio per season, 70 variables of the original 138 possibilities were evaluated for high collinearity using VIF analysis. MAP, DD5, and AMI all had high VIF values and were eliminated across all seasons. These variables had coarse gradations across the study area that were highly correlated with the geographic variables (e.g. east-to-west). Slope, TRI, and TRI2 also were highly correlated with each other and other variables and were eliminated for all seasons. The remaining variables had VIFs <10 in all seasons, and no additional variables were removed from seasonal models. Depending on the season, 19–23 different variables were included in each model.

Sample sizes for the seasonal location data used in the Maxent models ranged from 314 to 6,648 use locations for the years 2002–2020 combined (Table 4). The best performing RM based on AUCtest varied by season from 0.75 to 5.0 (Table 4). All models were able to predict caribou locations better than expected by random chance (Training AUC > 0.5). After re-running the models with the best performing RM and 100% of the data, the best performing model was for the mosquito season (AUC = 0.805) and the worst performing model was for the fall migration season (AUC = 0.619; Table 4). Test AUC was similar to training AUC in the top models, indicating that the models developed with the training data performed almost as well with separate test data. Clear distributional patterns and localized areas of high suitability were evident in all seasons (Figure 22).

In general, the variables with the highest relative permutation importance (>5) to the seasonal models included distance to coast, east-to-west distribution, the mean habitat

Table 4. Sample sizes and performance metrics for the species distribution model analysis for the NPRA survey area, 2002–2020. The regularization multiplier (RM) was varied (0.75, 1, 2, 3, 4, 5, 6, or 7), and the RM and Area under the curve (AUC) values for training sample and test sample of the best model based on the highest test AUC is provided, As well as the final test AUC when 100% of samples are ran with the top RM.

Season	Aerial Locations	Telemetry Locations	Total Locations	Regularization Multiplier	Training AUC	Test AUC	Final Training AUC
Winter	1,535	5,113	6,648	0.75	0.689	0.652	0.685
Spring Migration	458	627	1,085	0.75	0.745	0.703	0.746
Calving	1,704	202	1,906	2.00	0.657	0.635	0.653
Postcalving	1,789	92	1,881	1.00	0.672	0.668	0.671
Mosquito	88	226	314	5.00	0.809	0.774	0.805
Oestrid Fly	602	568	1,170	0.75	0.735	0.664	0.727
Late Summer	1,651	1,948	3,599	0.75	0.645	0.621	0.644
Fall Migration	2,239	3,574	5,813	2.00	0.623	0.614	0.619
Total	10,066	12,350	22,416				

proportion variables, and different measures of topography depending on the season (elevation, LED, TPI, gentle slopes, flat landforms, or ruggedness; Figures 23–30, Table 5). The geographic variables (distance to coast and/or east-to-west) were consistently in the top 3 for permutation importance. SWE only had a permutation importance >5 during spring. Daily NDVI, maxNDVI, biomass, and nitrogen did not have a permutation importance greater than 6.1 in any model and median snowmelt date and TWI were never greater than 5 in any model.

SUITABILITY BY SEASON

The training AUC in the winter season was moderate at 0.685. Based on the suitability map for the winter season, suitability tended to be lower in the GMT survey area with the highest suitability predominantly in northeast BTN and most the BTS (Figure 22). Suitability in the GMT survey area during winter was lowest in the far east and along streams and creeks, highest in the far northwest, and fairly uniform throughout the remainder of the survey area. The variables with the largest permutation importance to the model included elevation (30.7), distance to coast (12.1), flat landforms (11.3), west-to-east distribution (10.2), the mean proportion of tussock tundra (7.7), and the mean proportion of riverine habitat (5.3; Figure 23, Table 4). Based on the response curves, suitability was higher at higher elevations, further from the coast, with lower proportions of flat landforms, and farther west and caribou avoided wet habitats and preferred tussock tundra (Figure 23). Suitability was also higher in regions with moderate median SWE levels, and low at low maxNDVI values.

The training AUC for the spring migrations model had the second highest value of all seasonal models at 0.746. Based on the suitability map, the model predicted the highest suitability west of the GMT survey area, particularly in western BTN and central/mid-central BTS, with higher suitability in drainages or around lakes. The GMT survey area had relatively low predicted suitability in the eastern portion (Figure 22). The variables with the largest permutation importance to the model included west-to-east (33.1), distance to coast (15.9), elevation (13.8), SWE (6.1), and the proportion of gentle slopes (5.8; Figure 24, Table 4). Based on the response curves, suitability increased in the west, further from the coast, and as the mean proportion of gentle slopes increased (Figure 24). Suitability was very low at the highest

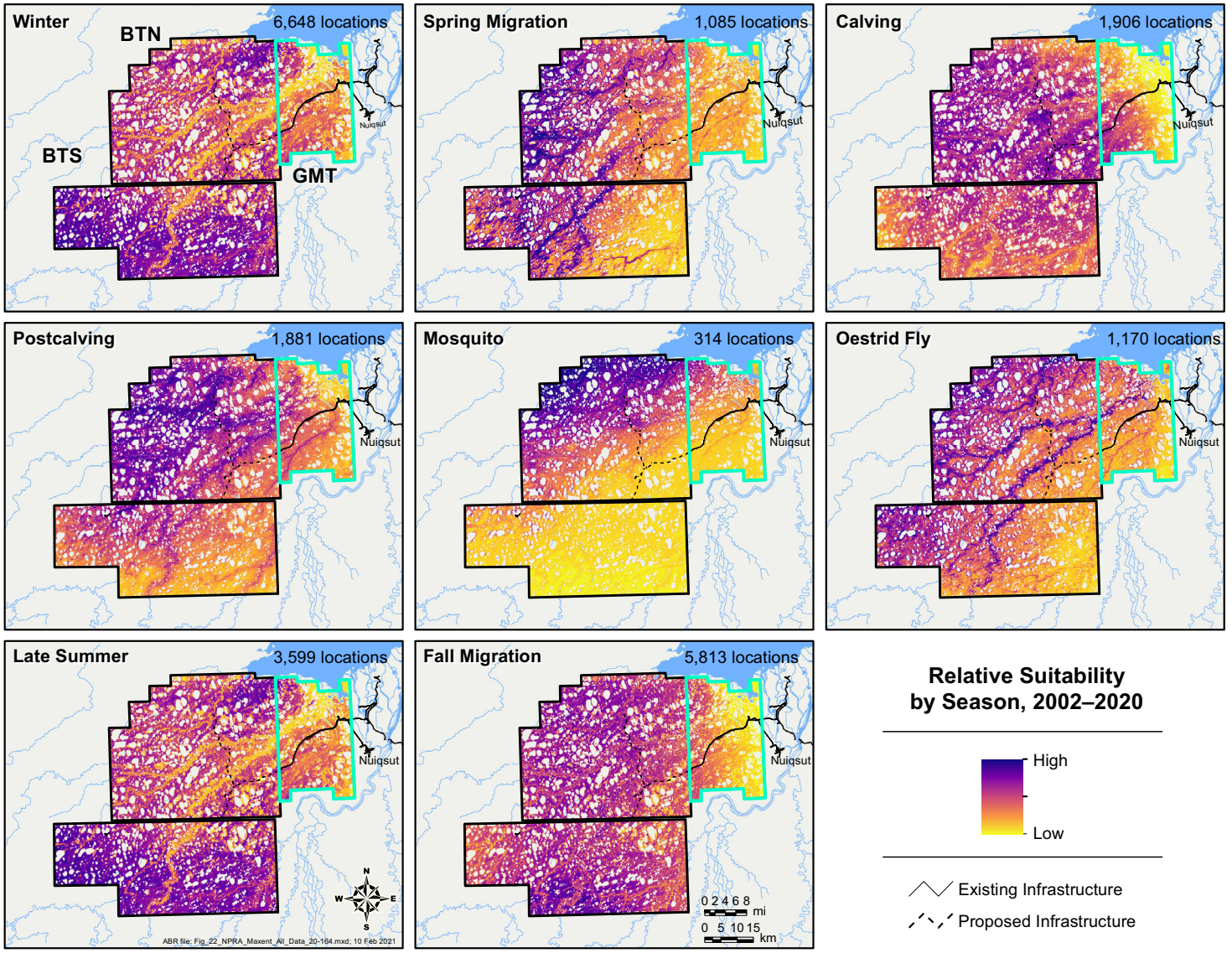

Figure 22. Predicted relative suitability for use of the NPRA survey area by caribou during 8 different seasons, 2002–2020, based on Maxent analysis. Relative probabilities calculated using the 2020 values for daily NDVI, biomass, and nitrogen.

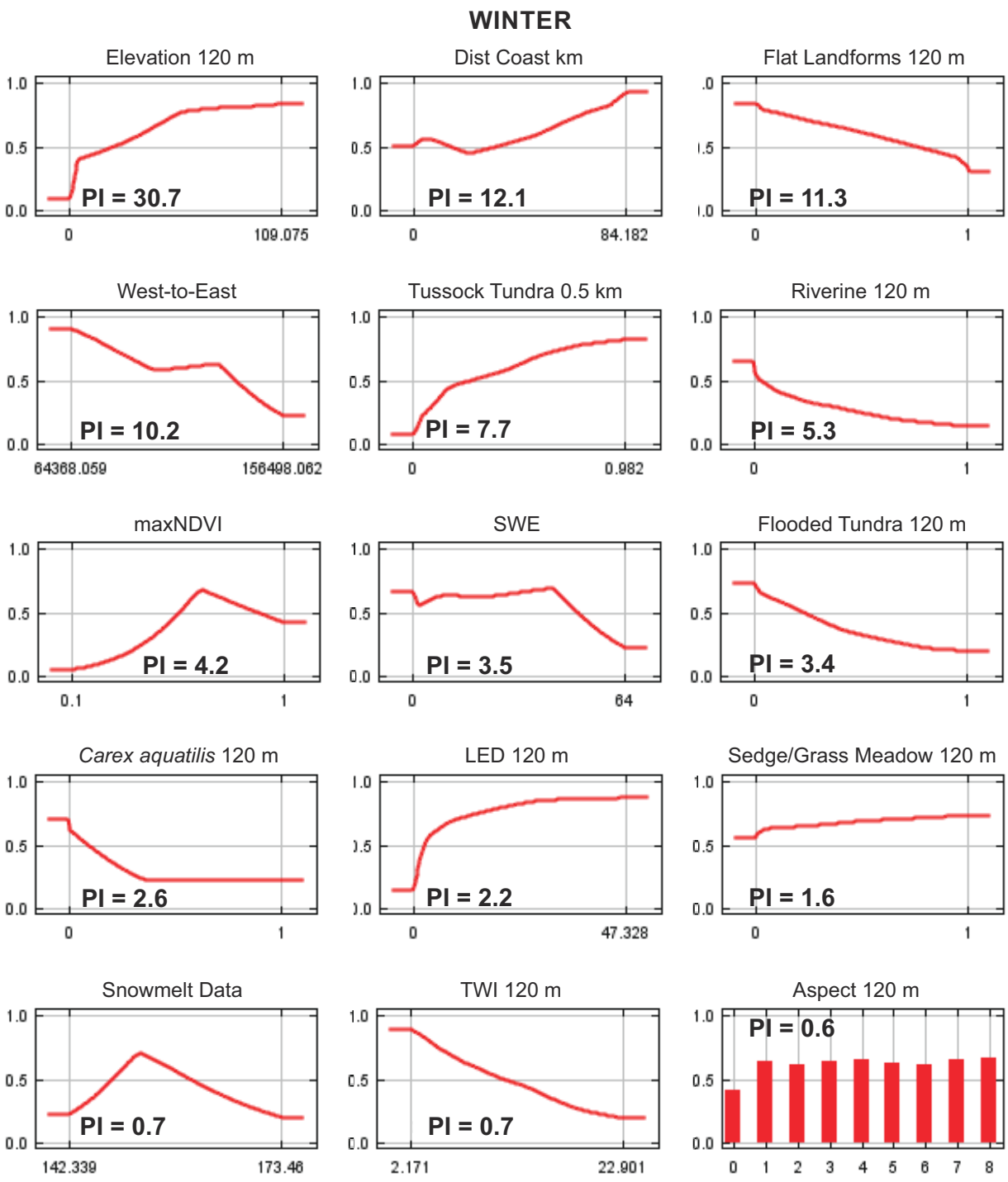

Figure 23. Response curves and permutation importance of the top 15 variables (based on permutation importance) included in models to predict caribou suitability in the GMT, BTN, and BTS surveys areas during the winter season. These plots reflect the dependence of predicted suitability both on the selected variable and on dependencies induced by correlations between the selected variable and other variables.

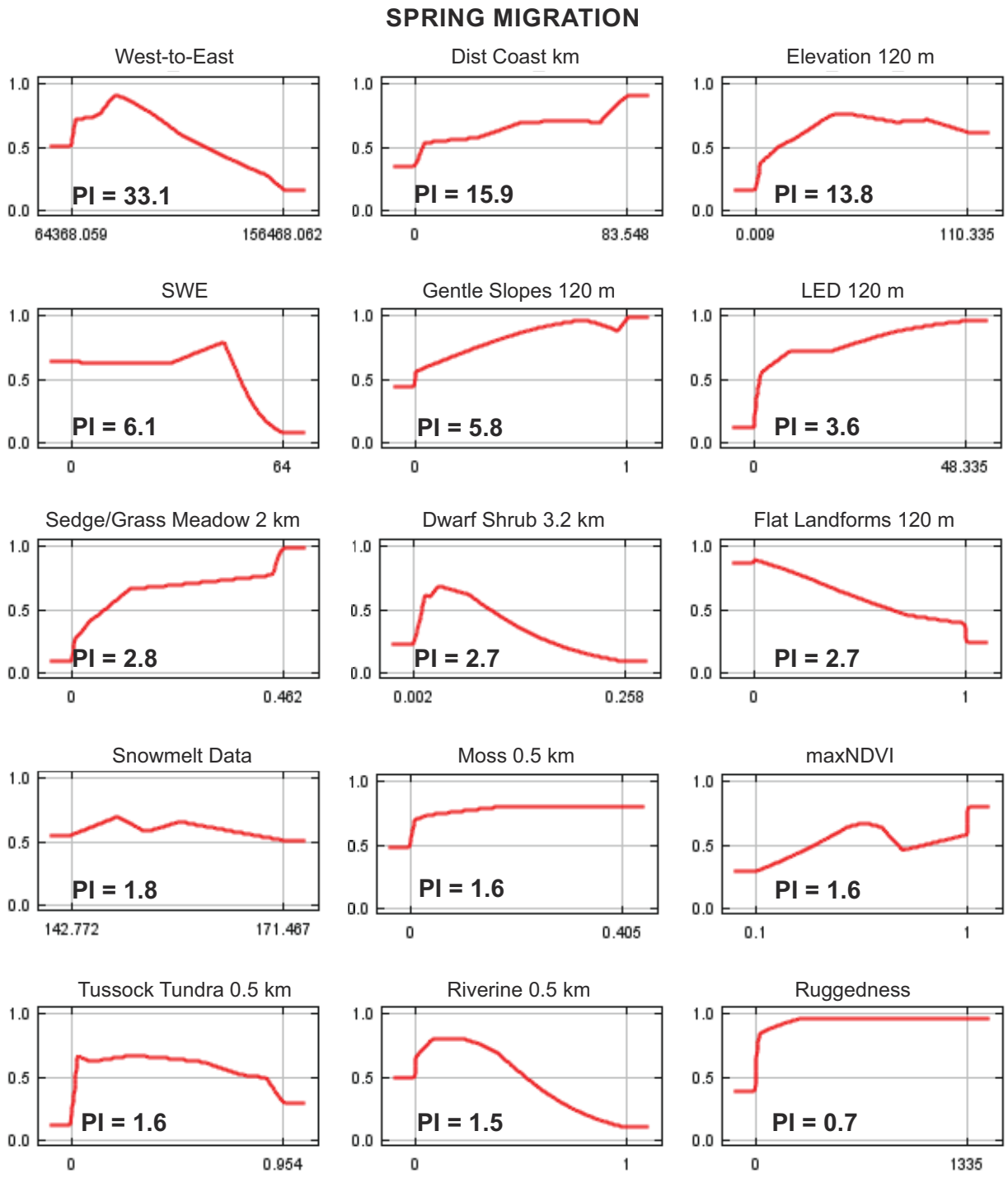

Figure 24. Response curves and permutation importance of the top 15 variables (based on permutation importance) included in models to predict caribou suitability in the GMT, BTN, and BTS surveys areas during the spring migration season. These plots reflect the dependence of predicted suitability both on the selected variable and on dependencies induced by correlations between the selected variable and other variables.

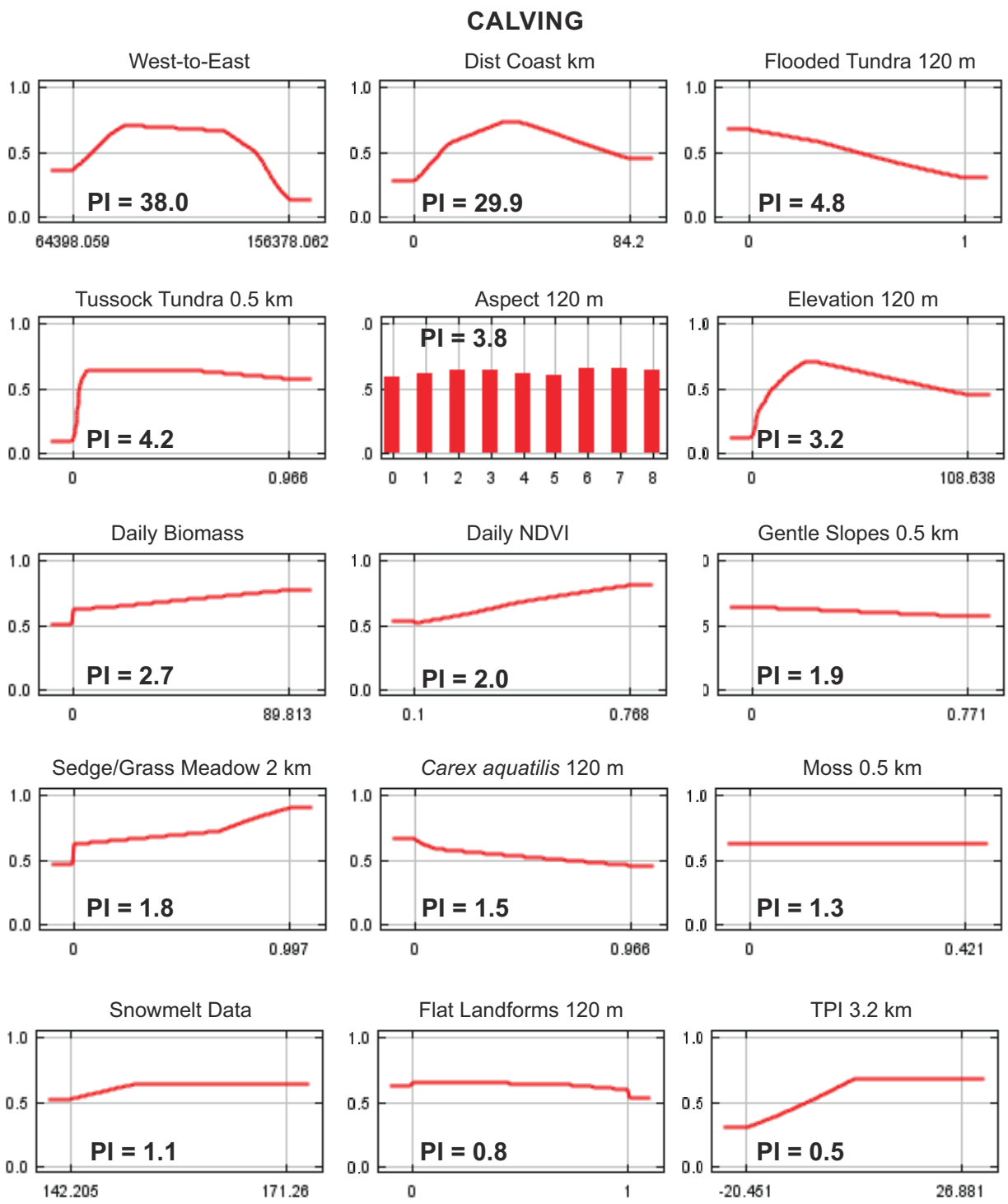

Figure 25. Response curves and permutation importance of the top 15 variables (based on permutation importance) included in models to predict caribou suitability in the GMT, BTN, and BTS surveys areas during the calving season. These plots reflect the dependence of predicted suitability both on the selected variable and on dependencies induced by correlations between the selected variable and other variables.

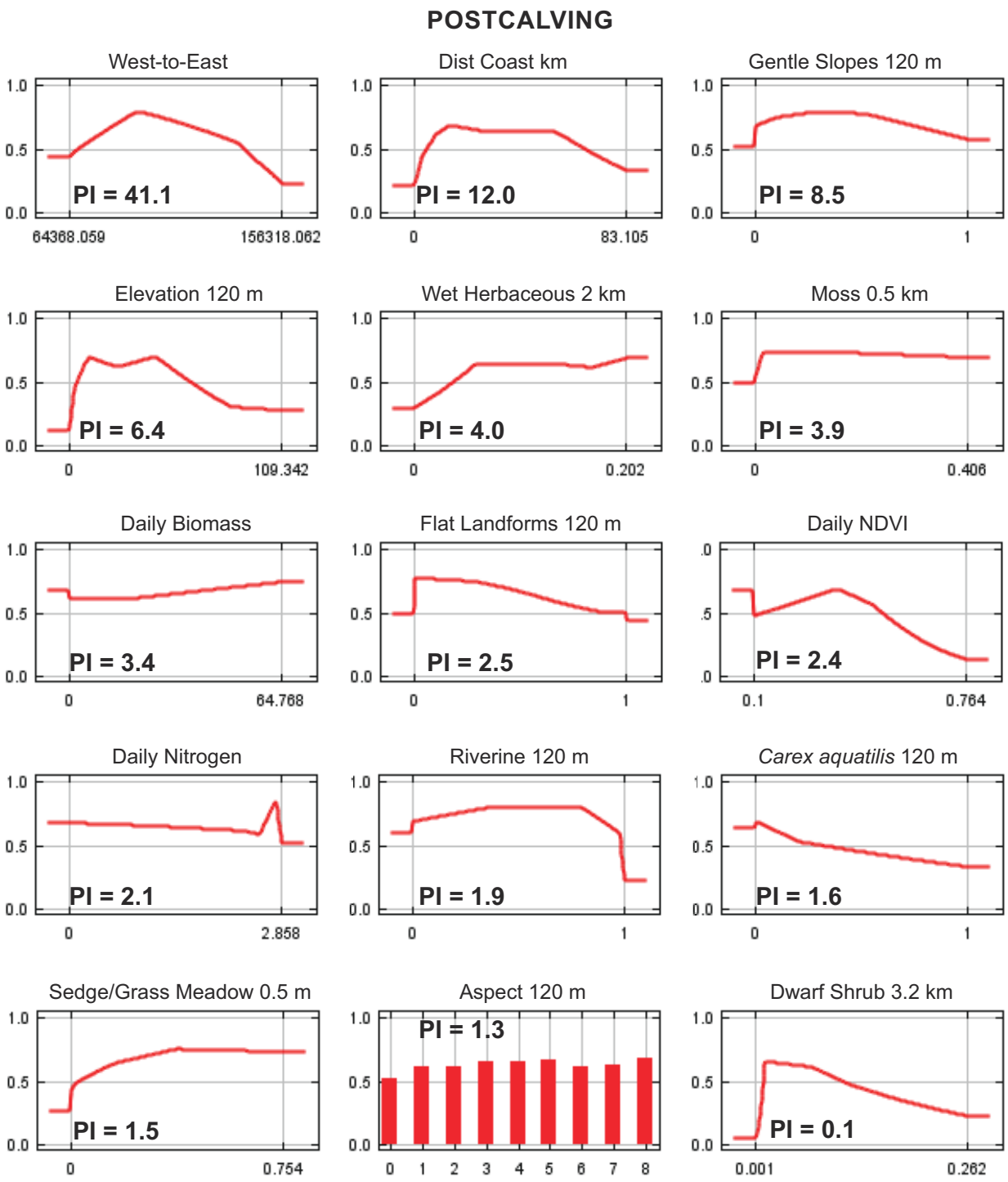

Figure 26. Response curves and permutation importance of the top 15 variables (based on permutation importance) included in models to predict caribou suitability in the GMT, BTN, and BTS surveys areas during the postcalving season. These plots reflect the dependence of predicted suitability both on the selected variable and on dependencies induced by correlations between the selected variable and other variables.

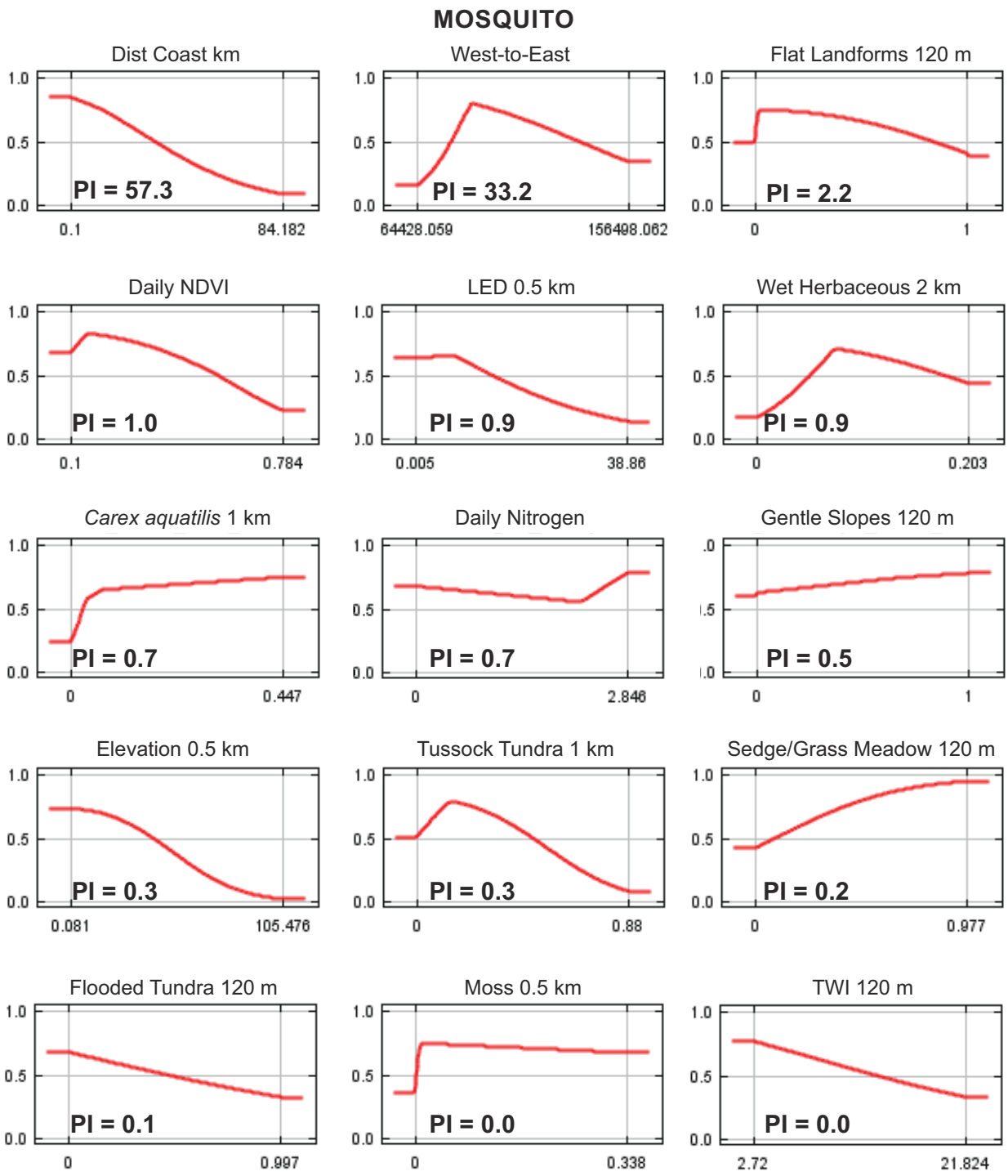

Figure 27. Response curves and permutation importance of the top 15 variables (based on permutation importance) included in models to predict caribou suitability in the GMT, BTN, and BTS surveys areas during the mosquito season. These plots reflect the dependence of predicted suitability both on the selected variable and on dependencies induced by correlations between the selected variable and other variables.

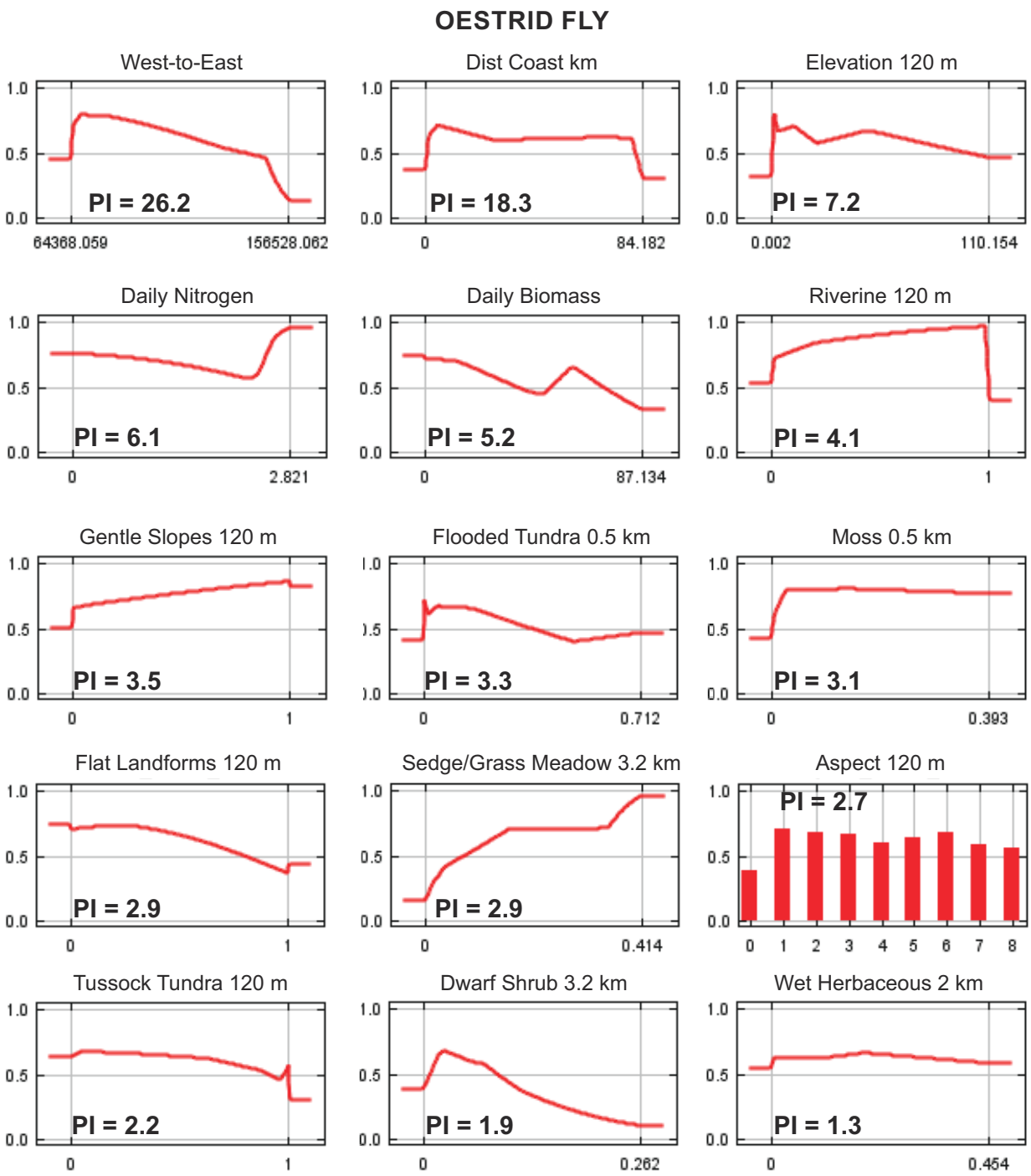

Figure 28. Response curves and permutation importance of the top 15 variables (based on permutation importance) included in models to predict caribou suitability in the GMT, BTN, and BTS surveys areas during the oestrid fly season. These plots reflect the dependence of predicted suitability both on the selected variable and on dependencies induced by correlations between the selected variable and other variables.

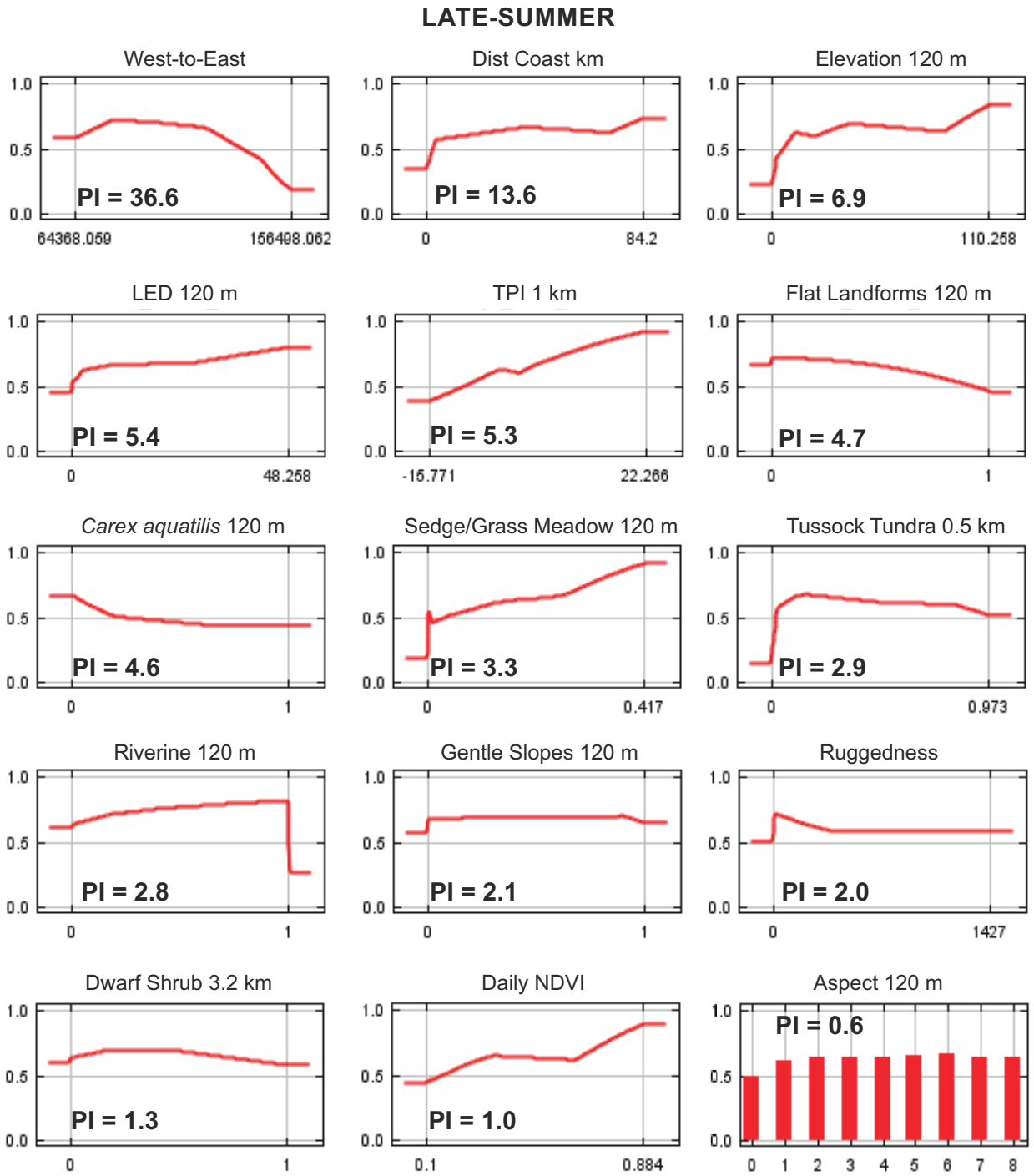

Figure 29. Response curves and permutation importance of the top 15 variables (based on permutation importance) included in models to predict caribou suitability in the GMT, BTN, and BTS surveys areas during late summer. These plots reflect the dependence of predicted suitability both on the selected variable and on dependencies induced by correlations between the selected variable and other variables.

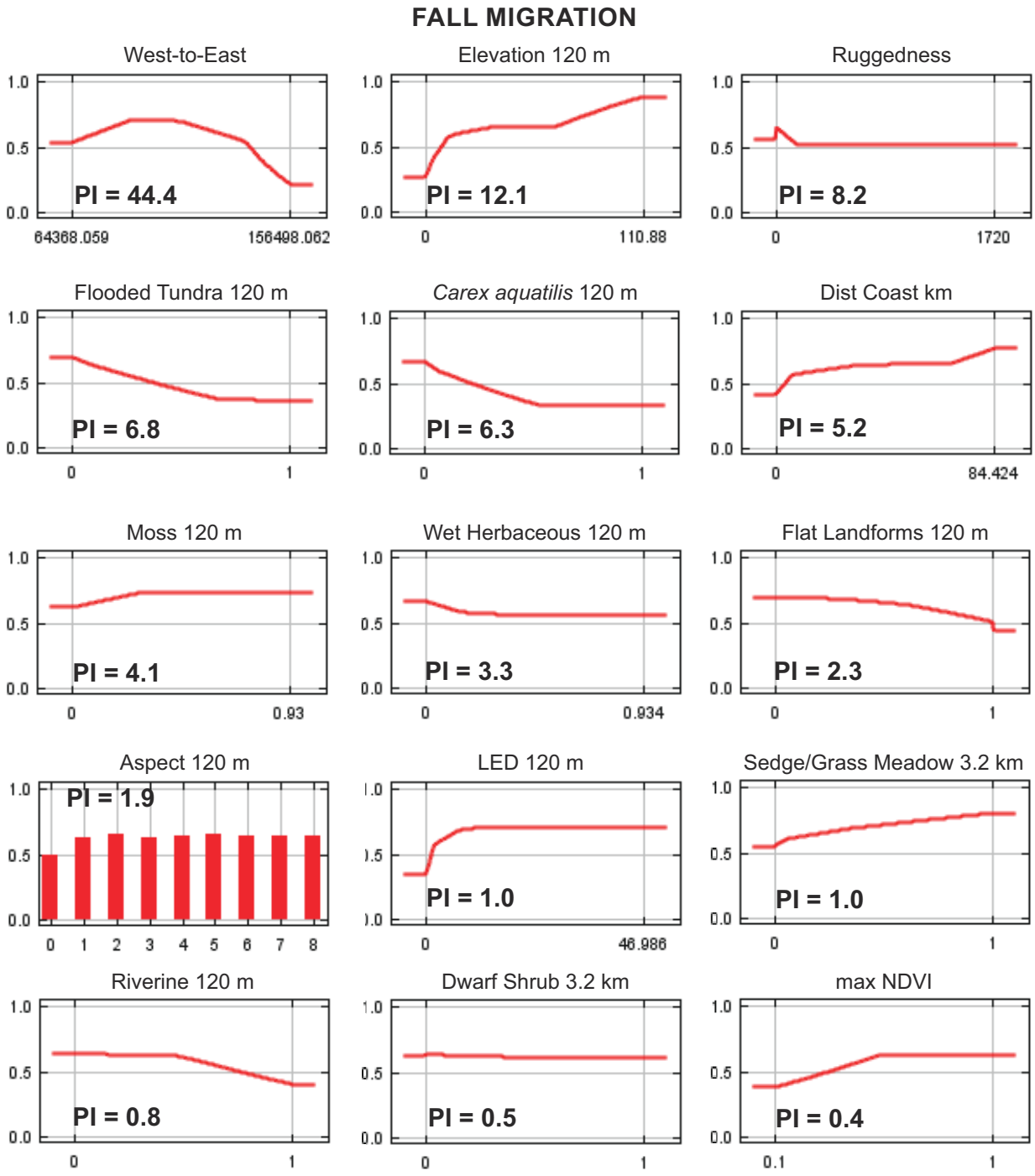

Figure 30. Response curves and permutation importance of the top 15 variables (based on permutation importance) included in models to predict caribou suitability in the GMT, BTN, and BTS surveys areas during the fall migration season. These plots reflect the dependence of predicted suitability both on the selected variable and on dependencies induced by correlations between the selected variable and other variables.

Table 5. Permutation Importance of variables used in species distribution models of caribou suitability in the GMT, BTN, and BTS survey areas during 8 different seasons, 2002–2020. Bold font indicates a permutation importance >5.

Variable	Winter	Spring Migration	Calving	Postcalving	Mosquito	Oestrid Fly	Late Summer	Fall Migration
Aspect 120m	0.6	0.0	3.8	1.3	0.1	2.7	0.6	1.9
Daily Biomass			2.7	3.4	0.5	**5.2**	0.9	
Dist Coast km	**12.1**	**15.9**	**29.9**	**12.0**	**57.3**	**18.3**	**13.6**	**5.2**
Carex aquatilis 1 km					0.7			
Carex aquatilis 120 m	2.6	1.2	1.5	1.6		0.2	4.6	**6.3**
Dwarf Shrub 3.2 km		2.7		0.1	0.9	1.9		
Dwarf Shrub 2.0 km	0.5							
Dwarf Shrub 120 m			0.2				1.3	0.5
Flooded Tundra 0.5 km		1.0				3.3		
Flooded Tundra 120 m	3.4		4.8	3.1	0.1		0.5	**6.8**
Moss 0.5 km		1.6	1.3	3.9	0.0	3.1		
Moss 120 m	0.7						1.0	4.1
Riverine 1 km			0.3					
Riverine 0.5 km		1.5						
Riverine 120 m	**5.3**			1.9	0.0	4.1	2.8	0.8
Sedge/Grass Meadow 3.2 km							3.3	
Sedge/Grass Meadow 2 km		2.0						
Sedge/Grass Meadow 0.5 km				1.5				
Sedge/Grass Meadow 120 m	1.6		1.8		0.2	2.9		1.0
Tussock Tundra 3.2 km				1.1				
Tussock Tundra 1 km					0.3			
Tussock Tundra 0.5 km	**7.7**	1.6	4.2				2.9	0.2
Tussock Tundra 120 m						2.2		

Table 5. Continued.

Variable	Winter	Spring migration	Calving	Postcalving	Mosquito	Oestrid Fly	Late Summer	Fall Migration
Wet Herbaceous 0.5 m						1.3		
Wet Herbaceous 2 km				4.0	0.9			
Wet Herbaceous 120 m	0.3	0.3	0.7				0.4	3.3
West-to-East	**10.2**	**33.1**	**38.0**	**41.1**	**33.2**	**26.2**	**36.6**	**44.4**
Elevation 0.5 km					0.3			
Elevation 120 m	**30.7**	**13.8**	3.2	**6.4**		**7.2**	**6.9**	**12.0**
Flat Landforms 120 m	**11.3**	2.7	0.8	2.5	2.2	2.9	4.7	2.3
Gentle Slopes 0.5 km			1.9			-		
Gentle Slopes 1 km								0.3
Gentle Slopes 120 m	0.5	**5.8**		**8.5**	0.5	3.5	2.1	
LED 0.5 km				0.9	0.9			
LED 2 km						0.9		
LED 120 m	2.2	3.6	0.4				**5.4**	1.0
maxNDVI	4.2	1.6	0.5	0.3	0.1	1.9	2.5	0.4
Daily NDVI			2.0	2.4	1.0	0.5	1.0	
Daily Nitrogen			0.3	2.1	0.7	**6.1**	0.7	
Ruggedness	0.9	0.7	0.2	1.8	0.0	1.7	2.0	**8.2**
Snowmelt Date	0.7	1.8	1.1			-		
SWE, spring		**6.1**						
SWE, winter	3.5							
TPI 1 km							**5.3**	
TPI 3.2 km	0.3		0.5	0.1	0.2	1.7		0.0
TPI 0.5 km		0.3						
TWI 120 m	0.7	1.9	0.1	0.0	0.0	2.2	0.9	1.2

SWE values, indicating they are avoiding the deepest or densest snow and was also lower at lower elevations.

The training AUC for the calving season indicated moderate predictive power at 0.653. Based on the suitability map, suitability for all survey regions was generally lowest in the eastern portions of GMT, lower along creeks and streams, and highest in the BTN survey area (Figure 22). The variables with the largest permutation importance to the model included west-to-east (38.0) and distance to coast (29.9; Figure 25, Table 4). The variables with the next highest permutation importance were the proportion of flooded tundra (4.8) and tussock tundra (4.2) habitats, aspect (3.8), and elevation (3.2). Based on the response curves, suitability was highest at mid-longitudes and moderate distances to coast (Figure 25). Suitability was lower as the proportion of flooded tundra increased, and very low at low proportions of tussock tundra and at lower elevations. The daily biomass variable had a permutation importance of 2.7 and suitability generally increased with increasing biomass on the landscape. The daily nitrogen and NDVI variables contributed 0.3 and 2.0, respectively. Median snowmelt date only had a permutation importance of 1.1 but had a slight positive relationship with suitability, suggesting that caribou tend to be distributed in regions with slightly later melting snow, but other variables are more powerful at predicting suitability.

The training AUC for the postcalving season indicated moderate predictive power at 0.671. Based on the suitability map, suitability in all survey areas across all survey areas was highest in the northwest and along drainages with the highest suitability in the GMT survey area along Fish Creek and lowest in the northeast and east (Figure 22). The variables with the largest permutation importance to the model included west-to-east (41.1), distance to coast (12.0), gentle slopes (8.5), and elevation (6.4; Figure 26, Table 4). Based on the response curves, suitability was higher at mid-longitudes, at close to mid-distances from coast (but not right along the coast), with a low or moderate proportion of gentle slopes, and at low to moderate elevations (Figure 26).

The training AUC value for the mosquito season was the highest of all the seasonal models at 0.805. Based on the suitability map, high suitability during this season was generally confined to the coast, the northwest portion of BTN, and lake margins (Figure 22). In the GMT survey area, suitability was highest along the coast and along drainages. The variables with the largest permutation importance to the model included distance to coast (57.3), west-to-east (33.2), flat landforms (2.2), and daily NDVI (1.0). No other variable had a contribution >1.0. Figure 27, Table 4). The response curve and the high permutation importance of the distance to coast variable indicates a strong selection for coastal areas (Figure 27). Suitability was higher close to the coast and at intermediate longitudes, with some evidence that lower proportions of flat landforms and lower NDVI values (like in coastal mudflats) were selected for.

The training AUC for the oestrid fly season was the third highest for the seasonal models at 0.727. Based on the suitability map, suitability for all survey areas generally increased from southeast to northwest and was highest along rivers and lake margins, especially Fish and Judy Creeks (Figure 22). The variables with the largest permutation importance to the model included west-to-east distribution (26.2), distance to coast (18.3), elevation (7.2), daily nitrogen (6.1), and daily biomass (5.2; Figure 28, Table 4). Based on the response curves, suitability increases to the west, is lowest in the extreme east and west of the study area, was higher at lower elevations, and was highest at the highest nitrogen levels.

The training AUC for the late summer season was low compared to other seasonal models at 0.644. Based on the suitability map, suitability was predicted to be lowest in the eastern GMT survey area, and higher in northwestern BTN, and along streams and some lake margins (Figure 22). The variables with the largest permutation importance to the model included west-to-east (36.6), distance to coast (13.6), elevation (6.9), LED (5.4), and TPI (5.3; Figure 29, Table 4). Based on the response curves, suitability was higher to the west, closer to the coast, at higher TPI values, and where mean LED was near zero.

The training AUC during the fall migration season was the lowest of all seasonal models at 0.619. Based on the suitability map, the lowest suitability was predicted to be in the eastern portion of GMT, highest in the southwest portion

of BTS and generally moderate in other areas (Figure 22). The variables with the largest permutation importance to the model included west-to-east (44.4), elevation (12.0), ruggedness (8.2), the proportion of flooded tundra (6.8), the proportion of *Carex aquatilis* (6.3), and distance to coast (5.2; Figure 30, Table 4). Based on the response curves, suitability was highest at mid-longitudes, at higher elevations, and slightly higher when ruggedness was near zero (Figure 30). Suitability decreased with increasing proportions of flooded tundra and *Carex aquatilis.*

DISTRIBUTION AND INFRASTRUCTURE

During all seasons, the distance to road variable increased the predictive power of the model. This suggests that the areas within 10 km of roads had somewhat different predicted suitability even after adjusting for the effects of other variables, however in some seasons the permutation importance of the distance to road model was small. The spring migration, oestrid fly, and fall seasons all had smooth response curves indicating lower than predicted suitability of the general area, but no noticeable decline in use of areas close to the roads (Figure 31). There was little data available to predict suitability during the mosquito season because caribou were primarily located > 10 km from the roads. During winter, calving, postcalving and late summer seasons, the response curve showed a nonlinear relationship with distance to road. During winter, there was a decline in suitability curve within ~5 km of roads. During the calving season, there was a small decline from ~4–6 km, a steeper decline from 0–4 km. During the postcalving and late summer seasons, there was a steep decline within ~1.0 km.

OTHER MAMMALS

In addition to caribou, we observed grizzly bears, muskoxen, and a single polar bear in the study areas in 2020. There were two observations of grizzly bear groups in the GMT or CRD survey areas in 2020. A sow with one cub was observed on the eastern Colville Delta on 19 August and a single adult bear was observed near the coast in the GMT survey area on 27 August (Figure 32). One adult polar bear was observed in the northwestern Colville Delta on 27 August. There were five observations of muskoxen near the Colville River in 2020 (Figure 24). Two adult muskoxen were observed in the southeastern GMT area on 6 October. The other four observations were outside the survey areas: there were two observations of single adults; one observation of three adults and one calf; and a group of 33 adults and approximately nine calves. ADFG also reported observing a similar size group of muskoxen (34 adults and 10 calves) in the area during mid-June (Lenart 2020). A single wolverine was observed west of the GMT area on 19 June (Figure 24).

DISCUSSION

WEATHER, SNOW, AND INSECT CONDITIONS

Weather conditions exert strong effects on caribou populations throughout the year in northern Alaska. Deep winter snow and icing events increase the difficulty of travel, decrease forage availability, and increase susceptibility to predation (Fancy and White 1985, Griffith et al. 2002, Bieniek et al. 2018). Severe cold and wind events can cause direct mortality of caribou (Dau 2005). Late snowmelt can delay spring migration, cause lower calf survival, and decrease future reproductive success (Finstad and Prichard 2000, Griffith et al. 2002, Carroll et al. 2005). In contrast, hot summer weather can depress weight gain and subsequent reproductive success by increasing insect harassment at an energetically stressful time of year, especially for lactating females (Fancy 1986, Cameron et al. 1993, Russell et al. 1993, Weladji et al. 2003).

Variability in weather conditions results in large fluctuations in caribou density during the insect season as caribou aggregate and move rapidly through the study area in response to wind conditions and changes in insect activity. On the central coastal plain (including the study area), caribou typically move upwind and toward the coast in response to mosquito harassment and then disperse inland when mosquito activity abates in response to cooler temperatures and increased winds (Murphy and Lawhead 2000, Yokel et al. 2009, Wilson et al. 2012).

The absence of mosquitoes during mid- to late June likely improves caribou body condition after

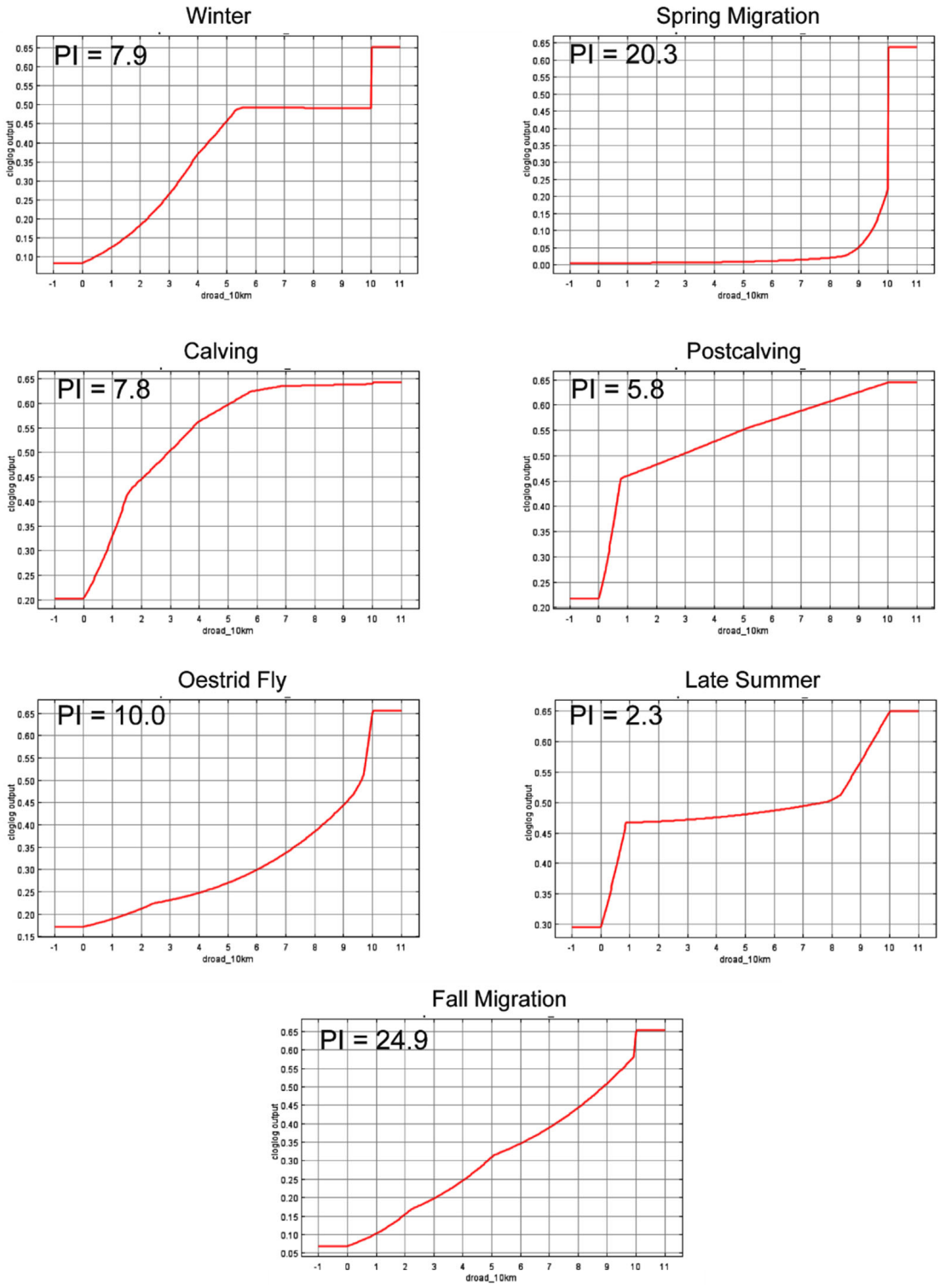

Figure 31. Response curves and permutation importance of the distance to road variable for a Maxent model with predicted seasonal suitability as one variable and distance to road as a second variable. Caribou locations were limited to those in 2019 and 2020 after the GMT2 road was built and distances greater than 10 km were set to 10 km to limit the zone of inference. The mosquito season was excluded due to a low sample size. Note some low values may represent normal interannual variability in caribou distribution or a low use of the general area that also occurred prior to construction (see text for details).

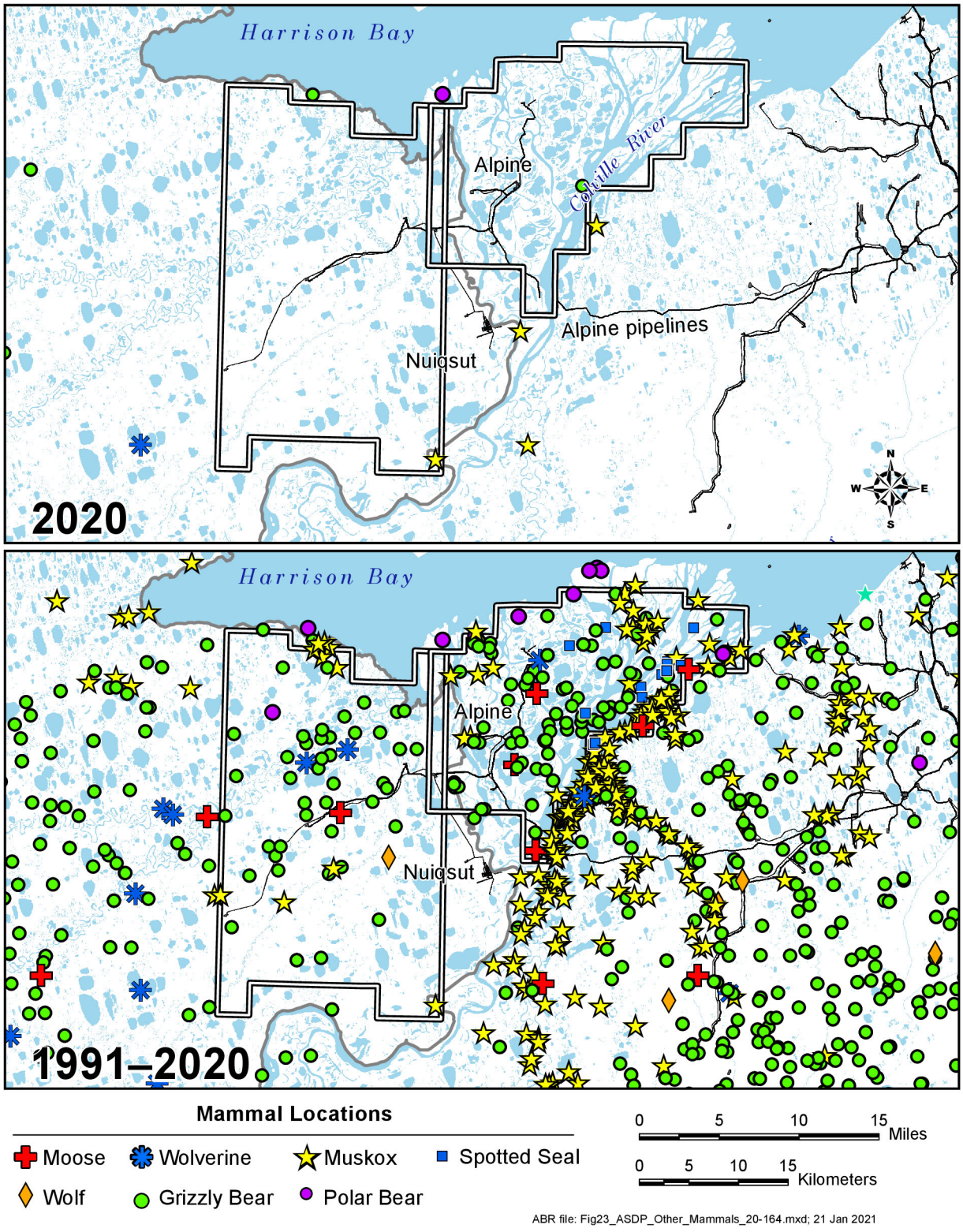

Figure 32. Distribution of other large mammals observed during aerial and ground surveys in the Colville River Delta or Greater Moose's Tooth survey areas, April–October 2020 and for the years 1992–2019 combined.

calving, and warm temperatures during July likely result in increased movement rates and decreased foraging, which can cause a decline in body condition. In 2020, multiple weather conditions were likely to be favorable for caribou. The timing of snowmelt was near normal, resulting in access to highly nutritious forage during calving, but the cool and windy weather was likely to result in low levels of insect harassment. Delayed onset of seasonal snow cover due high temperatures in September (typical of recent years on the coastal plain; Cox et al. 2017) may have allowed caribou to increase their forage rate and improve their body condition prior to the onset of winter, although forage quality is greatly diminished in the fall compared to the summer.

CARIBOU DISTRIBUTION AND MOVEMENTS

The TCH consistently uses the area west of the Colville River to some extent during all seasons of the year. Female TCH caribou numbers in the GMT and CRD survey areas are generally lowest during the calving and postcalving seasons, increase to their highest levels during the fall migration season, and then slowly decline through winter and spring migration. Male numbers, in contrast, are highest from calving–oestrid fly seasons, moderate during late summer and fall migration, and lowest during winter and spring migration. The CAH primarily uses the area east of the Colville River, although movements across the Colville River and onto the Colville River delta are not uncommon. CAH use of the CRD survey area is variable with rare episodic events, most frequently occurring during the mosquito and oestrid fly seasons, and low use during the remainder of the year. CAH caribou rarely use the GMT survey area, although several notable incursions have been recorded sporadically over the years, as described below.

Caribou density typically is lower in the GMT and CRD survey areas than in the BTN or BTS survey areas (Prichard et al. 2020d). Aerial transect surveys conducted since 2001 have demonstrated that only low levels of calving occur in the GMT and CRD survey areas. This result is consistent with analysis of telemetry data, which confirms that most TCH females calve around Teshekpuk Lake or areas to the west (Kelleyhouse 2001, Carroll et al. 2005, Person et al. 2007, Wilson et al. 2012, Parrett 2015a, Prichard et al. 2019a). East of the Colville River delta, high density calving occurs by CAH caribou (Prichard et al. 2020a). A few collared CAH females have switched to the TCH and calved west of the Colville River in isolated years (notably 2001), but it is a rare occurrence (Arthur and Del Vecchio 2009; Lenart 2009, 2015; Prichard et al. 2020b).

In 2020, we observed our highest density of caribou in the GMT survey area during the postcalving season. Telemetry data indicate that animals were still migrating north from wintering in the Brooks Range. These caribou are often males and non-parturient females (Person et al. 2007). A disproportionate number of male caribou winter in the central Brooks Range in most years (Prichard et al. 2019a) and some of these animals move through the GMT area during their return to the summer range. As a result, some of our estimates of caribou distribution and habitat suitability during calving and postcalving will differ depending on if the data is from telemetry collars which are deployed mostly on females, or from aerial surveys which count all caribou.

Transect surveys during mosquito season are inefficient for locating caribou aggregations because of the rapid speed of caribou movements during that period (Prichard et al. 2014) and the highly aggregated and unpredictable nature of caribou distributions. Since 2001, the only transect survey during which large groups of insect-harassed caribou (numbering from 200 to 2,400 animals) were found in the GMT survey area was on 2 August 2005 (Lawhead et al. 2006). In 2020, we did not conduct an aerial survey during the oestrid fly season in the GMT and CRD survey areas at the request of local subsistence hunters.

Caribou density decreased to relatively low levels in the GMT survey area during the late summer survey on 27 August but increased modestly during the early October survey as caribou dispersed inland and a portion of the herd moved towards the Brooks Range to winter. The highest average (0.6 caribou/km^2) and maximum (2.6 caribou/km^2) densities of caribou in the GMT survey area are usually in the fall migration season. High caribou densities have also been recorded

sporadically in the GMT survey region in late winter (e.g., 1.8 caribou/km² in April 2003).

Research to date shows that caribou are most likely to occur in the CRD survey area during the insect season (mosquito and oestrid fly periods, from late June to early August), and during the late summer season in late August when oestrid flies may still be active. In 2020, surveys of the CRD were not planned during the postcalving, oestrid fly, and late summer seasons due to predicted low use. Use of the area is primarily by CAH animals during the mosquito season and animals from both the TCH and CAH during the oestrid fly season. When mosquito harassment begins in late June or early July, caribou move toward the coast where lower temperatures and higher wind speeds prevail (Murphy and Lawhead 2000, Parrett 2007, Yokel et al. 2009, Wilson et al. 2012). The TCH typically moves to the area between Teshekpuk Lake and the Beaufort Sea, while the CAH typically moves to the coast east of the Colville River delta, often moving far to the east during late June and July. After oestrid fly harassment begins in mid-July, the large groups that formed in response to mosquito harassment begin to break up and caribou disperse inland, seeking elevated or barren habitats such as sand dunes, mudflats, and river bars, with some using shaded locations in the oilfields under elevated pipelines and buildings (Lawhead 1988, Murphy and Lawhead 2000, Person et al. 2007, Wilson et al. 2012).

Use of the Colville River delta by large numbers of caribou is relatively uncommon and does not occur annually. Large numbers have been recorded periodically in past summers (e.g., 1992, 1996, 2001, 2005, 2007, 2010, 2019) as aggregations moved onto or across the delta during or immediately after periods of insect harassment (Johnson et al. 1998, Lawhead and Prichard 2002, Lawhead et al. 2008). The most notable such instance was an unusually large movement westward onto the delta by at least 10,700 CAH caribou in the third week of July 2001, ~6,000 of which continued across the delta into northeastern NPRA (Lawhead and Prichard 2002, Arthur and Del Vecchio 2009) and moved west through the area traversed by the GMT1/MT6 road and planned GMT2/MT7 road. The highest number of caribou seen on Colville River delta transect surveys during 2001–2020 was recorded on 2 August 2005, when 994 caribou were found in the survey area (2.01 caribou/km²; Lawhead et al. 2006). At least 3,241 TCH caribou were photographed by ADFG on the outer delta on 18 July 2007 and up to several thousand more may have moved onto the delta by the end of July that year (Lawhead et al. 2008). Two large groups of caribou (>1,000 each) were recorded on the Colville River delta in July 2010 by time-lapse cameras set up to observe bird nests for a different study, but the herd affiliation of those animals was not clear (Lawhead et al. 2011). In late July 2020, a group of approximately 500 caribou were reported on the Colville Delta, near CD-3, in late July (R. McGhee, CPAI, pers. comm.), but no collared caribou were in the area at that time. Because such movements by large numbers of insect-harassed caribou often occur quickly, telemetry data are often more useful for describing caribou distribution and movements during the insect season than are periodic aerial transect surveys.

The ASDP and GMT infrastructure on and adjacent to the Colville River delta is encountered occasionally by caribou from both herds. Movements by satellite- and GPS-collared TCH and CAH caribou into the vicinity of ASDP infrastructure have occurred infrequently during the calving, mosquito, and oestrid fly seasons and during fall migration since monitoring began in the 1980s, well before any infrastructure was built. In the time since its construction in 2013–2014, only one collared caribou has crossed the CD-5 road (based on straight-line movements between locations), but very few crossings were recorded there in the years before construction either. In recent years, radio-collared TCH caribou and, to a lesser extent, CAH caribou have occasionally crossed the GMT1/MT6 or GMT2/MT7 road corridor alignments, with the highest crossing rates during fall migration and lowest during the postcalving and mosquito seasons.

The GMT2/MT7 alignment is located in a geographic area that currently receives low-density use by caribou during most seasons, however, during the 2020 late summer and fall migration season, many TCH caribou moved towards the GMT1/MT6 and GMT2/MT7 roads from the north and west with only a few individuals continuing on to cross the roads. Most caribou paralleled the road along the west side until they passed the

infrastructure. This apparent alteration of direction of travel followed by paralleling the road may be attributed to TCH caribou having less exposure to pipelines than CAH caribou as well as a natural tendency of caribou to follow linear features (LeResche and Linderman 1975, Bergerud et al. 1984, Lawhead et al. 1993, Prichard and Welch 2021). During the last two years, many TCH caribou have migrated towards Umiat in the fall and then spread out along the Colville River during winter with many moving back north along the west side of the river, increasing the likelihood that caribou encounter GMT infrastructure.

The harvest of caribou by Nuiqsut hunters tends to peak during the months of July and August, with fewer usually being taken in June and September–October and the smallest harvests occurring in other months (Pedersen 1995, Brower and Opie 1997, Fuller and George 1997, Braem et al. 2011, SRB&A 2017). Historically, the greatest proportion of the Nuiqsut caribou harvest has been taken by boat-based hunters during the open-water period (SRB&A 2017). The timing of hunting activity in relation to seasonal use of the study area by caribou suggests that caribou harvested on the Colville River delta by hunters in July and August could be from either herd, depending on the year. In contrast, caribou harvested upstream of the delta on the Colville River during the open-water period and west and south of Nuiqsut during October and the winter months are likely to be TCH animals.

Using harvest data (Braem et al. 2011) and telemetry data from 2003–2007, Parrett (2013) estimated that TCH caribou comprised 86% of the total annual harvest by Nuiqsut hunters during those years. Beginning in 2004, the distribution of the CAH during the insect season shifted farther eastward than had been observed in earlier years, so fewer caribou from that herd used the Colville River delta in summers 2004–2007. Since 2014, however, more CAH caribou have remained in the western portion of their range, near the Colville River, and have used the delta more in midsummer, similar to the years preceding 2004. The construction of the Nuiqsut Spur Road and CD-5 access road resulted in increased use of those roads for subsistence harvest of caribou (SRB&A 2017) and the new GMT1/MT6 and GMT2/MT7 roads are likely to increase subsistence hunter access to seasonal ranges used consistently year-round by TCH caribou.

SPECIES DISTRIBUTION MODEL

We chose to use a machine learning approach to model caribou distributions and habitat associations in 2020 because caribou resource selection is likely complex and difficult to predict; the highly flexible machine learning approach that can model nonlinear relationships and variable interactions may be more effective at capturing that complexity. Maxent builds flexible models with combinations of variables, variable transformations, and multiple variable interactions, including correlated variables, to find the best model for predicting a species' distribution (Phillips et al. 2006, 2017, Elith et al. 2011, Merow et al. 2013). Maxent can produce maps with high predictive power, but interpretation of variable importance and influence becomes more difficult, if not impossible, as model complexity increases (Phillips et al. 2006, Phillips 2017). For this reason, we reduced the number of variables included by using only the spatial scale for each variable with the greatest difference between used and random locations and by eliminating variables with high correlations with other variables.

Response curves are provided by the program, but these are generalizations of how each variable affects modeled suitability (Phillips 2017) and are dependent on the relationships between not only the predictor and the response, but correlations with other variables. Variables with no causal relationship with caribou selection may be correlated with important variables in the model or with a different variable that was not included in the model which is actually driving the relationship. Maxent may then assign importance to the non-important variable, or split importance among correlated variables depending on the path the model takes to arrive at the optimal solution. The model is capable of producing very similar and accurate predictions even if different variable combinations, percent contributions, or responses are used (Phillips 2017). Therefore, Maxent is generally more suited towards modeling a predictive space rather than identifying causal relationships and care must be taken in interpreting the importance and modeled relationship of each variable.

The two data sets (aerial transect surveys and radio telemetry) that were combined for the Maxent analysis provided complementary information for investigating broad patterns of resource selection. Telemetry data have higher spatial accuracy than do aerial survey data and are collected continuously throughout the year, albeit for a fairly small sample of individual caribou, mostly female. A single collared caribou that spends long periods of time within the study area can exert a large influence on distribution analysis. Because of the high variability in the amount of time spent in the study area by collared animals, we did not attempt to adjust for individual differences, other than limiting the frequency of locations in the analytical data set to one every 48 hours. In contrast, aerial transect survey data provide information on all caribou groups detected in the area (subject to sightability constraints) at the time of each survey, but the locations have lower spatial accuracy (~100 m) and surveys are conducted only periodically throughout the year. The lower spatial accuracy of aerial survey data was accommodated by using the mean proportion of habitats at spatial scales starting at 120m rather than the habitat types in individual 30-m pixels. Additionally, calculating mean proportions of habitat and other variables at multiple spatial scales allows evaluation of scale dependencies.

The two different data types also had different timing, especially during the winter season; only one aerial survey was conducted in that season in any given year (in mid–late April from 2002–2019 and in February 2020 for the BTS and BTN survey areas only), whereas telemetry locations were collected throughout the entire season. Despite these potential limitations, the combination of the two survey methods produced larger samples than were available for either data set alone and the resulting SDMs are broadly interpretable within the context of general patterns of caribou distributions on the central coastal plain.

Based on the guidelines on Hosmer and Lemeshow (2000), our mosquito season model performed excellently, our oestrid fly and spring migration models were adequate, and our winter, calving, postcalving, late summer, and fall migration models were below adequate, although better than a random model. This was not entirely unexpected. Caribou are a migratory species that range over a wide array of habitats and forage on a variety of plants. We used almost two decades of data from both aerial and telemetry data to predict caribou distributions. Therefore, lower AUC values most likely reflect the generalist habitats or non-selective movement patterns during some seasons.

Use of the aerial survey areas by caribou varies widely among seasons. These differences are related to west-to-east and distance to coast distributions, distribution of habitat types, topography, snow cover, and forage availability. In general, broad geographic patterns in distribution (west-to-east, distance to coast) were the strongest predictors of caribou distribution in almost every season, due in large part to the seasonal distribution patterns during key life cycle stages, but other factors such as topography and habitat proportions were also important seasonally. The important variables were similar to those identified with our RSF models (Prichard et al. 2020b). The flexible modeling framework of the Maxent, however, provides for better predictions and maps that more closely reflect where caribou have been recorded.

Because the GMT survey area is on the eastern edge of the TCH range, a natural west-to-east gradient of decreasing density occurs throughout much of the year. Few caribou are located in the far east of the GMT survey area year-round. During calving, the highest densities of TCH females typically calve near Teshekpuk Lake outside of the study area (Person et al. 2007, Wilson et al. 2012, Parrett 2015a). The past 3 years of aerial survey data in the BTN and BTS survey areas, as well as previous years of surveys in the GMT survey area, suggest limited calving activity. Therefore, our results likely reflect the suitability of non-parturient females and males, many of which are migrating north from the Brooks Range towards Teshekpuk Lake. Migrating caribou often cross the Colville River at Ocean Point and enter our study area near and southwest of GMT2/MT7.

During most seasons, the model was improved with some variable of topographic relief which tends to be higher along or adjacent to streams and creeks or lakes in the study area. Different studies have reported conflicting conclusions regarding the importance of topography, which may be related in part to the ways in which it has been calculated. Nellemann

and Thomsen (1994) and Nellemann and Cameron (1996) reported that CAH caribou selected areas of greater terrain ruggedness (as calculated by hand from topographic maps) in the Milne Point calving concentration area, but Wolfe (2000) and Lawhead et al. (2004), using a digital method of calculating terrain ruggedness, found no consistent relationship with terrain ruggedness in a larger calving area used by CAH females during calving. We used a number of different topographic relief metrics because the flexible nature of machine learning algorithms allows inclusion of many variables and the model determines which variable(s) are the best predictors of caribou occurrence. However, because of the inherent similarities of the topographic relief variables and because the Maxent model is often capable of calculating models that perform similarly well using a combination of variables, many of the topographic relief variables could be interchangeable. For example, the late summer season model used a combination of TPI and LED to highlight the importance of streams as good habitat. Had TPI and LED not been included in the model, Maxent could have arrived at a very similar model using, for example, greater contributions from ruggedness, gentle slopes, or riverine habitats. However, by including more variables, Maxent can create a map that likely has higher power for predicting overall suitability.

The avoidance of *Carex aquatilis*, Flooded Tundra, and Wet Tundra during fall and winter has been documented in previous years using different analyses (Lawhead et al. 2015, Prichard et al. 2020d), as well as selection of areas along Fish and Judy creeks during the postcalving, oestrid fly, and late summer seasons and avoidance of riverine habitat during winter. The riparian habitats along Fish and Judy creeks provide a complex interspersion of barren ground, dunes, and sparse vegetation that provide good oestrid fly-relief habitat near foraging areas (Nellemann and Thomsen 1994, Nellemann and Cameron 1996). Moss habitats are relatively rare on the landscape but are found primarily on the slopes adjacent to creeks and streams, an important area during the spring migration season

Comparison of caribou habitat use across studies is complicated by the fact that different investigators have used different habitat classifications. Kelleyhouse (2001) and Parrett (2007) reported that TCH caribou selected wet graminoid vegetation during calving and Wolfe (2000) reported that CAH caribou selected wet graminoid or moist graminoid classes; those studies used the vegetation classification by Muller et al. (1998, 1999). Using a habitat classification similar to the one developed by Jorgenson et al. (2003), Lawhead et al. (2004) found that CAH caribou in the Meltwater study area in the southwestern Kuparuk oilfield and the adjacent area of concentrated calving selected Moist Sedge–Shrub Tundra, the most abundant type in their study area, during calving. Wilson et al. (2012) used TCH telemetry data and the habitat classification of BLM and Ducks Unlimited (2002), as in this study, to investigate summer habitat selection at two different spatial scales, and concluded that TCH caribou consistently selected sedge/grass meadow and avoided flooded vegetation. In general, we also found that caribou appear to avoid wetter habitats (flooded tundra, *Carex aquatilus*) during most seasons (Prichard et al 2020a).

We used NDVI to estimate vegetative biomass in this study because other researchers have reported significant relationships between caribou distribution and biomass variables (NDVI_Calving, NDVI_621, and NDVI_Rate) during the calving period (Wolfe 2000, Griffith et al. 2002, Kelleyhouse 2001). The first flush of new vegetative growth that occurs in spring among melting patches of snow is valuable to foraging caribou (Kuropat 1984, Klein 1990, Johnstone et al. 2002), but the spectral signal of snow, ice, and standing water complicates NDVI-based inferences in patchy snow and recently melted areas. Snow, water, and lake ice all depress NDVI values. Therefore, estimates of NDVI variables change rapidly as snow melts and exposes standing dead biomass, which has positive NDVI values (Sellers 1985 [cited in Hope et al. 1993], Stow et al. 2004), and the initial flush of new growth begins to appear.

Johnson et al. (2018) used NDVI values as well as habitat type, distance to coast, and days from peak NDVI to develop models to predict biomass, nitrogen, and digestible energy for a given location on a given day. These models should, if successful, provide metrics that are more

directly related to caribou forage needs than NDVI alone. While daily biomass, nitrogen, and NDVI rarely had permutation importance values >5, one or more of these 3 variables were often more important than other environmental variables. We found evidence of a slight selection for areas that typically have higher biomass and NDVI during the calving season, higher biomass during the postcalving season, and higher nitrogen during the oestrid fly, but some of these relationships may have had more to do with habitat associations and distributional shifts due to insect avoidance. For instance, daily biomass had a permutation importance of 5.2 during the oestrid fly season, but the relationship was negative, likely because caribou were selecting for more non-vegetated habitats for insect relief. The relationships with these derived variables warrant further investigation.

It is possible that these models do not predict biomass and nitrogen well in this area. Johnson et al. (2018) used a land cover map (Boggs et al. 2016) based on a land cover map created by Ducks Unlimited for the North Slope Science Initiative (NSSI 2013) that has discontinuities in classification methodology and imagery in our analysis area. These discontinuities could translate into inaccurate forage metrics in our analysis area. Alternatively, caribou may not be selecting for forage nitrogen or forage biomass at this scale of selection and caribou distribution may be better predicted by high NDVI values which tend to be correlated with locations that have both large amounts of vegetation and less surface water in the pixel. Caribou movements are influenced by many factors other than forage and only a portion of GPS locations represent caribou that are actively feeding. It does not appear that our study area is heavily used by calving caribou and the study area likely has many non-parturient and migrating caribou present during this season. A demographically diverse local population could complicate modeling efforts, especially when one demographic is likely moving long distances and possibly not exhibiting highly selective behavior.

In this study, we found evidence that suitability in the winter and spring was consistent at low and moderate SWE levels but then dropped off quickly at higher levels, indicating an avoidance of deep snow. The daily SWE dataset was a new addition to the analysis for 2020 and initially appears to be a better predictor of caribou distribution than median snowmelt date during the winter and spring migration seasons. Previous studies have not produced consistent results concerning the calving distribution of northern Alaska caribou herds in relation to snow cover. Kelleyhouse (2001) concluded that TCH females selected areas of low snow cover during calving and Carroll et al. (2005) reported that TCH caribou calved farther north in years of early snow melt. Wolfe (2000) did not find any consistent selection for snow-cover classes during calving by the CAH, whereas Eastland et al. (1989) and Griffith et al. (2002) reported that calving PCH caribou preferentially used areas with 25–75% snow cover. Our results imply only a slight increase in suitability as median snowmelt date increases.

Interpretation of analytical results is complicated by the fact that caribou do not require snow-free areas in which to calve and are able to find nutritious forage even in patchy snow cover. The presence of patchy snow in calving areas is associated with the emergence of highly nutritious new growth of forage species, such as tussock cottongrass (Kuropat 1984, Griffith et al. 2002, Johnstone et al. 2002), and it also may increase dispersion of caribou and create a complex visual pattern that reduces predation (Bergerud and Page 1987, Eastland et al. 1989). Interpretation also is complicated by high annual variability in the extent of snow cover and the timing of snowmelt among years, as well as by variability in detection of snowmelt dates on satellite imagery because of cloud cover.

The current emphasis of this study is to monitor caribou distribution and movements in relation to the existing facilities in the ASDP/GMT study area and to compile predevelopment baseline data on caribou density and movements in the GMT2/MT7 portion of the survey area. Detailed analyses of the existing patterns of seasonal distribution, density, and movements are providing important insights about the ways in which caribou currently use the study area. Although both the TCH and CAH recently underwent sharp declines in population due to decreased survival of both adults and calves, particularly after the prolonged winter of 2012–2013, both herds increased in size in the latest counts from July 2017 (TCH) and July

2019 (CAH). In recent years, the TCH calving distribution has expanded both to the west and the southeast, whereas the winter distribution has varied widely among years (Parrett 2013, Prichard et al. 2019a). The CAH has shown indications of changes in seasonal distribution, with more caribou calving west of the Sagavanirktok River, remaining farther north longer during fall, wintering on the north side of the Continental Divide, and possibly more intermixing with adjacent herds (ADFG 2017, Prichard et al. 2020b).

We continue to compile data on caribou movements in the GMT area following construction of the roads. Seasonal patterns of movements can vary widely among years and the GMT area is near the eastern edge of the TCH range. Both of these factors make it difficult to draw inferences on impacts of infrastructure. We used Maxent to compare caribou distribution within 10 km of roads since 2018 with expected seasonal habitat suitability based on analysis of all data. This analysis suggested that the general area of the roads had somewhat lower use during the spring migration, oestrid fly, and fall migration seasons. This could be due to larger scale changes in seasonal movements or could just reflect the lower use of the area that occurred even prior to development. During the calving, postcalving, late summer, and winter seasons, there was some evidence of less use of the areas adjacent to roads, although the distance varied by season. There were few data in the area during the mosquito season because most TCH caribou are located near the coast during that season.

We caution that these results should be considered preliminary. Because of the large annual variability in movements, multiple years of data are required to understand large spatial changes. The distribution of TCH caribou during fall migration, winter, and spring migration were influenced by the proportion of caribou wintering in the Brooks Range, which varied annually. Previous research on the CAH has found that caribou do avoid active roads and pads during the calving season (Cameron et al. 1995, Lawhead et al. 2004, Johnson et al. 2020), but this avoidance declines following calving (Smith et al. 1994, Lawhead et al. 2004, Johnson et al. 2020, Prichard et al. 2020a). There is also evidence that impacts from development are largest right after construction and when caribou have had less previous exposure to infrastructure (Smith et al. 1994, Prichard et al. 2020a).

For this report, we incorporated several data collection methods and analyses to better understand the seasonal distributions, movements, and herd associations of caribou using the area. By conducting aerial surveys during different seasons over the course of 19 years in northeastern NPRA, we have compiled an extensive dataset that allows us to understand the seasonal patterns as well as the variability in caribou distribution over this specific area. The use of telemetry data provided high-resolution locations for a subset of caribou throughout the year. This large and growing database allows us to understand caribou movements through the area for the two different herds which use the area. It also allows us to put local caribou movements in the study area into the broader context of the annual herd ranges and seasonal herd distributions. Lastly, we incorporated aerial survey results and telemetry data with remote sensing information on land cover, vegetative biomass, and snow cover to better understand the factors determining seasonal distribution of caribou. This understanding of the underlying factors that are important to caribou is useful when evaluating potential future changes in caribou distribution that may be attributable to development or a changing climate.

OTHER MAMMALS

There were few observations of other mammals in the GMT and CRD survey areas in 2020, likely as a result of fewer observers working in the area. In the past, there have been regular sightings of grizzly bears, and occasional observations of moose, wolves, wolverines, and polar bears along the coast (Figure 24). Spotted seals are regularly observed hauled out in several locations of the Colville River delta during mid- to late summer.

In recent years, two mixed-sex groups of muskoxen were located in the area, one along the Colville River and delta and the other between the Kuparuk River delta and Milne Point (Prichard et al. 2018, 2019, Prichard and Welch 2020, 2021). In 2019, most of the muskoxen along the Kuparuk River moved to the Sagavanirktok River and in

2020, ADFG only observed 4 muskoxen along the Kuparuk River (Lenart 2020). The group along the Colville River was larger than had been observed in recent years.

The muskox population on the North Slope of Alaska has declined since 1999, evidently due to a combination of predation by grizzly bears, human interactions, disease, and unusual mortality events such as drowning (Reynolds et al. 2002, Shideler et al. 2007, Lenart 2015b). The decline was noted first in the Arctic National Wildlife Refuge but later was documented farther west on the central coastal plain. Population surveys by ADFG in late winter (April) found 216 muskoxen in 2006. The population on the central North Slope then remained relatively stable at approximately 190–200 animals for approximately a decade (Lenart 2015b, Arthur and Del Vecchio 2017). Calf production and survival have been high in recent years which appeared to result in an increase in the population. The minimum population was 298 animals in April 2020 (Lenart 2020). Predation by grizzly bears was the most common cause of death, responsible for an estimated 58% of calf mortalities and 62% of adult mortalities when a cause of death could be determined (Arthur and Del Vecchio 2017). Muskoxen have been observed in northeastern NPRA in the past, but in the pair observed in southeast GMT in 2020 are the first muskoxen observed west of the Colville River in recent years. The large group observed east of the Colville Delta may reflect high calf productivity in recent years and/or movements from other nearby groups.

Polar bears are observed periodically during aerial surveys in the area, with most observations occurring during late summer along the Beaufort Sea coast. With declining sea ice in summer and fall, more polar bears are expected to occur on the mainland and barrier islands during the open-water season (Schliebe et al. 2008). The proportion of radio-collared adult female polar bears coming ashore has tripled and the date of arrival on shore has advanced ~5 days/decade since the late 1990s (Atwood et al. 2016).

LITERATURE CITED

ADFG (Alaska Department of Fish and Game). 2017. Central Arctic caribou herd news. Winter 2016–17 edition. Alaska Department of Fish and Game, Division of Wildlife Conservation, Fairbanks, Alaska. 6 pp.

Anderson, R.P., and I. Gonzalez Jr. 2011. Species-specific tuning increases robustness to sampling bias in models of species distributions: an implementation with Maxent. Ecological Modeling 222: 2796–2811.

Arthur, S. M., and P. A. Del Vecchio. 2009. Effects of oil field development on calf production and survival in the Central Arctic Herd. Final research technical report, June 2001–March 2006. Federal Aid in Wildlife Restoration Project 3.46, Alaska Department of Fish and Game, Juneau, Alaska. 40 pp.

Bergerud, A. T., and R. E. Page. 1987. Displacement and dispersion of parturient caribou as antipredator tactics. Canadian Journal of Zoology 65: 1597–1606.

Bieniek, P.A., U.S. Bhatt, J.E. Walsh, R. Lader, B. Griffith, J. K. Roach, and R.L. Thoman. 2018. Assessment of Alaska rain-on-snow events using dynamical downscaling. Journal of Applied Meteorology and Climatology 57: 1847–1863.

BLM (Bureau of Land Management) and Ducks Unlimited. 2002. National Petroleum Reserve–Alaska earth-cover classification. U.S. Department of the Interior, BLM Alaska Technical Report 40, Anchorage, Alaska. 81 pp.

Boggs, K., L. Flagstad, T. Boucher, T. Kuo, D. Fehringer, S. Guyer, and M. Aisu. 2016. Vegetation Map and Classification: Northern, Western, and Interior Alaska. Second edition. Alaska Center for Conservation Science, University of Alaska Anchorage, Anchorage, Alaska. 110 pp.

Boyce, M. S., and L. L. McDonald. 1999. Relating populations to habitats using resource selection functions. Trends in Ecology and Evolution 14: 268–272.

Boyce, M. S., P. R. Vernier, S. E. Nielsen, and F. K. A. Schmiegelow. 2002. Evaluating resource selection functions. Ecological Modelling 157: 281–300.

Braem, N. M., S. Pedersen, J. Simon, D. Koster, T. Kaleak, P. Leavitt, J. Patkotak, and P. Neakok. 2011. Monitoring of annual caribou harvests in the National Petroleum Reserve in Alaska: Atqasuk, Barrow, and Nuiqsut, 2003–2007. Technical Paper No. 361, Alaska Department of Fish and Game, Division of Subsistence, Fairbanks, Alaska. 201 pp.

Brower, H. K., and R. T. Opie. 1997. North Slope Borough subsistence harvest documentation project: data for Nuiqsut, Alaska, for the period July 1, 1994 to June 30, 1995. North Slope Borough Department of Wildlife Management, Barrow, AK.

Brown, J., R. K. Haugen, and S. Parrish. 1975. Selected climatic and soil thermal characteristics of the Prudhoe Bay region. Pages 3–11 *in* J. Brown, editor. Ecological investigations of the tundra biome in the Prudhoe Bay region, Alaska. Biological Papers of the University of Alaska, Special Report No. 2, Fairbanks.

Burnham, K. P., and D. R. Anderson. 2002. Model Selection and Multimodel Inference: A Practical Information–Theoretic Approach. 2nd edition. Springer–Verlag, New York, NY. 488 pp.

Calcagno, V., and C. de Mazancourt. 2010. *glmulti*: an *R* package for easy automated model selection with (Generalized) Linear Models. Journal of Statistical Software 34: 1–29.

Cameron, R. D., W. T. Smith, and S. G. Fancy. 1989. Distribution and productivity of the Central Arctic Caribou Herd in relationship to petroleum development. Research progress report, Federal Aid in Wildlife Restoration Project 3.35, Alaska Department of Fish and Game, Juneau. 52 pp.

Cameron, R. D., D. J. Reed, J. R. Dau, and W. T. Smith. 1992. Redistribution of calving caribou in response to oil-field development on the Arctic Slope of Alaska. Arctic 45: 338–342.

Cameron, R. D., W. T. Smith, S. G. Fancy, K. L. Gerhart, and R. G. White. 1993. Calving success of female caribou in relation to body weight. Canadian Journal of Zoology 71: 480–486.

Cao, Y., R.E. DeWalt, J. L. Robinson, T. Tweddale, L. Hinz, and M. Pessino. 2013. Using Maxent to model the historic distributions of stonefly species in Illinois streams: the effects of regularization and threshold selections. Ecological Modelling. 259: 30– 39.

Carroll, G. M., A. K. Prichard, R. S. Suydam, L. S. Parrett, and D. A. Yokel. 2004. Unexpected movements of the Teshekpuk caribou herd. Paper presented at the 10th North American Caribou Workshop, 4–6 May 2004, Girdwood, AK. [abstract only]

Carroll, G. M., L. S. Parrett, J. C. George, and D. A. Yokel. 2005. Calving distribution of the Teshekpuk caribou herd, 1994–2003. Rangifer, Special Issue 16: 27–35.

CLS. 2016. Argos user's manual. CLS, Toulouse, France. Available online: http://www.argos-system.org/manual/ (accessed 16 February 2018).

Cox, C. J., R. S. Stone, D. C. Douglas, D. M. Stanitski, G. J. Divoky, G. S. Dutton, C. Sweeney, J. C. George, and D. U. Longenecker. 2017. Drivers and environmental responses to the changing annual snow cycle of northern Alaska. Bulletin of the American Meteorological Society 98: 2559–2577.

Crookston N and G. Rehfeldt. 2010. Degree-Days > 5 Degrees C (Based on Mean Monthly Temperature) Across All North America [raster digital data set]. U.S. Forest Service Rocky Mountain Research Station, Moscow Forestry Sciences Laboratory. Moscow, ID: http://forest.moscowfsl.wsu.edu/climate/current/.

Dau, J. R. 1986. Distribution and behavior of barren-ground caribou in relation to weather and parasitic insects. M.S. thesis, University of Alaska, Fairbanks. 149 pp.

Dau, J. 2005. Two caribou mortality events in northwestern Alaska: possible causes and management implications. Rangifer, Special Issue 16: 37–50.

Dau, J. R., and R. D. Cameron. 1986. Effects of a road system on caribou distribution during calving. Rangifer, Special Issue 1: 95–101.

Dick, B. L., S. L. Findholt, and B. K. Johnson. 2013. A self-adjusting expandable GPS collar for male elk. Journal of Wildlife Management 37: 887–892.

Duong, T. 2017. *ks*: Kernel Smoothing. *R* package version 1.10.7. Available online: https://CRAN.R-project.org/package=ks (accessed 16 February 2018).

Dunk, J. R., B. Woodbridge, T. M. Lickfett, G Bedrosian, B. R. Noon, D. W. LaPlante, J. L. Brown, and J. D. Tack. 2019. Modelling spatial variation in density of golden eagle nest sites in the western United States. PLoS ONE 14(9). e0223143. https://doi.org/10.1371/journal.pone.0223143

Eastland, W. G., R. T. Bowyer, and S. G. Fancy. 1989. Caribou calving sites relative to snow cover. Journal of Mammalogy 70: 824–828.

Elith, J., C. H. Graham, R. P. Anderson, et al., 2006. Novel methods improve prediction of species' distributions from occurrence data. Ecography. 29: 129–151.Elith, J., S. J. Phillips, T. Hastie, M. Dudik, Y. E. Chee, and C. J. Yates. 2011. A statistical explanation of MaxEnt for ecologists. Diversity and Distributions 17: 43–57.

Fancy, S. G. 1983. Movements and activity budgets of caribou near oil drilling sites in the Sagavanirktok River floodplain, Alaska. Arctic 36: 193–197.

Fancy, S. G. 1986. Daily energy budgets of caribou: a simulation approach. Ph.D. dissertation, University of Alaska, Fairbanks. 226 pp.

Fancy, S. G., and R. G. White. 1985. Energy expenditure by caribou while cratering in snow. Journal of Wildlife Management 49: 987–993.

Fancy, S. G., K. R. Whitten, N. E. Walsh, and R. D. Cameron. 1992. Population dynamics and demographics of caribou in developed and undeveloped areas of the Arctic Coastal Plain. Pages 1–21 *in* T. R. McCabe, D. B. Griffith, N. E. Walsh, and D. D. Young, editors. Terrestrial research: 1002 Area, Arctic National Wildlife Refuge. Interim report, 1988–1990. U.S. Fish and Wildlife Service, Anchorage.

Finstad, G. L., and A. K. Prichard. 2000. Climatic influence on forage quality, growth, and reproduction of reindeer on the Seward Peninsula, II: Reindeer growth and reproduction. Rangifer, Special Issue 12: 144 pp.

Fithian, W., J. Elith, T. Hastie, and D. A. Keith. 2015. Bias correction in species distribution models: pooling survey and collection data for multiple species. Methods in Ecology and Evolution 6: 424–438.

Fuller, A. S., and J. C. George. 1997. Evaluation of subsistence harvest data from the North Slope Borough 1993 census for eight North Slope villages for calendar year 1992. North Slope Borough Department of Wildlife Management, Barrow, AK.

Galante, P. J., B. Alade, R. Muscarella, S. A. Jansa, S. M. Goodman, and R. P. Anderson. 2018. The challenge of modeling niches and distributions for data-poor species: a comprehensive approach to model complexity. Ecography. 41: 726–736

Gasaway, W. C., S. D. DuBois, D. J. Reed, and S. J. Harbo. 1986. Estimating moose population parameters from aerial surveys. Biological Papers of the University of Alaska, No. 22, Fairbanks. 108 pp.

Gorelick, N., M. Hancher, M. Dixon, S. Ilyushchenko, D. Thau, and R. Moore. 2017. Google Earth Engine: planetary-scale geospatial analysis for everyone. Remote Sensing of Environment 202: 18–27.

Griffith, D. B., D. C. Douglas, N. E. Walsh, D. D. Young, T. R. McCabe, D. E. Russell, R. G. White, R. D. Cameron, and K. R. Whitten. 2002. Section 3: The Porcupine caribou herd. Pages 8–37 *in* D. C. Douglas, P. E. Reynolds, and E. B. Rhode, editors. Arctic Refuge coastal plain terrestrial wildlife research summaries. U.S. Geological Survey, Biological Resources Division, Biological Science Report USGS/BRD/BSR-2002-0001.

Hope, A. S., J. S. Kimball, and D. A. Stow. 1993. The relationship between tussock tundra spectral properties and biomass and vegetation composition. International Journal of Remote Sensing 14: 1861–1874.

Horne, J. S., E. O. Garton, S. M. Krone, and J. S. Lewis. 2007. Analyzing animal movements using Brownian bridges. Ecology 88: 2354–2363.

Hosmer, D. S. and S. Lemeshow. 2000. Applied Logistic Regression, 2nd Ed. Chapter 5, John Wiley and Sons, New York, NY. 160–164

Jenness J, B. Brost, and P. Beier. 2013. Land Facet Corridor Designer: Extension for ArcGIS. Flagstaff, AZ: Jenness Enterprises. http://www.jennessent.com/arcgis/land_facets.htm.

Jensen, P. G., and L. E. Noel. 2002. Caribou distribution in the northeast National Petroleum Reserve–Alaska, summer 2001. Chapter 3 *in* M. A. Cronin, editor. Arctic Coastal Plain caribou distribution, summer 2001. Report for BP Exploration (Alaska) Inc., Anchorage, by LGL Alaska Research Associates, Inc., Anchorage.

Johnson, C. B., B. E. Lawhead, J. R. Rose, M. D. Smith, A. A. Stickney, and A. M. Wildman. 1998. Wildlife studies on the Colville River delta, Alaska, 1997. Sixth annual report for ARCO Alaska, Inc., Anchorage, by ABR, Inc., Fairbanks. 144 pp.

Johnson, C. B., J. P. Parrett, T. Obritschkewitsch, J. R. Rose, K. B. Rozell, and P. E. Seiser. 2015. Avian studies for the Alpine Satellite Development Project, 2014. 12th annual report for ConocoPhillips Alaska, Inc., and Anadarko Petroleum Corp., Anchorage, by ABR, Inc., Fairbanks. 124 pp.

Johnson, H.E., T.S. Golden, L.G. Adams, D.D. Gustine, and E.A. Lenart. 2020. Caribou use of habitat near energy development in Arctic Alaska. Journal of Wildlife Management DOI: 10.1002/jwmg.21809

Johnson, H. E., D. D. Gustine, T. S. Golden, L. G. Adams, L. S. Parrett, E. A. Lenart, P. S. Barboza. 2018. NDVI exhibits mixed success in predicting spatiotemporal variation in caribou summer forage quality and quantity. Ecosphere 9: 10 pp.

Johnstone, J., D. E. Russell, and D. B. Griffith. 2002. Variations in plant forage quality in the range of the Porcupine caribou herd. Rangifer 22: 83–91.

Jorgenson, M. T., J. E. Roth, E. R. Pullman, R. M. Burgess, M. Raynolds, A. A. Stickney, M. D. Smith, and T. Zimmer. 1997. An ecological land survey for the Colville River delta, Alaska, 1996. Report for ARCO Alaska, Inc., Anchorage, by ABR, Inc., Fairbanks. 160 pp.

Jorgenson, M. T., J. E. Roth, M. Emers, S. Schlentner, D. K. Swanson, E. R. Pullman, J. Mitchell, and A. A. Stickney. 2003. An ecological land survey for the Northeast Planning Area of the National Petroleum Reserve–Alaska, 2002. Report for ConocoPhillips Alaska, Inc., Anchorage, by ABR, Inc., Fairbanks. 84 pp.

Jorgenson, M. T., J. E. Roth, M. Emers, W. Davis, E. R. Pullman, and G. V. Frost. 2004. An ecological land survey for the Northeast Planning Area of the National Petroleum Reserve–Alaska, 2003. Addendum to 2002 report for ConocoPhillips Alaska, Inc., and Anadarko Petroleum Corporation, Anchorage, by ABR, Inc., Fairbanks. 40 pp.

Kelleyhouse, R. A. 2001. Calving-ground selection and fidelity: Teshekpuk Lake and Western Arctic herds. M.S. thesis, University of Alaska, Fairbanks. 124 pp.

Klein, D. R. 1990. Variation in quality of caribou and reindeer forage plants associated with season, plant part, and phenology. Rangifer, Special Issue 3: 123–130.

Klimstra, R. 2018. Summary of Teshekpuk caribou herd photocensus conducted July 14, 2017. State of Alaska memorandum, Department of Fish and Game, Division of Wildlife Conservation (Northwest), Fairbanks. 6 pp.

Kranstauber, B., K. Safi, and F. Bartumeus. 2014. Bivariate Gaussian bridges: directional factorization of diffusion in Brownian bridge models. Movement Ecology 2: 5. doi.org/10.1186/2051-3933-2-5.

Kranstauber, B., M. Smolla, and A.K. Scharf. 2017. *Move*: visualizing and analyzing animal track data. *R* package version 3.0.1. Available online: https://CRAN.R-project.org/package=move (accessed 16 February 2018).

Kuropat, P. J. 1984. Foraging behavior of caribou on a calving ground in northwestern Alaska. M.S. thesis, University of Alaska, Fairbanks. 95 pp.

Lair, H. 1987. Estimating the location of the focal center in red squirrel home ranges. Ecology 68: 1092–1101.

Lawhead, B. E. 1988. Distribution and movements of Central Arctic Herd caribou during the calving and insect seasons. Pages 8–13 *in* R. Cameron and J. Davis, editors. Reproduction and calf survival. Proceedings of the 3rd North American Caribou Workshop. Wildlife Technical Bulletin No. 8, Alaska Department of Fish and Game, Juneau.

Lawhead, B. E., and A. K. Prichard. 2002. Surveys of caribou and muskoxen in the Kuparuk–Colville region, Alaska, 2001. Report for Phillips Alaska, Inc., Anchorage, by ABR, Inc., Fairbanks. 37 pp.

Lawhead, B. E., A. K. Prichard, M. J. Macander, and M. Emers. 2004. Caribou mitigation monitoring study for the Meltwater Project, 2003. Third annual report for ConocoPhillips Alaska, Inc., Anchorage, by ABR, Inc., Fairbanks. 104 pp.

Lawhead, B. E., A. K. Prichard, and M. J. Macander. 2006. Caribou monitoring study for the Alpine Satellite Development Program, 2005. First annual report for ConocoPhillips Alaska, Inc., Anchorage, by ABR, Inc., Fairbanks. 102 pp.

Lawhead, B. E., A. K. Prichard, and M. J. Macander. 2007. Caribou monitoring study for the Alpine Satellite Development Program, 2006. Second annual report for ConocoPhillips Alaska, Inc., Anchorage, by ABR, Inc., Fairbanks. 75 pp.

Lawhead, B. E., A. K. Prichard, and M. J. Macander. 2008. Caribou monitoring study for the Alpine Satellite Development Program, 2007. Third annual report for ConocoPhillips Alaska, Inc., Anchorage, by ABR, Inc., Fairbanks. 89 pp.

Lawhead, B. E., A. K. Prichard, and M. J. Macander. 2009. Caribou monitoring study for the Alpine Satellite Development Program, 2008. Fourth annual report for ConocoPhillips Alaska, Inc., Anchorage, by ABR, Inc., Fairbanks. 91 pp.

Lawhead, B. E., A. K. Prichard, and M. J. Macander. 2010. Caribou monitoring study for the Alpine Satellite Development Program, 2009. Fifth annual report for ConocoPhillips Alaska, Inc., Anchorage, by ABR, Inc., Fairbanks. 101 pp.

Lawhead, B. E., A. K. Prichard, and M. J. Macander. 2011. Caribou monitoring study for the Alpine Satellite Development Program, 2010. Sixth annual report for ConocoPhillips Alaska, Inc., Anchorage, by ABR, Inc., Fairbanks. 101 pp.

Lawhead, B. E., A. K. Prichard, and M. J. Macander. 2012. Caribou monitoring study for the Alpine Satellite Development Program, 2011. Seventh annual report for ConocoPhillips Alaska, Inc., Anchorage, by ABR, Inc., Fairbanks. 90 pp.

Lawhead, B. E., A. K. Prichard, M. J. Macander, and J. H. Welch. 2013. Caribou monitoring study for the Alpine Satellite Development Program, 2012. Eighth annual report for ConocoPhillips Alaska, Inc., Anchorage, by ABR, Inc., Fairbanks. 88 pp.

Lawhead, B. E., A. K. Prichard, M. J. Macander, and J. H. Welch. 2014. Caribou monitoring study for the Alpine Satellite Development Program, 2013. Ninth annual report for ConocoPhillips Alaska, Inc., Anchorage, by ABR, Inc., Fairbanks. 94 pp.

Lawhead, B. E., A. K. Prichard, M. J. Macander, and J. H. Welch. 2015. Caribou monitoring study for the Alpine Satellite Development Program, 2014. Tenth annual report for ConocoPhillips Alaska, Inc., Anchorage, by ABR, Inc., Fairbanks. 100 pp.

Lenart, E. A. 2009. GMU 26B and 26C, Central Arctic Herd. Pages 299–325 *in* P. Harper, editor. Caribou management report of survey and inventory activities, 1 July 2006–30 June 2008. Federal Aid in Wildlife Restoration Project 3.0, Alaska Department of Fish and Game, Juneau.

Lenart, E. A. 2015. Units 26B and 26C, Central Arctic. Chapter 18 *in* P. Harper and L. A. McCarthy, editors. Caribou management report of survey and inventory activities, 1 July 2012–30 June 2014. Alaska Department of Fish and Game, Species Management Report ADF&G/DWC/SMR-2015-4, Juneau.

Lenart, E. A. 2017. 2016 Central Arctic caribou photocensus results. State of Alaska memorandum, Department of Fish and Game, Division of Wildlife Conservation, Fairbanks. 5 pp.

Lenart, E. A. 2019. 2019 Central Arctic caribou photocensus results. State of Alaska Memorandum. Alaska Department of Fish and Game, Division of Wildlife Conservation. Fairbanks. 8 pp.

Macander, M. J., C. S. Swingley, K. Joly, and M. K. Raynolds. 2015. Landsat-based snow persistence map for northwest Alaska. Remote Sensing of Environment 163: 23–31.

Manly, B. F. J., L. L. McDonald, D. L. Thomas, T. L. McDonald, and W. P. Erickson. 2002. Resource selection by animals: statistical design and analysis for field studies. Second edition. Kluwer Academic Publishers, Dordrecht, The Netherlands. 209 pp.

McNay, R. S., J. A. Morgan, and F. L. Bunnell. 1994. Characterizing independence of observations in movements of Columbian black-tailed deer. Journal of Wildlife Management 58: 422–429.

Merow, C., M. J. Smith, and J. A. Silander, Jr. 2013. A practical guide to MaxEnt for modeling species' distributions: what it does, and why inputs and settings matter. Ecography 36: 1058–1069.

Mörschel, F. M. 1999. Use of climatic data to model the presence of oestrid flies in caribou herds. Journal of Wildlife Management 63: 588–593.

Muller, S. V., D. A. Walker, F. E. Nelson, N. A. Auerbach, J. G. Bockheim, S. Guyer, and D. Sherba. 1998. Accuracy assessment of a land-cover map of the Kuparuk River basin, Alaska: considerations for remote regions. Photogrammetric Engineering and Remote Sensing 64: 619–628.

Muller, S. V., A. E. Racoviteanu, and D. A. Walker. 1999. Landsat-MSS-derived land-cover map of northern Alaska: extrapolation methods and a comparison with photo-interpreted and AVHRR-derived maps. International Journal of Remote Sensing 20: 2921–2946.

Murphy, S. M., and B. E. Lawhead. 2000. Caribou. Chapter 4, pages 59–84 *in* J. Truett and S. R. Johnson, editors. The Natural History of an Arctic Oil Field: Development and the Biota. Academic Press, San Diego, CA.

Nellemann, C., and R. D. Cameron. 1996. Effects of petroleum development on terrain preferences of calving caribou. Arctic 49: 23–28.

Nellemann, C., and M. G. Thomsen. 1994. Terrain ruggedness and caribou forage availability during snowmelt on the Arctic Coastal Plain, Alaska. Arctic 47: 361–367.

Nicholson, K. L., S. M. Arthur, J. S. Horne, E. O. Garton, and P. A. Del Vecchio. 2016. Modeling caribou movements: seasonal ranges and migration routes of the Central Arctic Herd. PLoS One 11(4): e0150333. doi:10.1371/journal.pone.0150333.

Noel, L. E. 1999. Calving caribou distribution in the Teshekpuk Lake area, June 1998. Data report for BP Exploration (Alaska) Inc., Anchorage, by LGL Alaska Research Associates, Inc., Anchorage. 31 pp.

Noel, L. E. 2000. Calving caribou distribution in the Teshekpuk Lake area, June 1999. Report for BP Exploration (Alaska) Inc., Anchorage, by LGL Alaska Research Associates, Inc., Anchorage. 29 pp.

Noel, L. E., and J. C. George. 2003. Caribou distribution during calving in the northeast National Petroleum Reserve–Alaska, June 1998 to 2000. Rangifer, Special Issue 14: 283–292.

NSSI. 2013. North Slope Science Initiative land-cover mapping summary report. Report for NSSI by Ducks Unlimited, Inc., Rancho Cordova, CA. 51 p. + maps.

Parrett, L. S. 2007. Summer ecology of the Teshekpuk caribou herd. M.S. thesis, University of Alaska, Fairbanks. 149 pp.

Parrett, L. S. 2013. Unit 26A, Teshekpuk Caribou Herd. Pages 314–355 *in* P. Harper, editor. Caribou management report of survey and inventory activities, 1 July 2010–30 June 2012. Alaska Department of Fish and Game, Species Management Report ADF&G/DWC/SMR-2013-3, Juneau.

Parrett, L. S. 2015a. Unit 26A, Teshekpuk caribou herd. Chapter 17 *in* P. Harper and L. A. McCarthy, editors. Caribou management report of survey and inventory activities, 1 July 2012–30 June 2014. Alaska Department of Fish and Game, Species Management Report ADF&G/DWC/SMR-2015-4, Juneau.

Parrett, L. S. 2015b. Summary of Teshekpuk caribou herd photocensus conducted July 6, 2015. State of Alaska memorandum, Department of Fish and Game, Division of Wildlife Conservation (Northwest), Fairbanks. 6 pp.

Pebesma, E. J. 2004. Multivariate geostatistics in S: the *gstat* package. Computers & Geosciences 30: 683–691.

Pedersen, S. 1995. Nuiqsut. Chapter 22 *in* J. A. Fall and C. J. Utermohle, editors. An investigation of the sociocultural consequences of Outer Continental Shelf development in Alaska, Vol. V: Alaska Peninsula and Arctic. Technical Report No. 160, OCS Study MMS 95-014, Minerals Management Service, Anchorage.

Pennycuick, C. J., and D. Western. 1972. An investigation of some sources of bias in aerial transect sampling of large mammal populations. East African Wildlife Journal 10: 175–191.

Person, B. T., A. K. Prichard, G. M. Carroll, D. A. Yokel, R. S. Suydam, and J. C. George. 2007. Distribution and movements of the Teshekpuk caribou herd, 1990–2005: prior to oil and gas development. Arctic 60: 238–250.

Philo, L. M., G. M. Carroll, and D. A. Yokel. 1993. Movements of caribou in the Teshekpuk Lake herd as determined by satellite tracking, 1990–1993. North Slope Borough Department

of Wildlife Management, Barrow; Alaska Department of Fish and Game, Barrow; and U.S. Department of Interior, Bureau of Land Management, Fairbanks. 60 pp.

Phillips, S. J. 2017. A brief tutorial on Maxent. Available from: http://biodiversityinformatics.amnh.org/open_source/maxent/. Accessed on 15 June 2020.

Phillips, S. J., R. P. Anderson, and R. E. Schapire. 2006. Maximum entropy modeling of species geographic distributions. Ecological Modelling 190: 231–259.

Phillips, S. J., and M. Dudik. 2008. Modelling of species distributions with Maxent: new extensions and a comprehensive evaluation. Ocography. 31: 161–259

Phillips S. J., M. Dudík, and R. E. Schapire. 2020. Maxent software for modeling species niches and distributions (Version 3.4.1). Available from: http://biodiversityinformatics.amnh.org/open_source/maxent/. (accessed 15 September 2020)

Prichard, A.K., R. L. Klimstra, B. T. Person, and L. S. Parrett. 2019a. Aerial survey and telemetry data analysis of a peripheral caribou calving area in northwestern Alaska. Rangifer 43–58.

Prichard, A. K., B. E. Lawhead, E. A. Lenart, and J. H. Welch. 2020a. Caribou distribution and movements in a Northern Alaska Oilfield. Early View. Journal of Wildlife Management. https://doi.org/10.1002/jwmg.21932

Prichard, A. K., M. J. Macander, J. H. Welch, and B. E. Lawhead. 2017. Caribou monitoring study for the Alpine Satellite Development Program, 2015 and 2016. Twelfth annual report for ConocoPhillips Alaska, Inc., Anchorage, by ABR, Inc., Fairbanks. 62 p.

Prichard, A.K., L.S. Parrett, E.A. Lenart, J. Caikoski, K. Joly, and B.T. Person. 2020b. Interchange and overlap among four adjacent Arctic caribou herds. Journal of Wildlife Management. Journal of Wildlife Management. Early View. https://doi.org/10.1002/jwmg.21934

Prichard, A. K., and J. H. Welch. 2020. Mammal surveys in the Greater Kuparuk Area, northern Alaska, 2018–2019. Report for ConocoPhillips Alaska, Inc., and Greater Kuparuk Area, Anchorage, by ABR, Inc., Fairbanks.

Prichard, A. K., and J. H. Welch. 2021. Caribou us of the Greater Kuparuk Area, northern Alaska, 2020. Report for ConocoPhillips Alaska, Inc. Greater Kuparuk Area, Anchorage, by ABR, Inc., Fairbanks. 53 pp.

Prichard, A. K., J. H. Welch, and B. E. Lawhead. 2018a. Mammal surveys in the Greater Kuparuk Area, northern Alaska, 2017. Report for ConocoPhillips Alaska, Inc., Anchorage, by ABR, Inc., Fairbanks. 52 pp.

Prichard, A. K., J. H. Welch, M. J. Macander, and B. E. Lawhead. 2018b. Caribou monitoring study for the Alpine Satellite Development Program, 2017. Thirteenth annual report for ConocoPhillips Alaska, Inc., Anchorage, by ABR, Inc., Fairbanks. 63 pp.

Prichard, A. K., J. H. Welch, M. J. Macander, and B. E. Lawhead. 2019b. Caribou monitoring study for the Bear Tooth Unit Program, Arctic Coastal Plain, Alaska, 2018. Annual report for ConocoPhillips Alaska, Inc., Anchorage, by ABR, Inc., Fairbanks. 96 pp.

Prichard, A. K., J. H. Welch, M. J. Macander, and B. E. Lawhead. 2019c. Caribou monitoring study for the Alpine Satellite Development Program, 2018. Fourteenth annual report for ConocoPhillips Alaska, Inc., Anchorage, by ABR, Inc., Fairbanks. 88 pp.

Prichard, A. K., J. H. Welch, and M. J. Macander. 2020c. Caribou monitoring study for the Bear Tooth Unit Program, Arctic Coastal Plain, Alaska, 2019. Annual report for ConocoPhillips Alaska, Inc., Anchorage, by ABR, Inc., Fairbanks.

Prichard, A. K., J. H. Welch, and M. J. Macander. 2020d. Caribou monitoring study for the Alpine Satellite Development Program and Greater Moose's Tooth Unit, 2019. Annual report for ConocoPhillips Alaska, Inc., Anchorage, by ABR, Inc., Fairbanks.

Prichard, A. K., D. A. Yokel, C. L. Rea, B. T. Person, and L. S. Parrett. 2014. The effect of frequency of telemetry locations on movement-rate calculations in arctic caribou. Wildlife Society Bulletin 38: 78–88.

R Core Team. 2019. R: A language and environment for statistical computing. *R* Foundation for Statistical Computing, Vienna, Austria. URL: http://www.R-project.org.

Radosavljevic, A. and R. P. Anderson. 2014. Making better Maxent models of species distributions: complexity, overfitting and evaluation. Journal of Biogeography. 41: 629–643.Riggs, G. A., and D. K. Hall. 2015. MODIS snow products Collection 6 user guide. National Snow and Ice Data Center. Available online: https://nsidc.org/sites/nsidc.org/files/files/MODIS-snow-user-guide-C6.pdf (accessed 16 February 2018).

Riley S.J., S. D. DeGloria, and R. Elliot. 1999. A Terrain Ruggedness Index That Quantifies Topographic Heterogeneity. Intermountain Journal of Sciences. 5(1–4): 23-27.

Rouse, J. W., R. H. Haas, J. A. Schell, and D. W. Deering. 1973. Monitoring vegetation systems in the Great Plains with ERTS. Third Earth Resources Technology Satellite Symposium, Greenbelt, MD, NASA (SP-351) 1: 309–317.

Russell, D. E., A. M. Martell, and W. A. C. Nixon. 1993. Range ecology of the Porcupine caribou herd in Canada. Rangifer, Special Issue 8. 167 pp.

Salomonson, V. V., and I. Appel. 2004. Estimating fractional snow cover from MODIS using the normalized difference snow index. Remote Sensing of Environment 89: 351–360.

Sappington, J., K. M. Longshore, and D. B. Thompson. 2007. Quantifying landscape ruggedness for animal habitat analysis: a case study using bighorn sheep in the Mojave Desert. Journal of Wildlife Management 71: 1419–1426.

Schaaf, C., and Z. Wang. 2015. MCD43A4 MODIS/Terra+Aqua BRDF/Albedo Nadir BRDF Adjusted Ref Daily L3 Global - 500m V006. Distributed by NASA EOSDIS Land Processes DAAC, https://doi.org/10.5067/MODIS/MCD43A4.006

Sellers, P. J. 1985. Canopy reflectance, photosynthesis, and transpiration. International Journal of Remote Sensing 21: 143–183. [original not seen; cited in Hope et al. 1993]

Smith, W.T., R.D. Cameron, and D.J. Reed. 1994. Distribution and movements of caribou in relation to roads and pipelines, Kuparuk Development Area, 1978-1990. Alaska Department of Fish and Game Wildlife Technical Bulletin 12. 54 pp.

SRB&A. 2017. Nuiqsut caribou subsistence monitoring project: results of year 8 hunter interviews and household harvest surveys. Report for ConocoPhillips Alaska, Inc., Anchorage, by Stephen R. Braund & Associates, Anchorage. 47 pp. + appendices.

Stow, D. A., A. Hope, D. McGuire, D. Verbyla, J. Gamon, F. Huemmrich, S. Houston, C. Racine, M. Sturm, K. Tape, L. Hinzman, K. Yoshikawa, C. Tweedie, B. Noyle, C. Silapaswan, D. Douglas, B. Griffith, G. Jia, H. Epstein, D. Walker, S. Daeschner, A. Pertersen, L. Zhou, and R. Myneni. 2004. Remote sensing of vegetation and land-cover change in arctic tundra ecosystems. Remote Sensing of Environment 89: 281–308.

Theobald, D. 2011. Landscape Connectivity & Pattern Tools: Toolbox for ArcGIS. Fort Collins, CO: Colorado State University.

Thornton, P. E., M. M. Thornton, B. W. Mayer, Y. Wei, R. Devarakonda, R. S. Vose, and R. B. Cook. 2016. Daymet: Daily Surface Weather Data on a 1-km Grid for North America, Version 3. ORNL DAAC, Oak Ridge, Tennessee, USA. doi:10.3334/ORNLDAAC/1328

Walker, H. J. 1983. Guidebook to permafrost and related features of the Colville River delta, Alaska. Guidebook 2. Alaska Division of Geological and Geophysical Surveys, Anchorage. 34 pp.

Walker, H. J., and H. H. Morgan. 1964. Unusual weather and riverbank erosion in the delta of the Colville River, Alaska. Arctic 17: 41–47.

Warren, D. L. and S. N. Seifert. 2011. Ecological niche modeling in Maxent: the importance of model complexity and the performance of model selection criteria. Ecological Applications. 21: 335–342.

Weladji, R. B., G. Steinheim, Ø. Holand, S. R. Moe, T. Almøy, and T. Ådnøy. 2003. Use of climatic data to assess the effect of insect harassment on the autumn weight of reindeer (*Rangifer tarandus*) calves. Journal of Zoology 260: 79–85.

Wilson, M. F. J., B. O'Connell, C. Brown, J. C. Guinan, and A. J. Grehan. 2007. Multiscale Terrain Analysis of Multibeam Bathymetry Data for Habitat Mapping on the Continental Slope. Marine Geodesy. 30: 3-35. doi: 10.1080/01490410701295962.

White, R. G., B. R. Thomson, T. Skogland, S. J. Person, D. E. Russell, D. F. Holleman, and J. R. Luick. 1975. Ecology of caribou at Prudhoe Bay, Alaska. Pages 151–201 *in* J. Brown, editor. Ecological investigations of the tundra biome in the Prudhoe Bay region, Alaska. Biological Papers of the University of Alaska, Special Report No. 2, Fairbanks.

Wilson, R. R., A. K. Prichard, L. S. Parrett, B. T. Person, G. M. Carroll, M. A. Smith, C. L. Rea, and D. A. Yokel. 2012. Summer resource selection and identification of important habitat prior to industrial development for the Teshekpuk caribou herd in northern Alaska. PLoS One 7(11): e48697. doi:10.1371/journal.pone.0048697.

Wolfe, S. A. 2000. Habitat selection by calving caribou of the central arctic herd, 1980–95. M.S. thesis, University of Alaska, Fairbanks. 83 pp.

Yokel, D. A., A. K. Prichard, G. Carroll, L. Parrett, B. Person, and C. Rea. 2009. Teshekpuk caribou herd movement through narrow corridors around Teshekpuk Lake, Alaska. Alaska Park Science 8(2): 64–67.

Zuur, A. F., E. N. Ieno, N. J. Walker, A. A. Saveliev, and G. M. Smith. 2009. Mixed-effects models and extensions in ecology with *R*. Springer, New York, NY. 574 pp.

Appendix A. Full methods for calculating remote sensing metrics.

We analyzed 2020 snow cover and 2000–2020 vegetation greenness using gridded, daily reflectance and snow-cover products from MODIS Terra and Aqua sensors. The snow-cover data were added to the data compiled for 2000–2019 (see Lawhead et al. 2015 and Prichard et al. 2017 and 2018b for detailed description of methods). The entire vegetation index record, based on atmospherically corrected surface reflectance data, was processed to ensure comparability of greenness metrics.

For data from 2000–2015, we applied a revised cloud mask that incorporated snow-cover history to reduce false cloud detection during the active snowmelt season. However, the revised cloud mask did not work on the 2016–2020 imagery, probably due to changes in the data and data format from the aging MODIS sensors. For 2016–2020, we applied manual cloud masks for the snowmelt season and applied the standard cloud mask for images collected in June and later.

We analyzed and summarized the data using Google Earth Engine, a cloud computing service (Gorelick et al. 2017). For final analysis and visualization, we exported the results to the Alaska Albers coordinate system (WGS-84 horizontal datum) at 240-m resolution.

SNOW COVER

Snow cover was estimated using the fractional snow algorithm developed by Salomonson and Appel (2004). Only MODIS Terra data were used for snow mapping through 2016 because MODIS Band 6, which was used in the estimation of snow cover, was not functional on the MODIS Aqua sensor. However, a Quantitative Image Restoration algorithm has been applied to restore the missing Aqua Band 6 data to a scientifically usable state for snow mapping (Riggs and Hall 2015). The Terra sensor was no longer reliable for snow mapping in 2017, so we used MODIS Aqua data for snow mapping in 2017–2020. The 2018–2020 analysis was based on MYD10A1.006 data (MODIS/Aqua Snow Cover Daily L3 Global 500m Grid).

A time series of images covering the April–June period was analyzed for each year during 2000–2020. Pixels with >50% water (or ice) cover were excluded from the analysis. For each pixel in each year, we identified:

- The first date with 50% or lower snow cover (i.e., “melted”)
- The closest prior date with >50% snow cover (i.e., “snow”)
- The midpoint between the last observed date with >50% snow cover and the first observed date with <50% snow cover, which is an unbiased estimate of the actual snowmelt date (the first date with <50% snow cover)
- The duration between the dates of the two satellite images with the last observed “snow” date and the first observed “melted” date, providing information on the uncertainty in the estimate of snowmelt date. When the time elapsed between those two dates exceeded one week because of extensive cloud cover or satellite sensor malfunction, the pixel was assigned to the “unknown” category.

VEGETATIVE BIOMASS

The Normalized Difference Vegetation Index (NDVI; Rouse et al. 1973) is used to estimate the biomass of green vegetation within a pixel of satellite imagery at the time of image acquisition (Rouse et al. 1973). The rate of increase in NDVI between two images acquired on different days during green-up has been hypothesized to represent the amount of new growth occurring during that time interval (Wolfe

2000, Kelleyhouse 2001, Griffith et al. 2002). NDVI is calculated as follows (Rouse et al. 1973; http://modis-atmos.gsfc.nasa.gov/NDVI/index.html):

NDVI = (NIR – VIS) ÷ (NIR + VIS)

where:

NIR = near-infrared reflectance (wavelength 0.841–0.876 μm for MODIS), and

VIS = visible light reflectance (wavelength 0.62–0.67 μm for MODIS).

We derived constrained view-angle (sensor zenith angle ≤40°) maximum-value composites from daily surface reflectance composites acquired over targeted portions of the growing season in 2000–2020. The data products used were MOD09GA.006 (Terra Surface Reflectance Daily Global 1km and 500m) and MYD09GA.006 (MYD09GA.006 Aqua Surface Reflectance Daily L2G Global 1km and 500m). NDVI during the calving period (NDVI_Calving) was calculated from a 10-day composite period (1–10 June) for each year during 2000–2020 (adequate cloud-free data were not available to calculate NDVI_Calving over the entire study area in some years). NDVI values near peak lactation (NDVI_621) were interpolated based on the linear change from two composite periods (15–21 June and 22–28 June) in each year. NDVI_Rate was calculated as the linear change in NDVI from NDVI_Calving to NDVI_621 for each year. Finally, NDVI_Peak was calculated from all imagery obtained between 21 June and 31 August each year during 2000–2020. Due to the availability of new forage models, NDVI_Calving, NDVI_621, NDVI_Rate, and NDVI_Peak were not included in analyses of caribou distribution in 2020, but we included summaries of these metrics in this report for comparison with previous reports.

FORAGE MODELING

We applied forage models from Johnson et al. (2018) that incorporate daily NDVI values as well as habitat type, distance to coast, and days from peak NDVI to predict biomass, nitrogen, and digestible energy for a given location on a given day. These models may provide metrics that are more directly related to caribou forage needs than NDVI alone.

We used the MCD43A4.Version 6 daily product at 500-m resolution (Schaaf and Wang 2015). This is the Nadir Bidirectional Reflectance Distribution Function Adjusted Reflectance (NBAR) product, and it provides 500-meter reflectance data that are adjusted using a bidirectional reflectance distribution function (BRDF) to model the reflectance values as if they were collected from a nadir view (i.e., viewed from directly overhead). The NBAR data are produced daily within 16-day retrieval periods using data from both MODIS platforms (i.e., the Terra and Aqua satellites). The product is developed using a single observation from each 16-day period for each 500-m pixel, with priority given to the central day in each compositing period (i.e., the ninth day) to provide the most representative information possible for each period of the year. Other observations in the period are used to parameterize the BRDF model that is required to adjust the observation to nadir. Similar to other MODIS vegetation index products such as MOD13Q1, it has a 16-day composite period, but unlike other products it has a temporal frequency of one day, with the 16-day window shifting one day with each new image. Thus it avoids any artificial steps at the break between composite intervals, and is a good tool to assess daily phenology normals. It is more likely to provide an observation for a given day than true daily products such as the MOD09GA.006/MYD09GA.006 products used for the NDVI composite metrics (above).

Johnson et al. (2018) calibrated the forage models for 4 broad vegetation classes (tussock tundra, dwarf shrub, herbaceous mesic, and herbaceous wet). Following their approach, we used the Alaska Center for Conservation Science (ACCS) land cover map for Northern, Western, and Interior Alaska (Boggs et al. 2016), aggregated on the "Coarse_LC" attribute. This map is based on the North Slope Science Initiative

(NSSI 2013) with the addition of the aggregation field. We calculated the modal land cover class for each 500-m pixel.

Snow water equivalent (SWE) estimates were obtained from the Daymet Version 3 model output data (Thornton et al. 2016), which provided gridded estimates of daily weather parameters for North America and Hawaii at 1 km resolution. Daymet output variables include minimum temperature, maximum temperature, precipitation, and snow water equivalent. The dataset currently covers the period from January 1, 1980 to December 31, 2019 (2020 data will become available sometime in late winter of 2021). SWE was extracted based on the location and date.

For each date from the start of the calving season through the end of the late summer season (30 May–15 September) and for each year with telemetry locations (2002–2020) we mapped NDVI, annual NDVIMax, and days to NDVIMax. Then, we applied the equations from Johnson et al. (2018) to calculate forage nitrogen content and forage biomass for the 4 broad vegetation classes. We set the forage metrics to zero for water, snow/ice, and barren classes and set it to undefined for other vegetation classes that were not included in the Johnson et al. (2018) models. The areas with undefined forage metrics within the study area were primarily low and tall shrub types which comprise a small proportion of the surface area.

HABITAT CLASSIFICATION

We used the NPRA earth-cover classification created by BLM and Ducks Unlimited (2002; Figure 3) to classify habitats for analyses. The NPRA survey area contained 15 cover classes from the NPRA earth-cover classification (Appendix A), which we lumped into nine types to analyze caribou habitat use. The barren ground/other, dunes/dry sand, low shrub, and sparsely vegetated classes, which mostly occurred along Fish and Judy creeks, were combined into a single riverine habitat type. The two flooded-tundra classes were combined as flooded tundra and the clear-water, turbid-water, and *Arctophila fulv*a classes were combined into a single water type; these largely aquatic types are used very little by caribou, so the water type was excluded from the analysis of habitat preference.

Some previous reports (e.g., Lawhead et al. 2015) used a land-cover map created by Ducks Unlimited for the North Slope Science Initiative (NSSI 2013); however, discontinuities in classification methodology and imagery bisected our survey area and potentially resulted in land-cover classification differences in different portions of the survey area, and so we reverted to the BLM and Ducks Unlimited (2002) classification instead.

Appendix B. Cover-class descriptions of the NPRA earth-cover classification (BLM and Ducks Unlimited 2002).

Cover Class	Description
Clear Water	Fresh or saline waters with little or no particulate matter. Clear waters typically are deep (>1 m). This class may contain small amounts of *Arctophila fulva* or *Carex aquatilis*, but generally has <15% surface coverage by these species.
Turbid Water	Waters that contain particulate matter or shallow (<1 m), clear waterbodies that differ spectrally from Clear Water class. This class typically occurs in shallow lake shelves, deltaic plumes, and rivers and lakes with high sediment loads. Turbid waters may contain small amounts of *Arctophila fulva* or *Carex aquatilis*, but generally have <15% surface coverage by these species.
Carex aquatilis	Associated with lake or pond shorelines and composed of 50–80% clear or turbid water >10 cm deep. The dominant species is *Carex aquatilis*. Small percentages of *Arctophila fulva, Hippuris vulgaris, Potentilla palustris,* and *Caltha palustris* may be present.
Arctophila fulva	Associated with lake or pond shorelines and composed of 50–80% clear or turbid water >10 cm deep. The dominant species is *Arctophila fulva*. Small percentages of *Carex aquatilis, Hippuris vulgaris, Potentilla palustris,* and *Caltha palustris* may be present.
Flooded Tundra–Low-centered Polygons	Polygon features that retain water throughout the summer. This class is composed of 25–50% water; *Carex aquatilis* is the dominant species in permanently flooded areas. The drier ridges of polygons are composed mostly of *Eriophorum russeolum, E. vaginatum, Sphagnum* spp., *Salix* spp., *Betula nana, Arctostaphylos* spp., and *Ledum palustre*.
Flooded Tundra–Non-patterned	Continuously flooded areas composed of 25–50% water. *Carex aquatilis* is the dominant species. Other species may include *Hippuris vulgaris, Potentilla palustris,* and *Caltha palustris*. Non-patterned class is distinguished from low-centered polygons by the lack of polygon features and associated shrub species that grow on dry ridges of low-centered polygons.
Wet Tundra	Associated with areas of super-saturated soils and standing water. Wet tundra often floods in early summer and generally drains of excess water during dry periods, but remains saturated throughout the summer. It is composed of 10–25% water; *Carex aquatilis* is the dominant species. Other species may include *Eriophorum angustifolium*, other sedges, grasses, and forbs.
Sedge/Grass Meadow	Dominated by the sedge family, this class commonly consists of a continuous mat of sedges and grasses with a moss and lichen understory. The dominant species are *Carex aquatilis, Eriophorum angustifolium, E. russeolum, Arctagrostis latifolia,* and *Poa arctica*. Associated genera include *Cassiope* spp., *Ledum* spp., and *Vaccinium* spp.
Tussock Tundra	Dominated by the tussock-forming sedge *Eriophorum vaginatum*. Tussock tundra is common throughout the arctic foothills north of the Brooks Range and may be found on well-drained sites in all areas of the NPRA. Cottongrass tussocks are the dominant landscape elements and moss is the common understory. Lichen, forbs, and shrubs are also present in varying densities. Associated genera include *Salix* spp., *Betula nana*, *Ledum palustre*, and *Carex* spp.
Moss/Lichen	Associated with low-lying lakeshores and dry sandy ridges dominated by moss and lichen species. As this type grades into a sedge type, graminoids such as *Carex aquatilis* may increase in cover, forming an intermediate zone.

Appendix B. Continued

Cover Class	Description
Dwarf Shrub	Associated with ridges and well-drained soils and dominated by shrubs <30 cm in height. Because of the relative dryness of the sites on which this cover type occurs, it is the most species-diverse class. Major species include *Salix* spp., *Betula nana*, *Ledum palustre, Dryas* spp*., Vaccinium* spp*., Arctostaphylos* spp*., Eriophorum vaginatum,* and *Carex aquatilis.* This class frequently occurs over a substrate of tussocks.
Low Shrub	Associated with small streams and rivers, but also occurs on hillsides in the southern portion of the NPRA. This class is dominated by shrubs 0.3–1.5 m in height. Major species include *Salix* spp., *Betula nana*, *Alnus crispa*, and *Ledum palustre.*
Dunes/Dry Sand	Associated with streams, rivers, lakes and coastal beaches. Dominated by dry sand with <10% vegetative cover. Plant species may include *Poa* spp., *Salix* spp., *Astragalus* spp., *Carex* spp., *Stellaria* spp., *Arctostaphylos* spp., and *Puccinellia phryganodes*.
Sparsely Vegetated	Occurs primarily along the coast in areas affected by high tides or storm tides, in recently drained lake or pond basins, and in areas where bare mineral soil is being recolonized by vegetation. Dominated by non-vegetated material with 10–30% vegetative cover. The vegetation may include rare plants, but the most common species include *Stellaria* spp., *Poa* spp., *Salix* spp., *Astragalus* spp., *Carex* spp., *Arctostaphylos* spp., and *Puccinellia phryganodes*.
Barren Ground/ Other	Associated with river and stream gravel bars, mountainous areas, and human development. Includes <10% vegetative cover. May incorporate dead vegetation associated with salt burn from ocean water.

Appendix C. Snow depth (cm) and cumulative thawing degree-days (°C above freezing) at the Kuparuk airstrip, 1983–2020.

	Snow Depth (cm)			Cumulative Thawing Degree-days (ºC)						
Year	1 April	15 May	31 May	1–15 May	16–31 May	1–15 June	16–30 June	1–15 July	16–31 July	1–15 August
1983	10	5	0	0	3.6	53.8	66.2	74.7	103.8	100.3
1984	18	15	0	0	0	55.6	75.3	122.8	146.4	99.5
1985	10	8	0	0	10.3	18.6	92.8	84.7	99.4	100.0
1986	33	20	10	0	0	5.0	100.8	112.2	124.7	109.4
1987	15	8	3	0	0.6	6.7	61.4	112.2	127.8	93.1
1988	10	5	5	0	0	16.7	78.1	108.3	143.1	137.5
1989	33	–	10[a]	0	5.6	20.6	109.4	214.7	168.1	215.8
1990	8	3	0	0	16.1	39.7	132.2	145.0	150.0	82.5
1991	23	8	3	0	7.8	14.4	127.6	73.3	115.0	70.6
1992	13	8	0	0.3	20.3	55.0	85.3	113.9	166.1	104.2
1993	13	5	0	0	8.6	33.6	94.4	175.8	149.7	96.1
1994	20	18	8	0	4.4	49.2	51.7	149.7	175.8	222.2
1995	18	5	0	0	1.1	59.4	87.5	162.8	106.9	83.3
1996	23	5	0	8.1	41.7	86.1	121.1	138.9	168.1	95.8
1997	28	18	8	0	20.8	36.1	109.7	101.7	177.8	194.2
1998	25	8	0	3.6	45.8	74.2	135.0	158.9	184.4	174.4
1999	28	15	10	0	1.4	30.3	67.8	173.3	81.1	177.5
2000	30	23	13	0	0	36.7	169.7	113.3	127.5	118.6
2001	23	30	5	0	0.8	51.9	72.2	80.0	183.9	131.7
2002	30	trace	0	4.2	30.3	57.8	70.3	92.2	134.4	106.1
2003	28	13	trace	0	10.8	23.6	77.5	140.0	144.7	91.9
2004	36	10	5	0	8.9	26.4	185.6	148.1	151.4	153.3
2005	23	13	0	0	2.5	14.2	78.1	67.5	79.4	176.7
2006	23	5	0	0	23.3	93.3	153.1	82.2	186.1	109.7
2007	25	46	5	0	0	46.4	81.7	115.0	138.9	134.4
2008	20	18	0	0	32.8	71.7	138.9	172.2	132.5	86.1
2009	36	13	0	0	16.7	71.7	44.4	142.8	126.4	133.6
2010	41	43	13	0	1.4	53.3	51.1	126.7	168.9	149.2
2011[a]	25	18	0	0	27.8	12.5	101.2	122.4	171.6	143.2
2012[a]	48	53	2	0	1.7	26.8	137.3	140.2	195.2	143.5
2013	33	18	2	0	4.2	79.2	131.7	112.8	188.0	185.4

Appendix C. Continued.

Year	Snow Depth (cm)			Cumulative Thawing Degree-days (ºC)						
	1 April	15 May	31 May	1–15 May	16–31 May	1–15 June	16–30 June	1–15 July	16–31 July	1–15 August
2014	33	0[b]	0[b]	11.1	4.2	28.6	82.0	127.2	102.3	67.9
2015	38	14	3	1.4	46.4	78.9	197.2	117.9	95.7	106.9
2016	25	0	0	15.6	12.4	63.7	131.2	174.7	130.8	98.1
2017	36	14	0	0	12.1	5.2	121.3	173.4	174.5	150.5
2018	41	20	15	1.35	0	6.6	47.7	137.0	195.9	55.25
2019	23	13	0	1.1	11.9	31.1	108.5	180.3	181.3	118.0
2020	25.4	4.0	0	0.3	7.8	48.9	90.7	82.3	112.3	128.4
Mean	**25.5**	**14.2**	**3.1**	**1.2**	**11.7**	**41.6**	**101.8**	**128.2**	**144.9**	**125.1**

[a] Kuparuk weather data were not available for 17 June–9 December 2011, 4–14 August 2012, and 30–31 August 2012, so cumulative TDD for those periods were estimated by averaging Deadhorse and Nuiqsut temperatures (Lawhead and Prichard 2012).

[b] Kuparuk airport station reported no snow after 8 May 2014, whereas other weather stations nearby reported snow until 31 May and patchy snow was present in the GKA survey areas into early June. Therefore, if accurate, the airport information was not representative of the study area.

Page intentionally left blank.

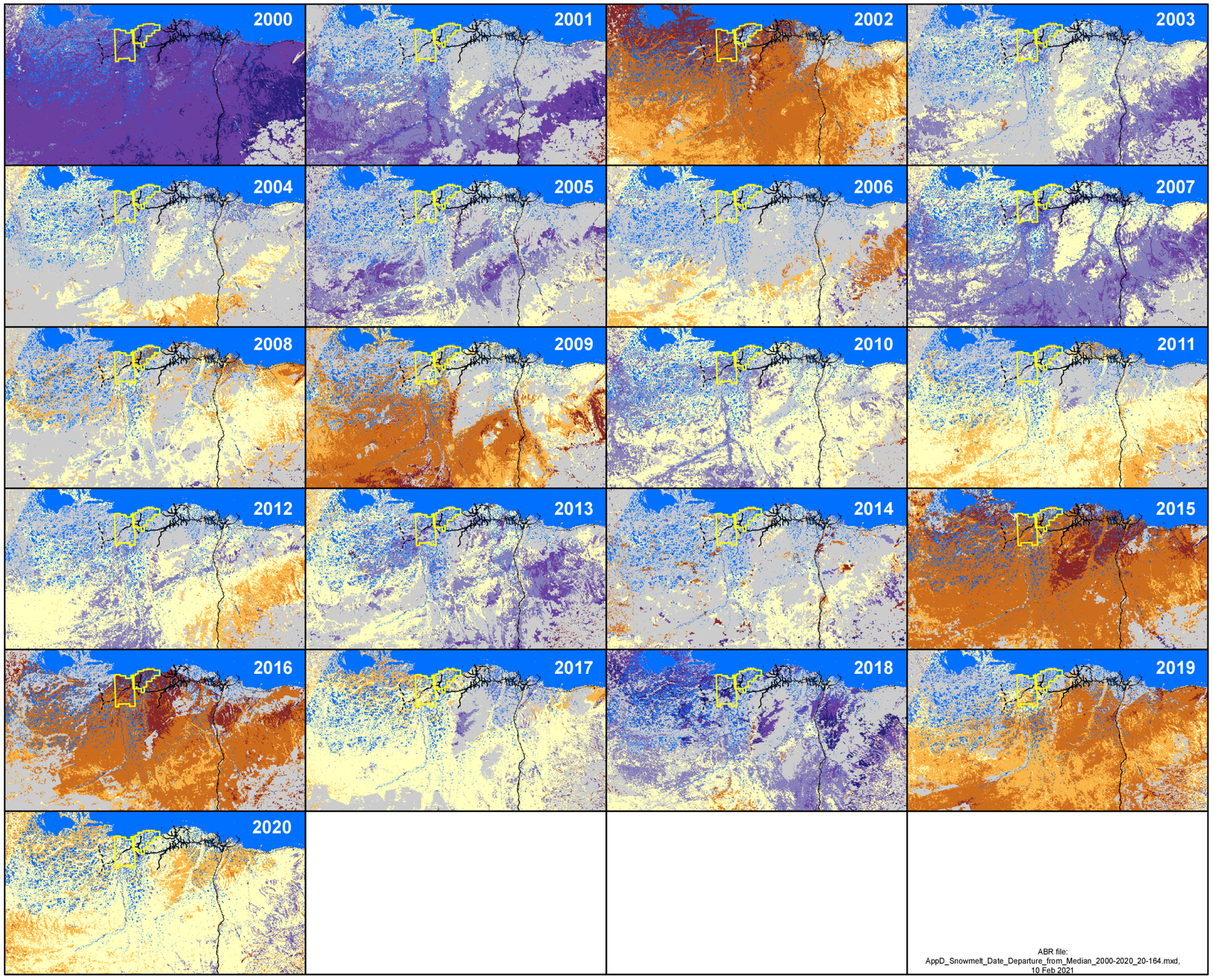

Timing of Snow Melt

Compared to Median (2000–2020)

- Date not known within one week
- > 14 days earlier than median
- 8–14 days earlier than median
- 4–7 days earlier than median
- Within 3 days of median
- 4–7 days later than median
- 8–14 days later than median
- > 14 days later than median
- >= 50% Water Cover

Aerial Survey Area

N
W E
S

0 20 40 60 80 100 Miles

0 50 100 150 Kilometers

Appendix D. Timing of annual snowmelt (<50% snow cover), compared with median date of snowmelt, on the central North Slope of Alaska during 2000–2020, as estimated from MODIS satellite imagery.

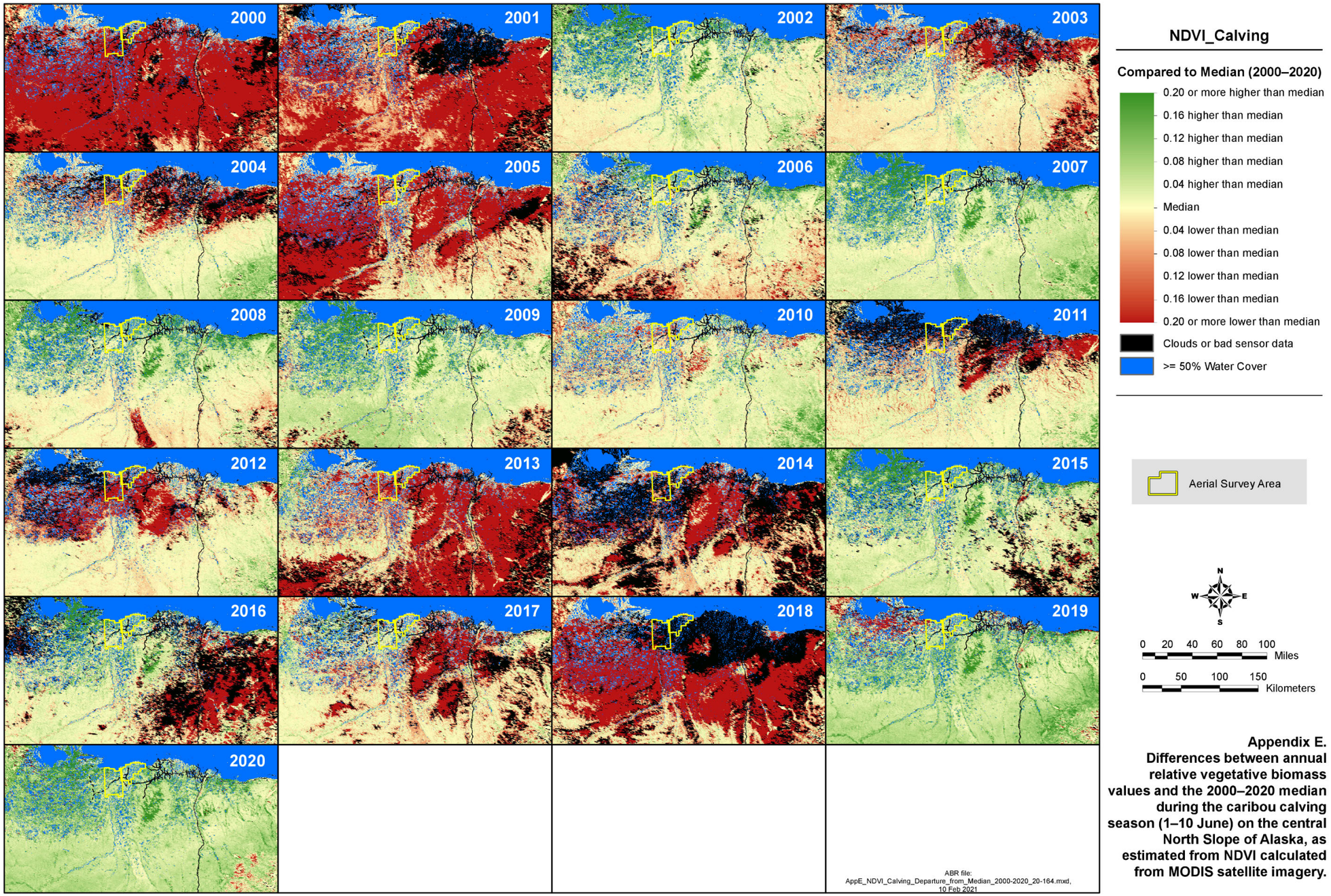

Appendix E. Differences between annual relative vegetative biomass values and the 2000–2020 median during the caribou calving season (1–10 June) on the central North Slope of Alaska, as estimated from NDVI calculated from MODIS satellite imagery.

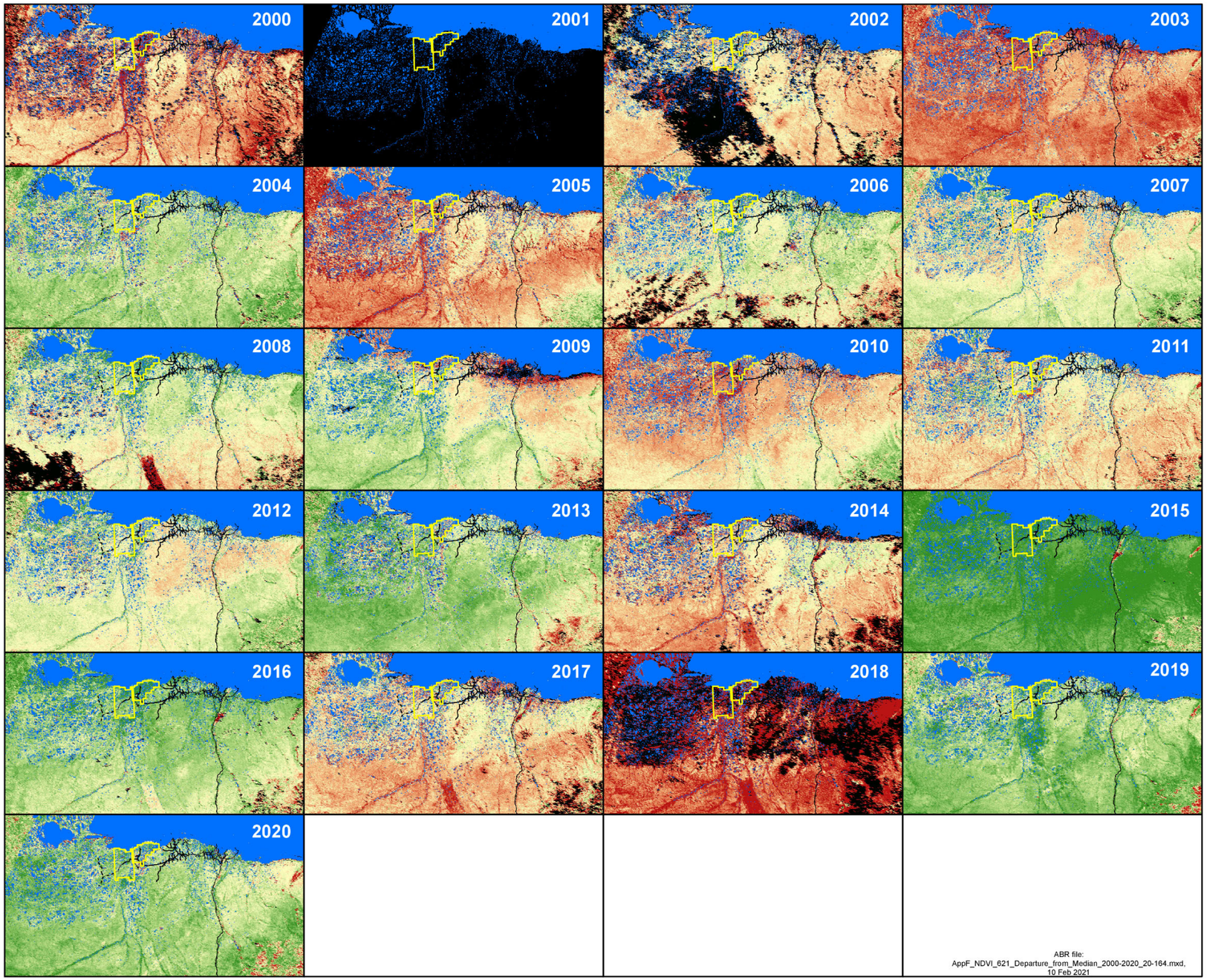

NDVI_621

Compared to Median (2000–2020)

- 0.10 or more higher than median
- 0.08 higher than median
- 0.06 higher than median
- 0.04 higher than median
- 0.02 higher than median
- Median
- 0.02 lower than median
- 0.04 lower than median
- 0.06 lower than median
- 0.08 lower than median
- 0.10 or more lower than median
- Clouds or bad sensor data
- >= 50% Water Cover
- Aerial Survey Area

N W E S

0 20 40 60 80 100 Miles

0 50 100 150 Kilometers

Appendix F.
Differences between annual relative vegetative biomass values and the 2000–2020 median at estimated peak lactation for caribou (21 June) on the central North Slope of Alaska, as estimated from NDVI calculated from MODIS satellite imagery.

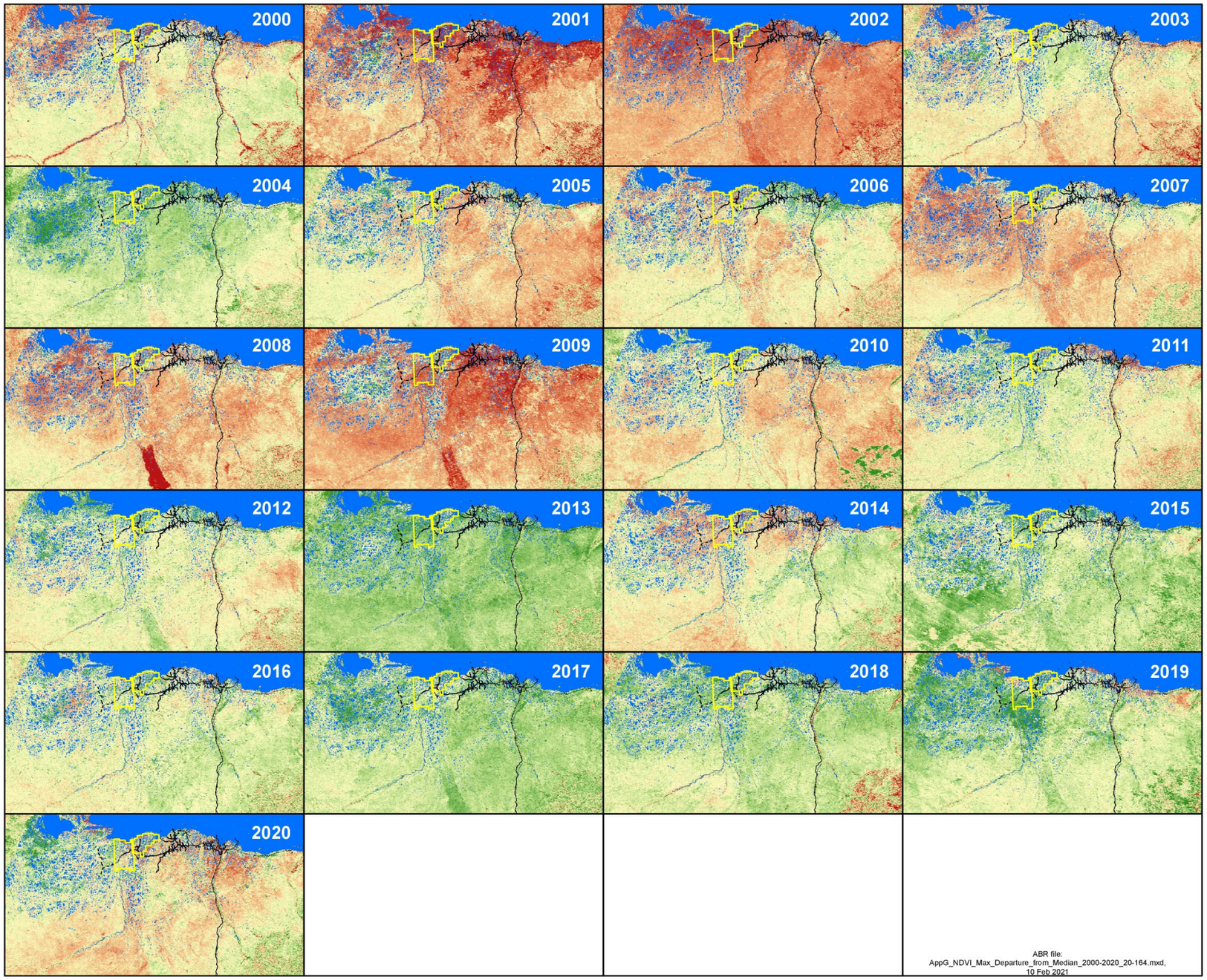

Appendix G. Differences between annual relative vegetative biomass values and the 2000–2020 median for estimated peak biomass on the central North Slope of Alaska, as estimated from NDVI calculated from MODIS satellite imagery.